Suite of Standards for Electromagnetic Material Characterization Using Mode Matching Theory

THESIS

Brian Witthoeft, 1Lt, USAF

AFIT/GE/ENG/09-49

DEPARTMENT OF THE AIR FORCE
AIR UNIVERSITY

AIR FORCE INSTITUTE OF TECHNOLOGY

Wright-Patterson Air Force Base, Ohio

APPROVED FOR PUBLIC RELEASE; DISTRIBUTION UNLIMITED.

The views expressed in this thesis are those of the author and do not reflect the official policy or position of the United States Air Force, Department of Defense, or the United States Government.

AFIT/GE/ENG/09-49

Suite of Standards for Electromagnetic Material Characterization Using Mode Matching Theory

THESIS

Presented to the Faculty

Department of Electrical and Computer Engineering

Graduate School of Engineering and Management

Air Force Institute of Technology

Air University

Air Education and Training Command

In Partial Fulfillment of the Requirements for the

Degree of Master of Science in Electrical Engineering

Brian Witthoeft, B.S.E.E.

1Lt, USAF

March 2008

APPROVED FOR PUBLIC RELEASE; DISTRIBUTION UNLIMITED.

AFIT/GE/ENG/09-49

Suite of Standards for Electromagnetic Material Characterization Using Mode Matching Theory

Brian Witthoeft, B.S.E.E.
1Lt, USAF

Approved:

Michael Havrilla — 17 Mar 2009
Dr. Michael J. Havrilla (Chairman) — date

17 MAR 2009
Dr. Peter J. Collins (Member) — date

17 Mar 2009
Dr. Anthony J. Terzuoli (Member) — date

Abstract

The objective of this research is to determine if an acceptable standard can be developed to access the accuracy and precision of measurements taken using waveguide systems. Tiny changes in material fabrication, processing, and environment can cause problems with accuracy and precision in measurement. There is a great deal of research on uncertainty analysis in the literature. A large portion of the effort will be to determine the levels of uncertainty caused by each of the dimensions of the waveguide insert and to develop a suitable standard capable of verifying system performance. The Mode-Matching Technique will be used to extract input and output S-parameters of a suite of metallic verification waveguide standards. This suite will be used to set a new standard for acceptable tolerances of waveguide systems. After running the theoretical values of Scattering parameters against measured values, it can be determined whether small changes to the parameters of uncertainty greatly effect the measurements. If these changes only cause small changes in measurement, this will be considered an effective standard.

Acknowledgements

First and foremost, I owe a large debt of gratitude to Dr. Michael Havrilla for all of the guidance and physical insight he provided. Secondly, a great debt of gratitude is owed to Dr. Greg Wilson of Berriehill Research Corp. for hours of help with the uncertainty portion of this thesis. I'd also like to thank my thesis committee for the time, effort, and knowledge they passed along reviewing my thesis. I'd also like to thank Capt. Neil Rogers for his tireless help. Without his help I may have gotten here, but it wouldn't have looked as good.

Brian Witthoeft

Table of Contents

Page

List of Figures

List of Tables

List of Symbols

List of Abbreviations

Suite of Standards for Electromagnetic Material Characterization Using Mode Matching Theory

I. Introduction

1.1 Background

In any electromagnetic material characterization measurement taken using a Network Analyzer (NWA), there are inherent errors caused by a variety of factors related to both the system environment and the user performing the measurement. Standards can be developed to compare measured values against true or "expected" values. These standards should allow simple theoretical calculations to determine true values. From here on this thesis will not use the term "expected" values because expected values holds a different meaning in statistical terms and will lead to confusion. There are three main areas of error in measurement: systematic, random, and drift. "Noise" or random errors can be caused by many factors in the environment of the NWA. These can be caused by simple things like how the cables are handled during measurement. Microwave equipment is sensitive in nature and must be handled with care. The air within a waveguide is not a perfect vacuum which may cause some changes to measurement. It is possible to remove some of this random error through things like averaging and IF Bandwidth Reduction. Errors that are systematic are predictable and deterministic in nature. These errors are caused by things like cable phase delay, coupler directivity, and load mismatch. Calibration is used as an effective tool to remove these types of errors from the system. Lastly, errors may be caused by drift to the system calibration. This usually occurs after systematic errors are removed through calibration. Environmental effects like changes in humidity and

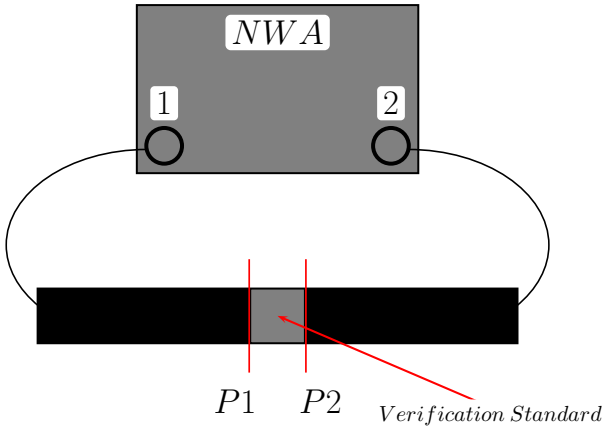

Figure 1.1: Model of Network Analyzer Connected to Waveguides

temperature may cause the level at calibration to vary slightly. This area can be improved by a tightly controlled environment. All three types of error may cause a bias and variance to the measurements being taken. A good standard will be one that introduces very little error due to fabrication and has fairly simple theory for determination of measurement parameters. Metallic standards have much more consistent material characteristics and there is a degree of control over machining of such standards. A metallic standard also makes it possible to fabricate into certain geometries which allow for simple analytic models. There is also very little breakdown of materials, dimensional changes from wear and tear, or humidity contamination. Figure 1.1 shows a typical set-up for measuring material characteristics.

In June of 2006, the Material Measurement Working Group (MMWG) was formed in part to develop a metallic verification standard to assess NWA accuracy and precision. In the paper, "Assessment of a Candidate Metallic Waveguide Standard, Based on S-Parameter Uncertainty Due To Dimensional Manufacturing Errors" [1], the MMWG studied the feasibility of using a metallic waveguide insert shown in Figure 1.2, as a NWA verification standard for interlaboratory comparisons. This group also performed an uncertainty study to determine if the verification standard was sensitive

to fabrication error. If small perfections lead to large uncertainty, the A600 would not be a good standard. A waveguide standard [1] as stated by this paper "is an object of known or accepted properties that can be measured using the waveguide procedure." More simply stated, this standard has a true value value that can be determined by theory. In the case of the A600 the MMWG was able to determine a true value using two separate modeling techniques.

The next part of the A600 analysis was to determine if small imperfections in the fabrication of the filter such as differences in height and depth of the filter, hole size and placement, and alignment led to measurement differences between true values and actual measurements of the filter. There were 14 separate parameters of uncertainty identified in their study. To determine how much care should be taken in fabrication, it was necessary for the group to determine relaxed tolerances and tight tolerances for each parameter. The MMWG Spring 2008 Meeting reported on an uncertainty analysis for the A600 [1] using two slightly different Monte-Carlo methods. There were two groups involved in the uncertainty analysis of the notch filter. The ATK group was included Dr. Greg Wilson and Dr. Thao Dinh[1]. The QinetiQ North America group included Dr. Kevin Lambert and Carol Kory. The ATK group used HFSS and the QinetiQ group used MWS to perform their analysis. In their presentation, it was shown that the 14 parameters of uncertainty present in the A600 each slightly affected the uncertainty. Results between the two groups showed similar responses for the A600. The A600 tended to be sensitive to be most sensitive to errors in slot width when it came to uncertainty. The A600 was also somewhat difficult to fabricate. A major advantage to the A600 was the fact that it provided one single standard that could be used from laboratory to laboratory. It would be helpful to know what is happening across the spectrum of S-parameters for all X-band frequencies. The disadvantage to having one single standard is that the A600 does not provide for varying values of S_{11} and S_{21}. The last disadvantage of the A600 comes in the area of computation time. For true values, computation time was

[1]Dr. Gregory Wilson and Dr. Thao Dinh are currently with Berriehill Research Corp (BRC)

roughly one hour. The Monte-Carlo uncertainty analysis done on the A600 however took days of computation time. Computation times are considerably improved when using alternative methods like Taylor Series and Equal Weight Cubature. Taylor Series could not be used with confidence for the A600. Equal Weight Cubature was not used as a method of uncertainty analysis for the A600. It may be possible to find an alternative standard that improves on some of the disadvantages of the A600 and this thesis will discuss one of these possible standards. In this case, however, it is a set of standards.

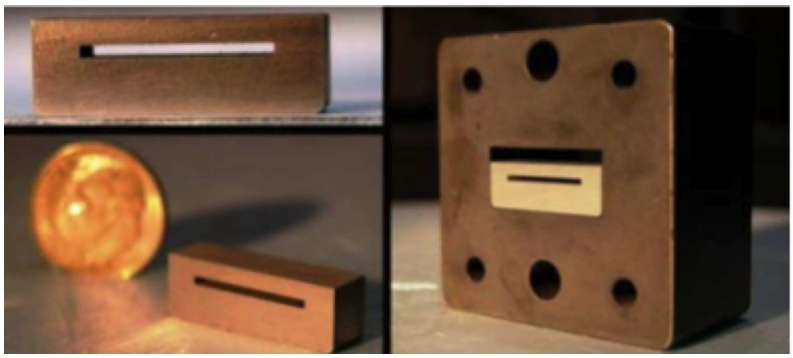

Figure 1.2: A WR-90 notch lter insert with a 0.6 inch wide slot; shown alone in two views (left) and in a material sample holder(right) [1] [4]

1.2 Goals

The purpose of this thesis is to determine if an alternative set of standards can be developed and characterized that will minimize the computational effort and the amount of uncertainty in material measurement calculations. This alternative set of standards will enable the use of a simplified theory called the Mode Matching Technique (MMT) because of the simplified geometry of this set of standards. The complicated geometry of the A600 notch filter requires more computationally robust modeling methods like that of MWS and HFSS. The MMT will be formulated in Chapter II and should decrease the computation time for expected values of the set of standards as well as for the uncertainty analysis. Once expected values of Scattering Parameters (S-Parameters) are determined, it's important to understand how even

slight changes to the specific parameters of Figure 2.1 like the width of the insert, ℓ, or the width of the opening of the insert in the 'x' direction, d might impact the expected values. Using metallic standards will decrease some of the causes of uncertainties described earlier. Performing an uncertainty analysis as in Chapter III will give expected "error bars" or boundaries for determining if the NWA system has any inherent errors in precision or accuracy. The terms precision and accuracy will be further defined in ChapterIII.

1.3 Procedures

The expected values for the possible alternative set of standards in this thesis come from the Mode Matching Technique which will be further developed in Chapter II. Without these true values or expected values, uncertainty becomes meaningless. `Matlab`® will be used for the majority of the analysis done in this thesis because of its versatility. The Mode Matching Technique creates 4N equations with 4N unknowns. This N or number of possible modes for determining S-parameters increases in accuracy as the number of modes increases. The disadvantage to increasing the number of modes is an increase to the amount of computation time. There should be a certain number of modes where the S-parameters computed become "slowly varying" or begin to converge on a value. The term "slowly varying" is somewhat subjective but this thesis will watch the third significant figure to determine the first place that the value is maintained for multiple mode increases. Once the number of modes is defined, the true values of the S-parameters will be locked in and set as the true values. 6 separate standard widths from a fully opened waveguide to an almost closed waveguide allows for an understanding of the whole spectrum of S-parameters for all X-band frequencies. As with the A600 analysis, it will be important to determine the sensitivity of these standards to variations in fabrication. This is done using an uncertainty analysis. To ensure continuity, three types of uncertainty analyses will be performed and should produce similar results: Taylor Series Method, Equal Weight

Cubature Method, and Monte-Carlo Method. Chapter III focuses on a brief introduction to those uncertainty analysis methods which is information largely gained through collaboration with Dr. Gregory Wilson, BRC.

1.4 Summary

It is vital for the Air Force and the material measurement community that the measurements taken using a NWA are accurate and precise. This thesis will determine the feasibility of a set of standards to increase the confidence in measurement independent of environment. Fabrication of these standards takes a relatively short amount of time (a matter of a couple of days) and the simplistic geometry of these standards should increase the precision of each parameter of uncertainty, i.e. $'d'$ and $'\ell'$. If small variations in $'d'$ and $'\ell'$ produce large uncertainty values, this set of standards has little value. However, if variations in $'d'$ and $'\ell'$ produce small uncertainty values, than these standards may be used to check NWA values Air Force wide.

II. Mode Matching Method

2.1 Theory

Electromagnetic modeling methods like MWS and HFSS often take large amounts of computation time to complete. These methods can be very accurate but lend themselves to large costs in time and money. The difficulty of the A600 is that the geometry is fairly complicated and expected S-parameter values are most accurately defined using modeling techniques like MWS and HFSS. The geometry of the set of alternate standards described in this thesis lends itself to a simpler technique for determining expected S-parameter values. The Mode Matching Technique (MMT) is accomplished using these three main steps:

(1) Expand Fields

(2) Apply Boundary Conditions

(3) Apply Testing Operations

The system described in this thesis is defined in Figure 2.1. There are three main regions that must be thoroughly defined through field expansion. Region I defines the area in the following equations when $z < 0$. Regions II defines the area in the following equations when $0 < z < \ell$. Finally Region III defines the area in the following equations when $z > \ell$.

2.1.1 Field Expansion. Field Expansion is the first step necessary to define exactly what is happening in each region of the waveguide system. There are an infinite number of modes that are propagated through the waveguide which are defined by the variable 'n'. a_1^+ is considered to be the forward coefficients for the $\bar{E}$ and $\bar{H}$ fields in Region I. a_n^- are the infinite number of coefficients that make up the return fields of Region I. b_n^+ and b_n^- are the forward and reverse coefficients for Region II. c_n^+

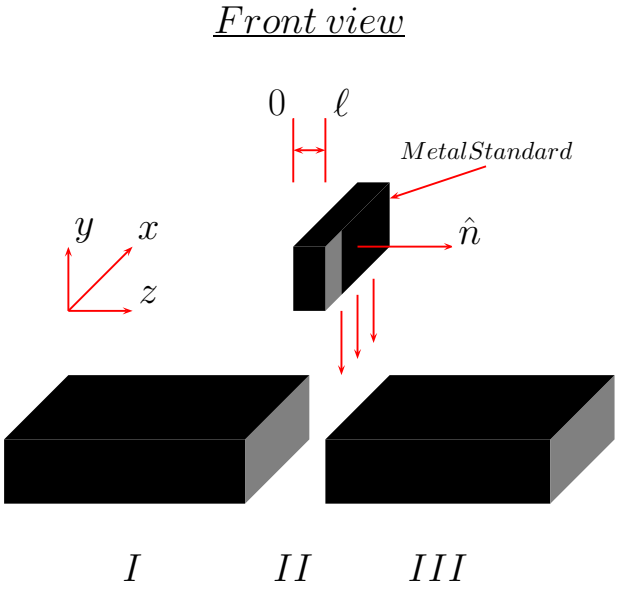

Figure 2.1: X-Band Waveguide System Illustration

contains the forward coefficients for Region III.

$$\bar{E} = a_1^+(\bar{e}_1 + \hat{z}e_{z1})e^{-\gamma_1 z} + \sum_{n=1}^{\infty} a_n^-(\bar{e}_n - \hat{z}e_{zn})e^{\gamma_n z} ... z < 0 \tag{2.1}$$

$$\bar{H} = a_1^+(\bar{h}_1 + \hat{z}h_{z1})e^{-\gamma_1 z} + \sum_{n=1}^{\infty} a_n^-(-\bar{h}_n + \hat{z}h_{zn})e^{\gamma_n z} ... z < 0 \tag{2.2}$$

$$\bar{E} = \sum_{n=1}^{\infty} b_n^+(\bar{\tilde{e}}_n + \hat{z}\tilde{e}_{zn})e^{-\tilde{\gamma}_n z} + \sum_{n=1}^{\infty} b_n^-(\bar{\tilde{e}}_n - \hat{z}\tilde{e}_{zn})e^{\tilde{\gamma}_n z} ... 0 < z < \ell \tag{2.3}$$

$$\bar{H} = \sum_{n=1}^{\infty} b_n^+(\bar{\tilde{h}}_n + \hat{z}\tilde{h}_{zn})e^{-\tilde{\gamma}_n z} + \sum_{n=1}^{\infty} b_n^-(-\bar{\tilde{h}}_n + \hat{z}\tilde{h}_{zn})e^{\tilde{\gamma}_n z} ... 0 < z < \ell \tag{2.4}$$

$$\bar{E} = \sum_{n=1}^{\infty} c_n^+(\bar{e}_n + \hat{z}e_{zn})e^{-\gamma_n (z-\ell)} ... z > \ell \tag{2.5}$$

$$\bar{H} = \sum_{n=1}^{\infty} c_n^+(\bar{h}_n + \hat{z}h_{zn})e^{-\gamma_n (z-\ell)} ... z > \ell \tag{2.6}$$

2.1.2 Apply Boundary Conditions. The waveguide is considered to be a PEC for the formulation of this theory section. Since the waveguide is considered PEC, the tangential $\bar{E}$ fields are known to be '0'. Also, the fields across each section boundary in free space are continuous. This is where the following equations come from. $\hat{n}$ or the normal with respect to the waveguide inserts is the $\hat{z}$ direction. $\hat{z}$ crossed with the $\hat{z}$ vector produces zero. Therefore the only remaining components are the x and y components. In this case the dominant mode is the TE_{10} mode. The incident excitation is y-invariant and the boundaries of regions I, II, & III are y-invariant, therefore only the TE_{m0} modes will be scattered.

$$\hat{n} \times \bar{E}(z = 0^-) = \begin{cases} \hat{n} \times \bar{E}(z = 0^+) & \text{if } 0 < x < d; \\ 0 & \text{if } d < x < a. \end{cases} \tag{2.7}$$

$$\hat{n} \times \bar{H}(z = 0^-) = \hat{n} \times \bar{H}(z = 0^+) \qquad \text{if } 0 < x < d \tag{2.8}$$

$$\hat{n} \times \bar{E}(z = \ell^+) = \begin{cases} \hat{n} \times \bar{E}(z = \ell^-) & \text{if } 0 < x < d; \\ 0 & \text{if } d < x < a. \end{cases} \tag{2.9}$$

$$\hat{n} \times \bar{H}(z = \ell^-) = \hat{n} \times \bar{H}(z = \ell^+) \qquad \text{if } 0 < x < d \tag{2.10}$$

$$\hat{z} \times \left[a_1^+(\bar{e}_1 + \hat{z}e_{z1}) + \sum_{n=1}^{\infty} a_n^-(\bar{e}_n - \hat{z}e_{zn}) \right] \tag{2.11}$$

$$= \begin{cases} \hat{z} \times [\sum_{n=1}^{\infty} b_n^+(\bar{\tilde{e}}_n + \hat{z}\tilde{e}_{zn}) + b_n^-(\bar{\tilde{e}}_n - \hat{z}\tilde{e}_{zn})] & \text{if } 0 < x < d; \\ 0 & \text{if } d < x < a. \end{cases}$$

$$\hat{z} \times \left[a_1^+(\bar{h}_1 + \hat{z}h_{z1}) + \sum_{n=1}^{\infty} a_n^-(-\bar{h}_n + \hat{z}h_{zn}) \right] \tag{2.12}$$

$$= \hat{z} \times \left[\sum_{n=1}^{\infty} b_n^+(\bar{\tilde{h}}_n + \hat{z}\tilde{h}_{zn}) + b_n^-(-\bar{\tilde{h}}_n + \hat{z}\tilde{h}_{zn}) \right] \text{if } 0 < x < d$$

$$\hat{z} \times \left[\sum_{n=1}^{\infty} c_n^+(\bar{e}_n + \hat{z}e_{zn}) \right] \tag{2.13}$$

$$= \begin{cases} \hat{z} \times \left[\sum_{n=1}^{\infty} b_n^+(\bar{\tilde{e}}_n + \hat{z}\tilde{e}_{zn}) e^{-\tilde{\gamma}_n \ell} + \sum_{n=1}^{\infty} b_n^-(\bar{\tilde{e}}_n - \hat{z}\tilde{e}_{zn}) e^{\tilde{\gamma}_n \ell} \right] & \text{if } 0 < x < d; \\ 0 & \text{if } d < x < a. \end{cases}$$

$$\hat{z} \times \left[\sum_{n=1}^{\infty} c_n^+(\bar{h}_n + \hat{z}h_{zn}) \right] \tag{2.14}$$

$$= \hat{z} \times \left[\sum_{n=1}^{\infty} b_n^+(\bar{\tilde{h}}_n + \hat{z}\tilde{h}_{zn}) e^{-\tilde{\gamma}_n \ell} + \sum_{n=1}^{\infty} b_n^-(-\bar{\tilde{h}}_n + \hat{z}\tilde{h}_{zn}) e^{\tilde{\gamma}_n \ell} \right] \text{if } 0 < x < d$$

Dividing out a_1^+ and substituting Eq. 2.15 into Eqs. 2.11-2.14 produces Eqs. 2.17-2.20. There are an infinite number of possible modes from Eqs. 2.11-2.14. This must be truncated at 'N' modes for practical implementation. Determining the 'N' will be part of the results chapter of this thesis. The following equations produce all of the reflection and transmission coefficients for all 'N' equations. However, only the 'N' = 1 equations are needed because all other modes are evanescing.

$$R_n = \frac{a_n^-}{a_1^+}, \quad t_n = \frac{b_n^+}{a_1^+}, \quad r_n = \frac{b_n^-}{a_1^+}, \quad T_n = \frac{c_n^+}{a_1^+} \tag{2.15}$$

$$R_1 = \frac{a_1^-}{a_1^+} = S_{11}, \quad T_1 = \frac{c_1^+}{a_1^+} = S_{21} \tag{2.16}$$

This leaves 4N Linearly Independent equations and 4N unknowns:

$$\bar{e}_1 + \sum_{n=1}^{N} R_n \bar{e}_n = \begin{cases} \sum_{n=1}^{N} \left(t_n \bar{\bar{e}}_n + r_n \bar{\bar{e}}_n\right) & \text{if } 0 < x < d; \\ 0 & \text{if } d < x < a. \end{cases} \tag{2.17}$$

$$\bar{h}_1 - \sum_{n=1}^{N} R_n \bar{h}_n = \sum_{n=1}^{N} \left(t_n \bar{\bar{h}}_n - r_n \bar{\bar{h}}_n\right) \qquad \text{if } 0 < x < d; \tag{2.18}$$

$$\sum_{n=1}^{N} T_n \bar{e}_n = \begin{cases} \sum_{n=1}^{N} \left(t_n \bar{\bar{e}}_n e^{-\tilde{\gamma}_n \ell} + r_n \bar{\bar{e}}_n e^{\tilde{\gamma}_n \ell}\right) & \text{if } 0 < x < d; \\ 0 & \text{if } d < x < a. \end{cases} \tag{2.19}$$

$$\sum_{n=1}^{N} T_n \bar{h}_n = \sum_{n=1}^{N} \left(t_n \bar{\bar{h}}_n e^{-\tilde{\gamma}_n \ell} - r_n \bar{\bar{h}}_n e^{\tilde{\gamma}_n \ell}\right) \quad \text{if } 0 < x < d \tag{2.20}$$

2.1.3 Apply Testing Operators. Testing operators will help solve the 4N equations necessary to fill the $Ax = b$ matrix. In this case, because of the unchanging nature of the y-component, only the x-components need be integrated.

$$\int_0^a \bar{e}_m \cdot \{(2.17), (2.19)\}\, dx \quad ...m = 1, 2, 3, ..., N$$

$$\int_0^d \bar{\bar{h}}_m \cdot \{(2.18), (2.20)\}\, dx \quad ...m = 1, 2, 3, ..., N$$

These testing operators were chosen from the geometry of the waveguide system and are applied to each side of Eqs. 2.17-2.20. $\bar{e}_m$ is integrated between 0 to a from the field expansion of sections I & III of the waveguide in Figure 2.1. These sections of the waveguide are fully open and the $\bar{E}$ field equations are used over the entire opening. The region from d to a is fully determined by the $\bar{E}$ field being exactly zero at the PEC because of the uniqueness theorem. This means that $\bar{H}$ fields are not necessary in that region. This is why $\bar{\bar{h}}_m$ is only used between regions 0 to d.

$$\int_0^a \bar{e}_m \cdot \bar{e}_1 dx + \sum_{n=1}^{N} R_n \int_0^a \bar{e}_m \cdot \bar{e}_n dx = \sum_{n=1}^{N} \left(t_n \int_0^d \bar{e}_m \cdot \bar{\bar{e}}_n dx + r_n \int_0^d \bar{e}_m \cdot \bar{\bar{e}}_n dx \right) \tag{2.21}$$

$...m = 1, ..., N$

$$\int_0^d \bar{\bar{h}}_m \cdot \bar{h}_1 dx - \sum_{n=1}^{N} R_n \int_0^d \bar{\bar{h}}_m \cdot \bar{h}_n dx = \sum_{n=1}^{N} \left(t_n \int_0^d \bar{\bar{h}}_m \cdot \bar{\bar{h}}_n dx - r_n \int_0^d \bar{\bar{h}}_m \cdot \bar{\bar{h}}_n dx \right) \tag{2.22}$$

$...m = 1, ..., N$

$$\sum_{n=1}^{N} T_n \int_0^a \bar{e}_m \cdot \bar{e}_n dx \quad = \sum_{n=1}^{N} \left(t_n \int_0^d \bar{e}_m \cdot \bar{\bar{e}}_n dx \cdot e^{-\tilde{\gamma}_n \ell} + r_n \int_0^d \bar{e}_m \cdot \bar{\bar{e}}_n dx \cdot e^{\tilde{\gamma}_n \ell} \right) \tag{2.23}$$

$...m = 1, ..., N$

$$\sum_{n=1}^{N} \left(t_n \int_0^d \bar{\bar{h}}_m \cdot \bar{\bar{h}}_n dx \cdot e^{-\tilde{\gamma}_n \ell} - r_n \int_0^d \bar{\bar{h}}_m \cdot \bar{\bar{h}}_n dx \cdot e^{\tilde{\gamma}_n \ell} \right) = \sum_{n=1}^{N} T_n \int_0^d \bar{\bar{h}}_m \cdot \bar{h}_n dx \tag{2.24}$$

$...m = 1, ..., N$

The next step requires getting Eqs. 2.21-2.24 into a form $Ax = b$ where the x vector contains the reflection and transmission coefficients for each of the 4N equations. The following terms are substituted into the 4N equations for simplification:

'A' matrix substitutions

$$A_{mn} = \int_0^a \bar{e}_m \cdot \bar{e}_n dx \qquad E_{mn} = \int_0^d \bar{e}_m \cdot \bar{\bar{e}}_n dx \cdot e^{-\tilde{\gamma}_n \ell}$$

$$B_{mn} = \int_0^d \bar{e}_m \cdot \bar{\bar{e}}_n dx \qquad F_{mn} = \int_0^d \bar{e}_m \cdot \bar{\bar{e}}_n dx \cdot e^{\tilde{\gamma}_n \ell}$$

$$C_{mn} = \int_0^d \bar{\bar{h}}_m \cdot \bar{h}_n dx \qquad G_{mn} = \int_0^d \bar{\bar{h}}_m \cdot \bar{\bar{h}}_n dx \cdot e^{-\tilde{\gamma}_n \ell}$$

$$D_{mn} = \int_0^d \bar{\bar{h}}_m \cdot \bar{\bar{h}}_n dx \qquad H_{mn} = \int_0^d \bar{\bar{h}}_m \cdot \bar{\bar{h}}_n dx \cdot e^{\tilde{\gamma}_n \ell}$$

'b' vector substitutions

$$X_{m1} = \int_0^a \bar{e}_m \cdot \bar{e}_1 dx \qquad Y_{m1} = \int_0^d \bar{\bar{h}}_m \cdot \bar{h}_1 dx$$

After substition and reordering of some of the terms, Eqs. 2.25-2.28 are now in a usable form.

$$\sum_{n=1}^{N} A_{mn}R_n - \sum_{n=1}^{N} B_{mn}r_n - \sum_{n=1}^{N} B_{mn}t_n = -X_{m1} \tag{2.25}$$

$$...m = 1, ..., N$$

$$\sum_{n=1}^{N} C_{mn}R_n - \sum_{n=1}^{N} D_{mn}r_n + \sum_{n=1}^{N} D_{mn}t_n = Y_{m1} \tag{2.26}$$

$$...m = 1, ..., N$$

$$\sum_{n=1}^{N} F_{mn}r_n + \sum_{n=1}^{N} E_{mn}t_n - \sum_{n=1}^{N} A_{mn}T_n = 0 \tag{2.27}$$

$$...m = 1, ..., N$$

$$\sum_{n=1}^{N} H_{mn}r_n - \sum_{n=1}^{N} G_{mn}t_n + \sum_{n=1}^{N} C_{mn}T_n = 0 \tag{2.28}$$

$$...m = 1, ..., N$$

In matrix form the 4N equations look like the matrix equation below where each variable of the A matrix contains NxN values and each variable of the b matrix contains Nx1 values.

$$\begin{bmatrix} A & -B & -B & 0 \\ C & -D & D & 0 \\ 0 & F & E & -A \\ 0 & H & -G & C \end{bmatrix} \begin{bmatrix} R \\ r \\ t \\ T \end{bmatrix} = \begin{bmatrix} -X \\ Y \\ 0 \\ 0 \end{bmatrix}$$

Matlab® is used as a large matrix mathematical solver for the S-parameters. Matlab® uses Gaussian elimination to determine the x vector which contains the S-parameters. S_{11} and S_{21} are found in the 1st row of the x vector and the $3N+1$ row of the x vector as shown in Equation 2.16.

2.1.4 Necessary Equations. In order to solve the matrix equation some additional variables must be defined. The wave number in the x direction is defined by the equations:

$$k_{xm} = \frac{m\pi}{a} \qquad \tilde{k}_{xm} = \frac{m\pi}{d},$$

where a is the width of the waveguide and d is the width of the insert. In the following equations, tilde denotes the changing aperture region between 0 and d and non-tilde functions denote the fully open region between 0 and a $\bar{e}_m$ and $\bar{h}_m$ are representative of the TE_{m0} modes for the fully open aperture region. $\bar{\tilde{e}}_m$ and $\bar{\tilde{h}}_m$are representative of the TE_{m0} modes for the semi-closed aperture region.

$$\bar{e}_m = \hat{y} \cdot \sqrt{\frac{2}{a}} sin(k_{xm}x)$$

$$\bar{\tilde{e}}_m = \hat{y} \cdot \sqrt{\frac{2}{d}} sin(\tilde{k}_{xm}x),$$

$$\bar{h}_m = \frac{\hat{z} \times \bar{e}_m}{Z_{TE_m^z}} = -\hat{x}\frac{1}{Z_{TE_m^z}}\sqrt{\frac{2}{a}} sin(k_{xm}x),$$

$$\bar{\tilde{h}}_m = \frac{\hat{z} \times \bar{e}_m}{\tilde{Z}_{TE_m^z}} = -\hat{x}\frac{1}{\tilde{Z}_{TE_m^z}}\sqrt{\frac{2}{d}}sin(\tilde{k}_{xm}x)$$

The wave impedance is defined by the following equations:

$$Z_{TE_m^z} = \frac{j\omega\mu}{\gamma_{zm}},$$

$$\tilde{Z}_{TE_m^z} = \frac{j\omega\mu}{\tilde{\gamma}_{zm}},$$

where $\omega = 2\pi f$(f = frequency) and $\mu = permeability$ of the material. It is important to determine the wave number k_{zm} to determine the propagation characteristics of this model. Readers may be familiar with the expression $k_{zm} = \sqrt{k^2 - k_{xm}^2 + k_{ym}^2}$ or $\tilde{k}_{zm} = \sqrt{k^2 - \tilde{k}_{xm}^2 + \tilde{k}_{ym}^2}$ with $k_{ym} = 0$ in this case due to y-invariance. The following relation is used because there are two solutions for k_{zm}. A decaying wave is what should be happening in this case but if the solution leads to a +j, a growing wave is actually calculated by $k_{zm} = \sqrt{k_x^2 - k^2}$ where square root denotes the principal square root function.

$$\gamma_m = jk_{zm} = \sqrt{k_x^2 - k^2}$$

For simplification and error analysis, the following normalizes the components of the above matrix:

$$\begin{aligned} A_{mn} = \int_0^a \bar{e}_m \cdot \bar{e}_n dx &= \frac{2}{a}\int_0^a sin(k_{xm}x)sin(k_{xn}x)dx \\ &= \frac{2}{a}\int_0^a sin(\frac{m\pi x}{a})sin(\frac{n\pi x}{a})dx \\ &= \frac{2}{a}\begin{cases} 0 & \text{if } m \neq n; \\ \frac{a}{2} & \text{if } m = n. \end{cases} \end{aligned}$$

This is true because of orthogonality. Therefore,

$$A_{mn} = \delta_{mn} \; and \; X_m = A_{m1} = \delta_{mn}$$

.

$$B_{mn} = \int_0^d \bar{e}_m \cdot \bar{\tilde{e}}_n dx = \frac{2}{\sqrt{ad}} \int_0^d sin(k_{xm}x) sin(\tilde{k}_{xn}x) dx$$
$$= \begin{cases} \frac{2}{\sqrt{ad}} \frac{(-1)^n \tilde{k}_{xn} sin(k_{xm}d)}{(k_{xm}^2 - \tilde{k}_{xn}^2)} & \text{if } k_{xm} \neq \tilde{k}_{xn}; \\ \sqrt{\frac{d}{a}} & \text{if } k_{xm} = \tilde{k}_{xn}. \end{cases}$$

$$C_{mn} = \int_0^d \bar{\tilde{h}}_m \cdot \bar{h}_n dx = \frac{1}{\tilde{Z}_m Z_n} \int_0^d \bar{\tilde{e}}_m \cdot \bar{e}_n dx = \frac{1}{\tilde{Z}_m \tilde{Z}_n} B_{nm}$$
$$= \frac{1}{\tilde{Z}_m Z_n} \begin{cases} \frac{2}{\sqrt{ad}} \frac{(-1)^m \tilde{k}_{xm} sin(k_{xn}d)}{(k_{xn}^2 - \tilde{k}_{xm}^2)} & \text{if } \tilde{k}_{xm} \neq k_{xn}; \\ \sqrt{\frac{d}{a}} & \text{if } \tilde{k}_{xm} = k_{xn}. \end{cases}$$

$$D_{mn} = \int_0^d \bar{\tilde{h}}_m \cdot \bar{\tilde{h}}_n dx = \frac{1}{\tilde{Z}_m \tilde{Z}_n} \int_0^d \bar{\tilde{e}}_m \cdot \bar{\tilde{e}}_n dx$$

$$\text{By orthogonality, } = \frac{1}{\tilde{Z}_m \tilde{Z}_n} \delta_{mn}$$

$$E_{mn} = \int_0^d \bar{e}_m \cdot \bar{\tilde{e}}_n dx \cdot e^{-\tilde{\gamma}_n \ell} = B_{mn} e^{-\tilde{\gamma}_n \ell}$$

$$F_{mn} = \int_0^d \bar{e}_m \cdot \bar{\tilde{e}}_n dx \cdot e^{\tilde{\gamma}_n \ell} = B_{mn} e^{\tilde{\gamma}_n \ell}$$

$$G_{mn} = \int_0^d \bar{\tilde{h}}_m \cdot \bar{\tilde{h}}_n dx \cdot e^{-\tilde{\gamma}_n \ell} = D_{mn} e^{-\tilde{\gamma}_n \ell}$$

$$H_{mn} = \int_0^d \bar{\tilde{h}}_m \cdot \bar{\tilde{h}}_n dx \cdot e^{\tilde{\gamma}_n \ell} = D_{mn} e^{\tilde{\gamma}_n \ell}$$

The Mode Matching Technique determines expected or true values for the S-parameters

of this system. Once true values are established, an uncertainty analysis can be completed to determine if small manufacturing imperfections produce large uncertainties. To increase the confidence in the results of the uncertainty analysis, multiple types of uncertainty analysis will be used.

III. Uncertainty Study

3.1 Uncertainty

The Mode Matching Technique is used as a method to find true values of S-parameters of the inserts being developed. In order to determine if these standards are good standards, it is necessary to determine how small errors in fabrication affect measurement. These small errors determine the uncertainty inherent in the system. First, the term uncertainty must be defined. One definition from Nick Ridler, Brian Lee, Jon Martens, and Ken Wong's paper entitled "Measurement Uncertainty, Traceability, and the GUM" states that uncertainty is "an interval that is likely to contain the "true value" of the quantity being measured" [2].

The term "true value" normally introduces some new problems when talking about measurement. Where does the "true value" come from? Who determines what the "true value" is? What are the assumptions made when deciding on a "true value"? In this thesis when the term "true value" is used, it will be referring to values of S-parameters based on specific d and ℓ values. The term repeatability is often used as a means of indicating "the closeness of agreement between successive results of measurements that are usually made under essentially the same conditions" [2]. This is unhelpful when there are systemic errors that repeatedly give the wrong measurement. Perhaps a better choice of terms would be accurate and precise.

Accuracy will be used to describe the value of the measurement [3]. This is the so-called "true value" or how close to the center of the bulls-eye a measurement is. Precision is a quantitative measure used to describe how close repeated measurements are in proximity to the mean value [4]. The terms "bias", the symbol β, and "variance", the symbol σ^2, are also related to these terms. Bias is the difference between the mean and the true value. In Figure 3.1 the mean is represented by the center of the data points, while the true value is represented by the bulls-eye. Variance describes the spread of the data about the mean. Thus, a small variance indicates precision, while a small variance together with a small bias indicates accuracy[1]. When the mean

[1]Accuracy implies precision, but not conversely.

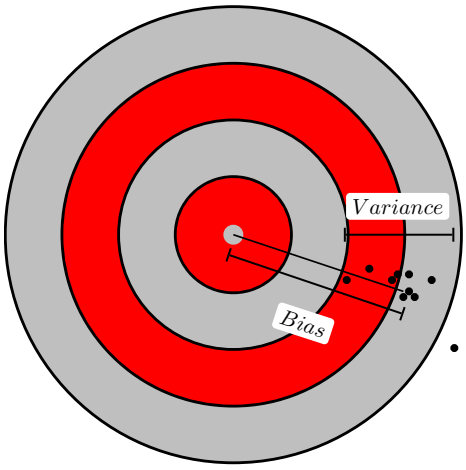

(a) Small Variance, Large Bias
Precise But Not Accurate

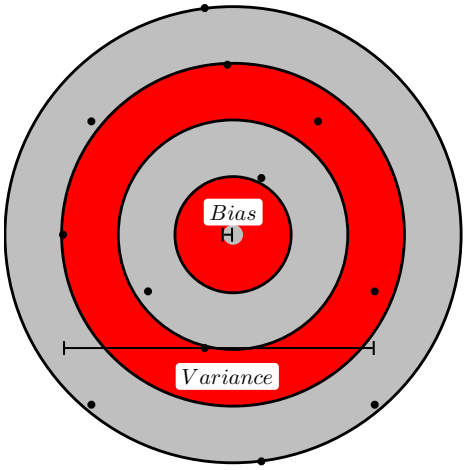

(b) Large Variance, Small Bias
Neither Precise Nor Accurate

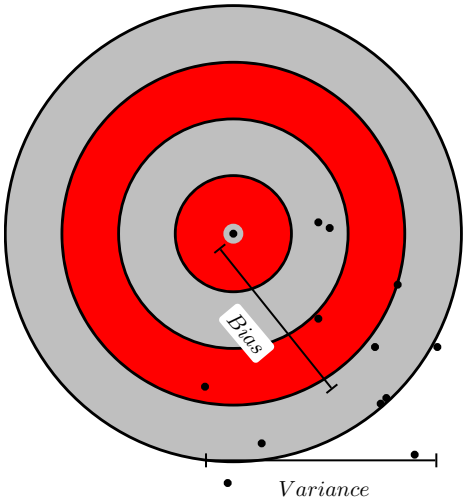

(c) Large Variance, Large Bias
Neither Precise Nor Accurate

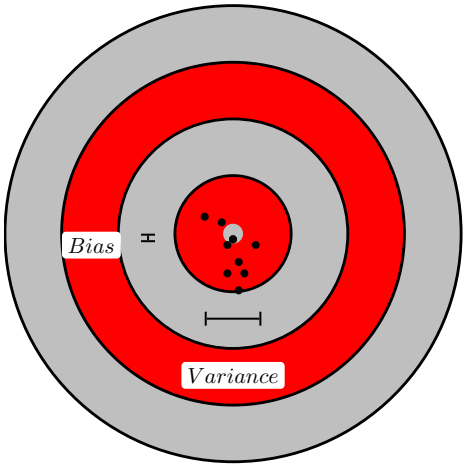

(d) Small Variance, Small Bias
Precise and Accurate

Figure 3.1: Visual Aid to Understanding Variance and Bias

value is closest to the center of the bulls-eye, i.e. the bias is very small, there can still be a large error. This would mean that the distribution is spread out widely over the bulls-eye, i.e. a large variance. It's important to note that it is the combination of these two things that determine the uncertainty. In this thesis, uncertainty will be defined as Root Mean Squared Error (RMSE).

$$U_{RMSE} = \sqrt{\sigma^2 + |\beta|^2}$$

When U_{RMSE} is small, both the β and σ^2 are small, leading to accuracy. The plots included in Chapter IV give RMSE uncertainty as a function of X-band frequencies in magnitude and phase. Magnitude and phase are used as they provide a better physical understanding then real and imaginary plots. There may be multiple points of uncertainty in any system. In this NWA system which uses waveguides to measure electromagnetic characteristics, there are two main parameters[2] of uncertainty:

1) the z-direction thickness of the standard is labeled as the variable ℓ
2) the x-direction width of the insert opening is labeled as the variable d

There are two separate types of uncertainty that will be used in this thesis: component and composite. Component uncertainty determines the uncertainty of each individual parameter (i.e. the d alone or the ℓ alone). Composite uncertainty takes all of the components together and determines the total effect those components have on the uncertainty (i.e. both the d and the ℓ). Three distinct methods of uncertainty analysis are described in this chapter and used to develop an analysis of these standards: Taylor Series, Equal Weight Cubature, and Monte-Carlo.

[2]Review Figure 2.1 for a visual understanding of each parameter of uncertainty

3.2 Taylor Series Method

The Taylor Series (TS) method of uncertainty will be used in this thesis for performing a component analysis of both the d and ℓ parameters. In the following equations taken from Dr. Greg Wilson's Estimation of Material Parameter Uncertainty [4], x is used as a variable for either d or ℓ. For simplicity, S_{11} will be used in most equations for $f(x)$. In the results Chapter IV, S_{21} is also graphed as it also contains easily determined true values. S_{22} and S_{12} could also have been used for this analysis. If S_{11} is chosen and just the d component is used the basic taylor series equation is of the form:

$$S_{11}(d+\Delta d) \approx S_{11}(d) + \frac{\delta S_{11}}{\delta d}\Delta d + \frac{\delta^2 S_{11}}{\delta d^2}\frac{\Delta d^2}{2!} + \frac{\delta^3 S_{11}}{\delta d^3}\frac{\Delta d^3}{3!} + ...$$

Therefore,

$$S_{11}(d+\Delta d) - S_{11}(d) \approx \Delta S_{11} \approx \sum_{k=1}^{K} \frac{\delta^k S_{11}}{\delta d^k}\frac{\Delta d^k}{k!}$$

The bias and variance are determined from the following equations from Dr. Wilson's manuscript [4]:

$$\begin{aligned}
&\beta_{\hat{x}} = \langle \Delta x \rangle = \langle \hat{x} \rangle - x, \\
&\beta_y = \langle \Delta y \rangle = \langle \hat{y} \rangle - y, \\
&\Delta x \equiv \hat{x} - x \\
&Var(\Delta x) = \sigma_x^2 = \langle |\hat{x}|^2 \rangle - |\langle \hat{x} \rangle|^2, \\
&Var(\Delta y) = \sigma_y^2 = \langle |\hat{y}|^2 \rangle - |\langle \hat{y} \rangle|^2,
\end{aligned}$$

where $\hat{x}$ is a Random Variable (RV) estimate of x and x is a true value which is constant and denotes the expected value (mean) of the RV Δx. In this case x is either d or ℓ. S_{11} has been inserted to substitute for the variable y for clarity but

could also be S_{21}:

$$\beta_{S_{11}} = \langle \Delta S_{11} \rangle = \langle \hat{S}_{11} \rangle - S_{11},$$
$$Var(\Delta S_{11}) = \sigma^2_{\hat{S}_{11}} = \langle |\hat{S}_{11}|^2 \rangle - |\langle \hat{S}_{11} \rangle|^2,$$

where $\hat{S}_{11}$ is a RV estimate or the average distribution around the mean and S_{11} is a true value constant from the MMT of Chapter II. Here is a reiteration of the RMSE equations with S_{11} inserted for y:

$$U_{RMSE} = \sqrt{|\beta_{S_{11}}|^2 + Var(\Delta S_{11})} \tag{3.1}$$

Considering $S_{11} = f(x)$, where x represents the variables of d and ℓ and i, j, and k represent the order of the partial derivative. Derivation of the following equations for bias and variance can be found in Appendix A of this thesis.

$$\beta_{S_{11}} \approx \beta_0 + \sum_{k=1}^{K} \frac{f^{(k)}(x)}{k!} \langle (\Delta x)^k \rangle, \tag{3.2}$$

$$Var(\Delta S_{11}) \approx \sum_{i=1}^{K} \sum_{j=1}^{K} \frac{f^{(i)}(x)}{i!} \left(\frac{f^{(j)}(x)}{j!} \right)^* Cov[(\Delta x)^i, (\Delta x)^j], \tag{3.3}$$

where $\Delta x = \hat{x} - x$, $x \in \{d, \ell\}$, $\hat{x} \in \{\hat{d}, \hat{\ell}\}$, and K is a positive integer. In this case β_0 or initial bias is equal to zero because there is no bias due to the determination of S_{11} whenever $\Delta d = \Delta \ell = 0$. [4] Equations for the the individual moments for each parameter of uncertainty and covariance necessary to determine bias and variance are:

$$\langle \Delta x^k \rangle = \frac{1}{k+1} \sum_{i=0}^{k} a^i b^{k-i} \quad (\text{assuming } \Delta x \sim U[a,b])$$
$$Cov((\Delta x)^i, (\Delta x)^j) = \langle (\Delta x)^i (\Delta x)^j \rangle - \langle (\Delta x)^i \rangle \langle (\Delta x)^j \rangle \tag{3.4}$$

The following equations are the first four partials for the S-parameters which are necessary to find the bias and variance of the first four moments. The derivative with respect to d is shown below but the derivative with respect to ℓ can be found in the same manner. The Taylor Series, Monte-Carlo and Equal Weight Cubature methods are compared in the next chapter. In this thesis, the Taylor Series method is restricted to component analysis. Its complexity lends itself to various errors in finding partial derivatives which are increased greatly using a composite analysis. The Equal Weight Cubature and Monte-Carlo method apply to both component and composite uncertainty. Once all the uncertainty estimation methods are validated against each other under the component analysis, the Equal Weight Cubature and Monte-Carlo methods can be used with confidence for a composite analysis. In order to solve the MMT from Chapter II, consider the equation $Ax = b$. The 'A' matrix and the 'b' vector contain known constant values. The following equations will be used to solve for the unknown 'x' vector which contain the terms used to solve for the

bias and variance of the S-parameters.

$$\frac{\delta \bar{x}}{\delta d} = A^{-1}\left[\frac{\delta b}{\delta d} - \frac{\delta A}{\delta d}\bar{x}\right]$$

$$\frac{\delta^2 \bar{x}}{\delta d^2} = A^{-1}\left[\frac{\delta^2 b}{\delta d^2} - \frac{\delta^2 A}{\delta d^2}\bar{x} - 2\frac{\delta A}{\delta d}\frac{\delta \bar{x}}{\delta d}\right]$$

$$\frac{\delta^3 \bar{x}}{\delta d^3} = A^{-1}\left[\frac{\delta^3 b}{\delta d^3} - \frac{\delta^3 A}{\delta d^3}\bar{x} - 3\frac{\delta^2 A}{\delta d^2}\frac{\delta \bar{x}}{\delta d} - 3\frac{\delta A}{\delta d}\frac{\delta^2 \bar{x}}{\delta d^2}\right]$$

$$\frac{\delta^4 \bar{x}}{\delta d^4} = A^{-1}\left[\frac{\delta^4 b}{\delta d^4} - \frac{\delta^4 A}{\delta d^4}\bar{x} - 4\frac{\delta^3 A}{\delta d^3}\frac{\delta \bar{x}}{\delta d} - 6\frac{\delta^2 A}{\delta d^2}\frac{\delta^2 \bar{x}}{\delta d^2} - 4\frac{\delta A}{\delta d}\frac{\delta^3 \bar{x}}{\delta d^3}\right]$$

The partial derivatives for each part of this matrix equation will be determined analytically in Chapter IV using `Matlab`® 's symbolic toolbox and Wolfram's *Mathematica*® 7. They were also determined numerically to check computer coding. The Taylor Series is the most complicated method of the three methods considered, and much of the effort was spent error checking the partial derivatives, particularly those related to the higher orders, K = 3 and 4, appearing in equations 3.2-3.3.

Advantages:

1) Can increase K until convergence is achieved, resulting in high confidence that the Taylor Series is being evaluated inside its region of convergence.

2) Analytic process that can be checked with multiple methods

3) Component analysis runs somewhat quickly once all partial derivatives are determined

Disadvantages:

1) Somewhat difficult to program and check derivatives

2) Easy to make typographical errors when filling in multiple partial derivative matrices

3) Composite analysis partials adds greatly to already complicated equations

4) Mixed partials required for composite analysis appear in complicated analogs of equations 3.2-3.3

This method is helpful because it results in high confidence when convergence is shown. The biggest problem is that this method requires a great deal of detailed calculations to perform. It may be most effective using component analysis as a means of giving confidence to a simpler method of uncertainty analysis such as Equal Weight Cubature.

3.3 Equal Weight Cubature

Equal Weight Cubature (EWC) is a method of uncertainty that uses a Weighting function to help solve the functions S_{11} and S_{21} between the values of a and b which are the minimum and maximum Δd and $\Delta \ell$. Between these minimum and maximum values if the function behaves like a 3rd order polynomial or less, Equal Weight Cubature will give exact values for the uncertainty of S_{11} and S_{21}. Outside of this area, the function is given a weight of zero. For these cases, EWC gives an equal weight to each value over the function from a to b and then sums the parts as a means of integration. Higher order polynomials may produce poor results which is why another method such as Taylor Series must be used to determine the utility of EWC. The Probability Density Function of x (PDF(x)) is exactly zero outside of the uniform distribution from a to b. Using the following equations, the bias and variance can be determined.

$$W(x) = PDF(x) = \begin{cases} \frac{1}{b-a} & a < x < b; \\ 0 & \text{if } elsewhere. \end{cases}, \tag{3.5}$$

$$\langle \hat{S}_{11} \rangle = \int_D S_{11}(x) W(x) dx, \tag{3.6}$$

$$\langle |\hat{S}_{11}|^2 \rangle = \int_D |S_{11}(x)|^2 W(x) dx, \tag{3.7}$$

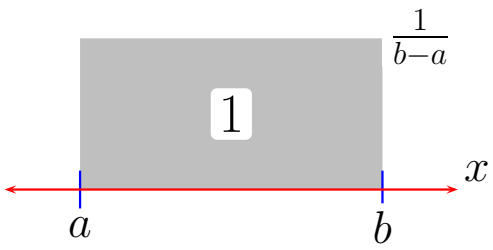

Figure 3.2: Weighting Function Illustration

where x can be substituted for either d or ℓ, $\hat{S}_{11}$ is a RV estimate and S_{11} is a constant true value from the MMT of Chapter II, and D is the support of W(i.e. $D = [a, b]$). Inserting $\langle \hat{S}_{11} \rangle$ into the β equation and $\langle |\hat{S}_{11}|^2 \rangle$ into the σ^2 equation and then inserting into U_{RMSE} gives the solution for EWC uncertainty. [4]

$$\beta_{S_{11}} = \langle \Delta S_{11} \rangle = \langle \Delta \hat{S}_{11} \rangle - S_{11}, \tag{3.8}$$

$$\sigma^2_{\hat{S}_{11}} = \langle |\hat{S}_{11}|^2 \rangle - |\langle \hat{S}_{11} \rangle|^2, \tag{3.9}$$

$$U_{RMSE}(\hat{S}_{11}) = \sqrt{\sigma^2_{\hat{S}_{11}} + |\beta_{S_{11}}|^2} \tag{3.10}$$

Advantages:

1) Better accuracy with far fewer function evaluations than Monte-Carlo Method

2) Does not require partial derivatives

3) Component and Composite analysis runs quickly

Disadvantages:

1) Cannot use alone for uncertainty analysis (must verify using other methods)

2) May not produce accurate results if f is not well approximated by a cubic within the interval [a,b].

EWC computes very quickly for both component and composite analysis. Once

Taylor Series and Equal Weight Cubature methods validate one another for a component analysis, a composite analysis can be performed. The Monte-Carlo method is an excellent method for producing accurate results and will be used to validate the EWC composite results.

3.4 Monte-Carlo Method

The Monte-Carlo method is a method of uncertainty analysis "coined by S. Ulam and Nicholas Metropolis in reference to games of chance, a popular attraction in Monte-Carlo, Monaco." according to a website on "Monte-Carlo Simulation Basics" [5]. Equations taken from Greg Wilson's paper [4] are used to find the Root Mean Squared Uncertainty using the Monte-Carlo method. It is an effective tool for validating faster methods. For results in Chapter IV, the `Matlab`® 's random number generator was used. `Matlab`® 's random number generator uses a uniform distribution to produce the pseudorandom numbers. The method 'twister' was used for this analysis which is the default setting. The Monte-Carlo method evaluates the RMSE uncertainty using the following equations:

$$
\begin{aligned}
&\Delta\hat{S}_{11}(i) = \hat{S}_{11}(i) - S_{11},\\
&\beta_{S_{11}} = \langle \Delta S_{11}(i) \rangle = \langle \hat{S}_{11}(i) - S_{11}, \rangle\\
&Var(\Delta S_{11}) = \langle |\hat{S}_{11}(i) - S_{11}|^2 \rangle - |\langle |\hat{S}_{11}(i) - S_{11}, \rangle|^2\\
&U_{RMSE} = \sqrt{|\beta_{S_{11}}|^2 + Var(\Delta S_{11}(i))},\\
&= \sqrt{|\langle \hat{S}_{11}(i) - S_{11} \rangle|^2 + \langle |\hat{S}_{11}(i) - S_{11}|^2 \rangle - |\langle |\hat{S}_{11}(i) - S_{11} \rangle|^2},\\
&= \sqrt{\langle |\hat{S}_{11}(i) - S_{11}|^2 \rangle} \approx \sqrt{\frac{1}{N}\sum_{i=1}^{N} |\hat{S}_{11}(i) - S_{11}|^2}
\end{aligned}
$$

Therefore,

$$U_{RMSE} \approx \sqrt{\frac{1}{N}\sum_{i=1}^{N} |\hat{S}_{11}(i) - S_{11}|^2} \tag{3.11}$$

where N is chosen large enough to meet a prescribed convergence tolerance, $\hat{S}_{11}$(i) is

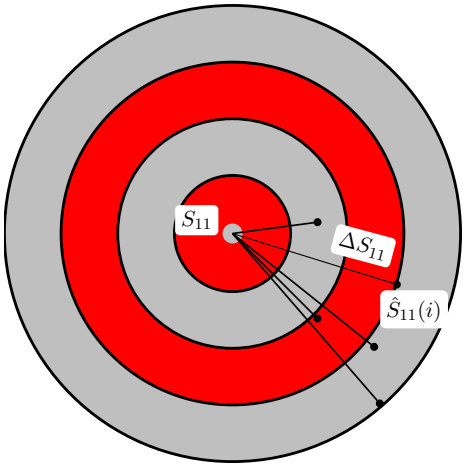

Figure 3.3: Monte-Carlo Illustration

an estimate of S_{11} corresponding to a pseudo random number representing $\hat{\ell}$ (or $\hat{d}$). Where $\hat{\ell} = \ell + \Delta\ell$ and $\hat{d} = d + \Delta d$. Returning to the bulls-eye demonstration from earlier in the chapter helps somewhat with understanding the Monte-Carlo method. Each data point is a value of $\hat{S}_{11}$(i) up to $i = N$ and the center of the bulls-eye is the true value of S_{11}. The distance between these data points is the vector ΔS_{11}. In this case pseudo random numbers are generated to produce a pair of slightly varying $\hat{\ell}$ and $\hat{d}$ components which are the values of $\hat{S}_{11}(i)$.

Advantages:

1) Any random distribution may be used

2) Can analyze multiple sources of uncertainty

3) Simple to understand and develop

4) `Matlab`® contains a built in Random Number Generator for both Normal and Uniform distributions.

5) Excellent tool for validation of faster methods.

Disadvantages:

1) Often takes many thousands of function evaluations before convergence takes place

2) Is particularly impractical whenever f is costly (in terms of execution time).

This method is the simplest of methods, but takes such a great amount of time to compute that it is only useful as a validation method for faster methods like EWC. The next chapter will show each of these methods performed in relation to producing RMSE uncertainty values. It's important to note that if these methods produce similar results, a good amount of confidence is gained that the values of uncertainty are correct. This does not necessarily mean that the standards are good standards. If there is a high amount of uncertainty when manufacturing errors occur this standard is not a good standard. As stated in Chapter **??**, the purpose of this thesis is to determine a standard that can be used from laboratory to laboratory while minimizing the uncertainty related to fabrication of the standards.

IV. Results

4.1 Number of Modes Determination

The Mode Matching Technique used in the theory from Chapter II leaves us with 4N equations and 4N unknowns. The true value of S_{11} and S_{21} require a determination of the number of modes to incorporate. A greater number of modes increases the accuracy of the S-parameter values by reducing truncation error, but increases the computation time. For the the true values it increased runtime from an order of seconds for a single mode to several minutes for a hundred modes. An uncertainty analysis for Taylor Series took around 40 minutes for a hundred modes. If computation time is cost prohibitive, it is important to find a good stopping point so that the methods that require a much larger computation time such as Monte-Carlo are still able to be used to verify results. Appendix D shows an excel file that was used to identify a "slowly varying" point for each value of d. When the data stops varying for 3 significant figures for up to 10 modes, the data was highlighted. This was checked for several frequencies in the X-band and for modes up to 100. This becomes somewhat of a subjective determination. Certainly more modes and a more strict determination of "slowly varying" can be used in further study of these waveguide standards but for the purpose of practicality 35 modes were selected. The following figures are an example of the graphs used in determination of a good stopping point for the amount of modes used.

Shown in Figure 4.1 and 4.2 are mode increases for the real parts of S_{11} . An excel file is included in Appendix D that marks the place where each value of S_{11} becomes slowly varying. At $d = .15in$ and $d = .90in$ the point of slow variance was almost instantaneous while the slowest values to converge were $d = .45in$ and $d = .6in$.

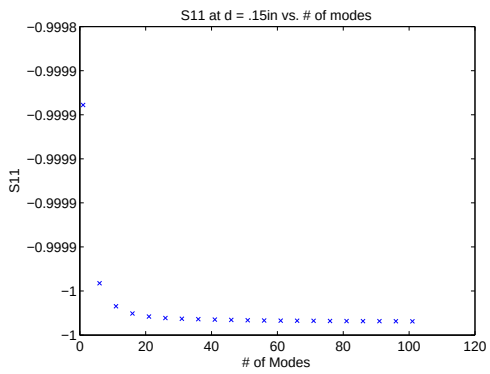

(a) d = 0.15in

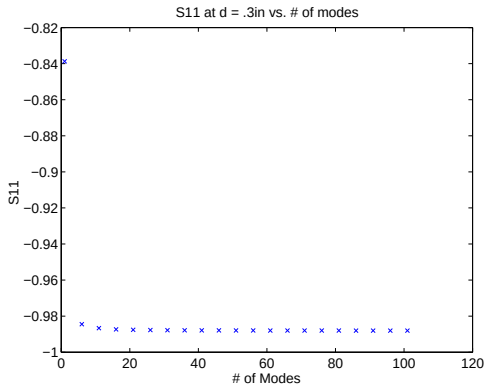

(b) d = 0.30in

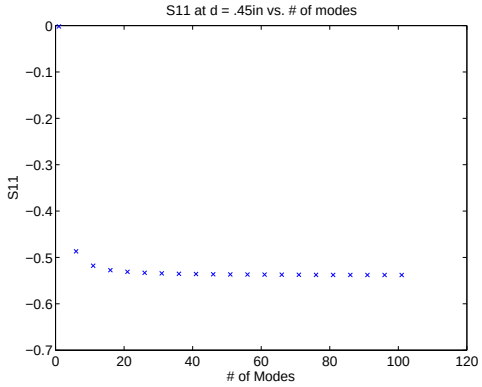

(c) d = 0.45in

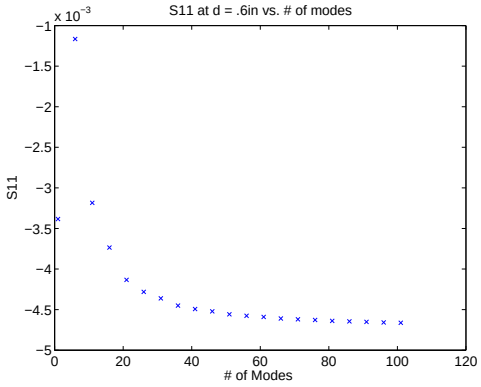

(d) d = 0.60in

Figure 4.1: First 4 $'d'$ widths with increasing mode inclusion with respect to real S_{11}

Now that there is a determination of the number of modes, 201 data points can be used to model the S-parameters between a fully open waveguide and a fully closed one. 201 data points were selected because the default setting of Network Analyzers is 201 and this can be used to ensure stability of the system. The uncertainty analysis however, will often use 20 points for speed of computation and for clearer understanding of figures.

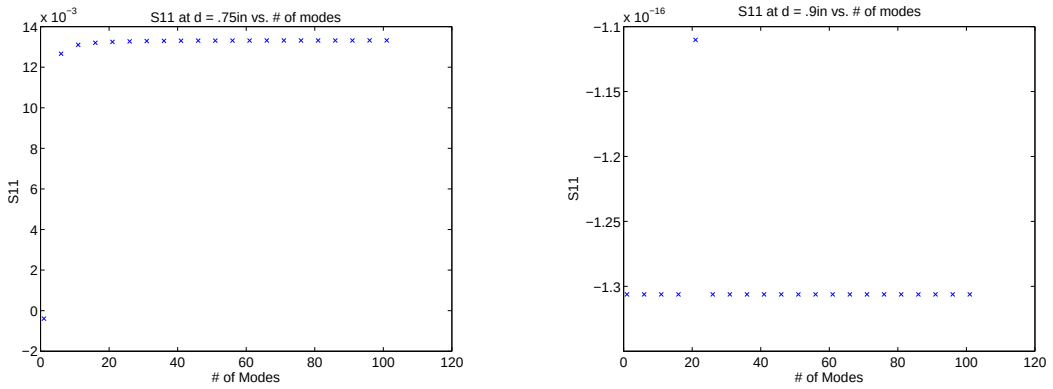

(a) d = 0.75in (b) d = 0.90in

Figure 4.2: Last 2 d widths with increasing mode inclusion with respect to real S_{11}

4.2 Multiple Frequency

S-parameter variance is shown in this section as a function of frequency. As stated in the previous section, the number of data points selected was 20. This study includes only X-band waveguides so the frequency band used was 8.2GHz to 12.4GHz.

True values of each of the six insert standards for S_{11} and S_{21} from Figure 4.2 were produced using the MMT as stated in Chapter II. These values are shown in values of magnitude and phase because in this case there is no need to worry about confusion in the phase as there is only one cycle to worry about. Real and imaginary parts would normally be used to avoid that confusion caused by the cyclic nature of phase. If the cyclic nature of phase was a problem, the phase would be very sporadic in nature. As the following graphs will show only the $d = .90in$ case for S_{11} is sporadic. The reason this happens is because the magnitude goes to zero and in that case the phase has very little meaning. Using magnitude and phase allows for a better physical understanding. As d increases and the waveguide begins to open up it can be shown as expected that S_{11} decreases and S_{21} increases. It can also be shown that as frequency increases, $|S_{11}|$ decreases and $|S_{21}|$ increases. The dominant mode of this waveguide is the TE_{m0} mode because it is the mode with the lowest cutoff frequency

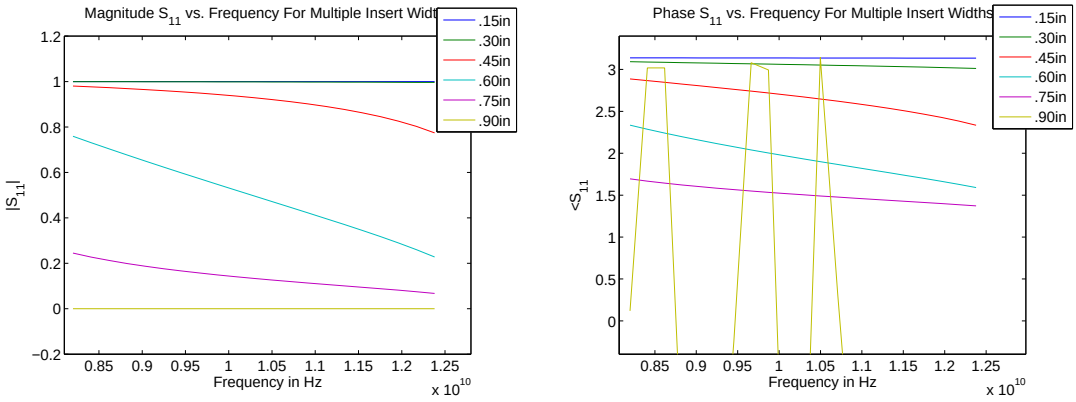

(a) Magnitude of S_{11}

(b) Phase of S_{11}

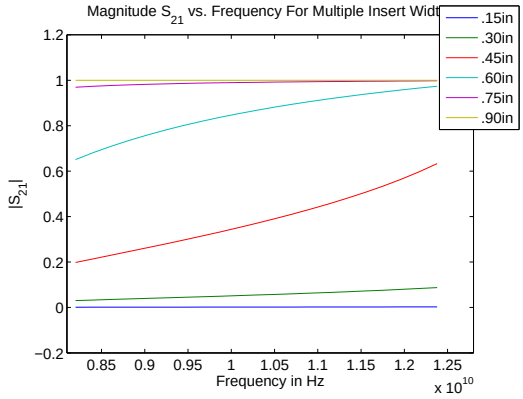

(c) Magnitude of S_{21}

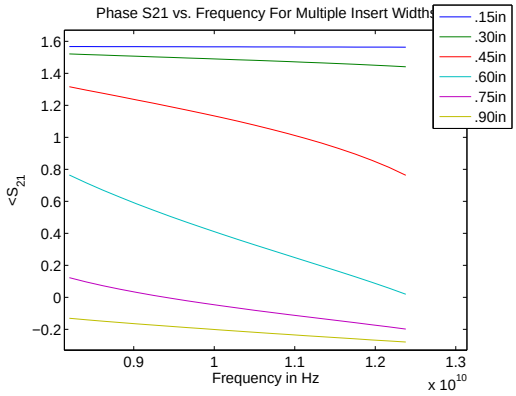

(d) Phase of S_{21}

Figure 4.3: Magnitude and Phase of S-Parameters for 35 Modes and 201 Data Points

for this geometry. Therefore,

$$k_z^2 = k_0^2 - k_c^2,$$
$$k_c^2 = k_x^2 + k_y^2 = (\frac{m\pi}{a})^2 + (\frac{n\pi}{b})^2,$$
$$n = 0, \text{therefore } \; k_c^2 = k_x^2,$$

It follows then that,

$$
\begin{aligned}
k_z &= \sqrt{k_0^2 - k_c^2} \\
k_c &= w_{co}\sqrt{\epsilon_0\mu_0} = \frac{m\pi}{d}, \text{ where } w_{co} \text{ is the angular cutoff frequency} \\
k_0 &= w_{op}\sqrt{\epsilon_0\mu_0}, \text{ where } w_{op} \text{ is the angular operating frequency} \\
k_z &= k_0\sqrt{1 - (\frac{k_c}{k_0})^2} \\
&= k_0\sqrt{1 - (\frac{f_c}{f_0})^2} \\
f_c &= \frac{mc}{2d}
\end{aligned}
$$

While f_{op} is greater than f_{co}, the wave continues to propagate through the waveguide insert opening. When f_{op} falls below f_{co}, the operating frequency is in the evanescent range meaning that the wave decays exponentially by distance through the waveguide insert. The greater the width of ℓ, the smaller the value of S_{21} through the waveguide opening in the evanescent modes. When fully closed S_{21} has a value of close to zero but in this case the MMT equations break down at $d = 0$. The first standard value will be $d = .15$ which is close to a fully closed waveguide. As d begins to open, Fig. 4.4a shows the values of S_{11} decreasing and Fig 4.4b shows values of S_{21} increasing. When d is fully open, S_{11} has a magnitude of almost zero. This makes phase values very difficult to validate and true values are mostly trivial. Magnitude values of S_{21} grow to $+1$ with a phase of approximately zero.

Just to ensure that conservation of energy is being maintained, Figure 4.5 shows all values of d maintain the equation:

$$|S_{11}|^2 + |S_{21}|^2 = 1$$

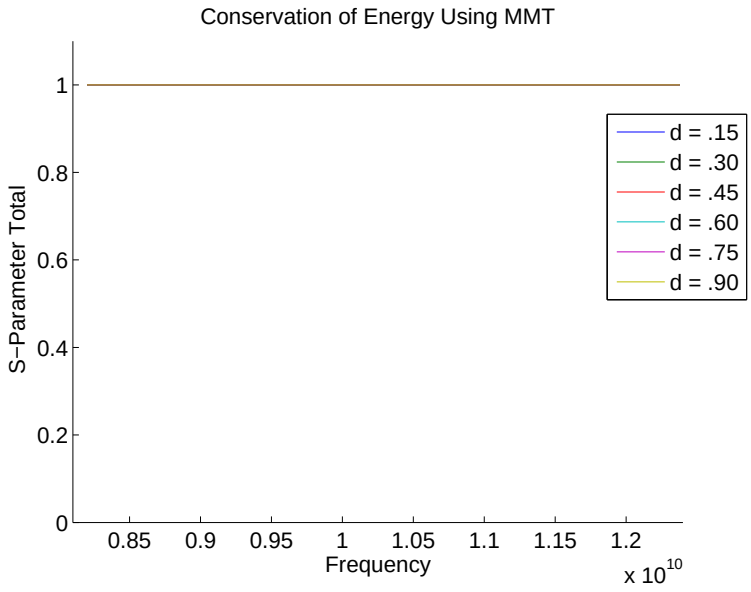

Figure 4.4: Conservation of Energy is Maintained For All Values of d

This is only true if the waveguide is considered a PEC and vacuum filled. Otherwise the equation would be $<$ rather than $=$ as there would be some loss in the system. Because this is the ideal case, all values of the waveguide from open to closed fall exactly on top of one another.

The next part of this analysis, uncertainty, will be determined using the true values as a baseline. If uncertainty can be modeled "accurately", a determination can be made as to whether this is a good standard to use. One of the purposes of this uncertainty analysis is to determine which of the two parameters of uncertainty have a greater impact on the values obtained for the S-parameters. This will determine if one or both of the parameters will need to have a tighter tolerance when being machined.

4.3 Taylor Series and Equal Weight Cubature Component Uncertainty Results

This section highlights the component analysis done using the Taylor Series Method and Equal Weight Cubature Methods described in Chapter III. Each of the two parameters of uncertainty, d and ℓ were done separately as a component analysis. Once it's determined that results for Taylor Series and Equal Weight Cubature model each other accurately, a combined analysis using Equal Weight Cubature and the Monte-Carlo technique will be used to measure the total uncertainty of the two variables d and ℓ. A loose tolerance was used for d and ℓ at a value of $0.01in$ for all measurements unless explicitly stated. These values were chosen as loose tolerance even though the fabrication shop was able to make actual tolerances of about $0.001in$ because at the tight tolerance of $0.001in$, uncertainty values were almost imperceptable as will be shown in the last part of this chapter.

4.3.1 Component d. This section includes the component uncertainty analysis for component d for a Taylor Series and Equal Weight Cubature analysis. They are shown side by side to demonstrate the continuity between the two methods. The dimensions of the X-band waveguide are such that the TE_{10} is the dominant mode. This means that the first mode is the only mode that propagates. All other modes are evanescing. While evanescing modes still add somewhat to the magnitude, phase values do not change. When discussing the following figures, consider that cutoff frequencies of the 2nd mode tend to be much higher than the operating frequencies of the X-band waveguide. The largest uncertainty occurs for a magnitude of approximately ± 0.025 for S_{11} and approximately ± 0.03 for S_{21} at $d = .45in$ and for the phase S_{11} was approximately $\pm 0.0425rad$ and approximately $\pm 0.04rad$ for S_{21}. All the largest values of uncertainty occurred as expected when approaching cutoff frequency.

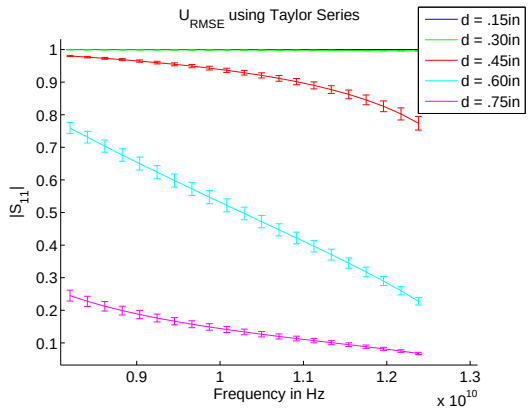

(a) $|S_{11}|$ Taylor Series RMSE Uncertainty Component d

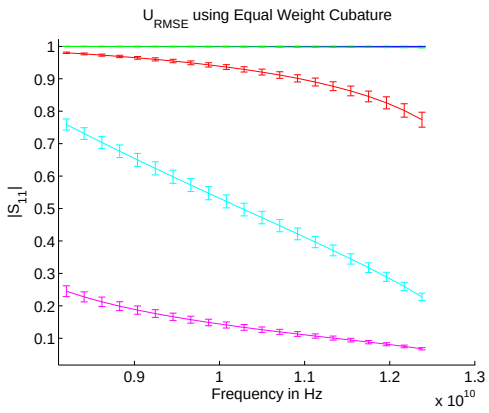

(b) $|S_{11}|$ Equal Weight Cubature RMSE Uncertainty Component d

Figure 4.5: $|S_{11}|$ Component d EWC vs. Taylor Series

For the component analysis above, when $d = .15in,\ .30in$, the cutoff frequency of the first mode is so high that small changes in d do not bring the mode out of evanescence. At $d = .45in$ it can be seen that the higher frequencies approach the cutoff frequency increasing the amount of energy that propagates. This makes little changes important to d at these frequencies. For $d = .60in,\ .75in$, the lower frequencies remain in evanescence and small changes to d effect the amount of energy decaying in the waveguide insert. Once it passes the cutoff frequencies of 9.84GHz and 7.87GHz for $d = .60in$ and $d = .75in$ respectively, the waves are now propagating.

With the phase of S_{11}, when $d = .15in,\ .30in$, the cutoff frequency of the first

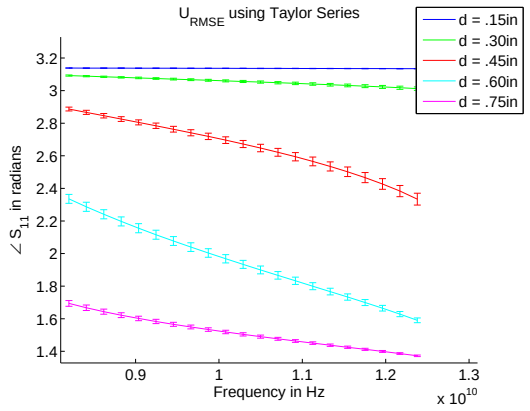

(a) $\angle S_{11}$ Taylor Series RMSE Uncertainty Component d

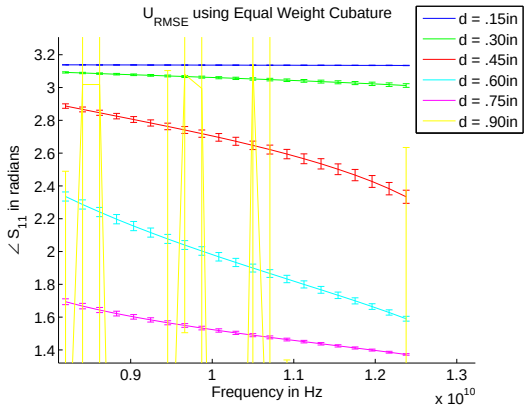

(b) $\angle S_{11}$ Equal Weight Cubature RMSE Uncertainty Component d

Figure 4.6: $\angle S_{11}$ Component d EWC vs. Taylor Series

mode is so high that small changes in d do not bring the mode out of evanescence. This means there is very little additional interaction caused by reflections within the waveguide insert as the waves are decaying. At $d = .45in$ it can be seen that the higher frequencies approach the cutoff frequency. This means that little changes to d will cause more reflections within the insert which will in turn add or subtract phase from S_{11}. For $d = .60in$, $.75in$, the lower frequencies remain in evanescence and small changes to d effect the amount of energy decaying in the waveguide insert and in turn effect reflected waves that will interact with those in the first region. Once it passes the cutoff frequencies of 9.84GHz and 7.87GHz for $d = .60in$ and $d = .75in$ respectively, the waves are now propagating. Closer to the cutoff frequency, slight changes in d effect where the cutoff frequency happens and therefore effect the change in phase. As d grows to $.9in$, the magnitude of S_{11} decreases to zero as there is nothing to reflect the wave back to the source. This leads to a problem with phase. Without any magnitude, phase becomes a meaningless quantity and very sporadic. Results in this case were so large and irrational that they were left off of the Taylor Series figure and somewhat cropped out of the EWC figure.

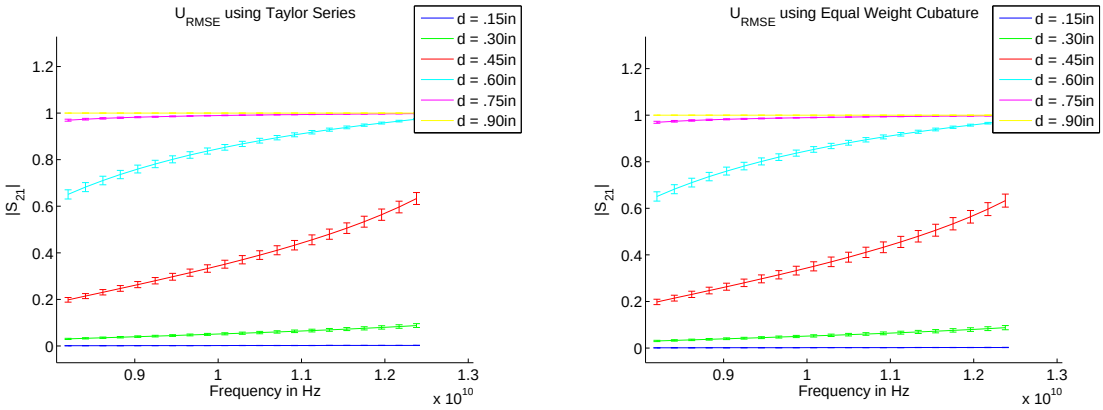

(a) $|S_{21}|$ Taylor Series RMSE Uncertainty Component d

(b) $|S_{21}|$ Equal Weight Cubature RMSE Uncertainty Component d

Figure 4.7: $|S_{21}|$ Component d EWC vs. Taylor Series

With the case of S_{21}, which is the energy that travels to port 2, the $d = .15in$ case has a cutoff frequency that is so high that small changes in d do not bring the mode out of evanescence. While in evanescence, the further the operating frequency is from cutoff, the more decay happens in the waveguide. Physically this begins to look like a short and in this case equates to almost exactly zero magnitude. For $d = .30in$, the waveguide is now slightly open. The cutoff frequency is not as high and at higher frequencies, some energy propagates through. The uncertainty is still very small because changing the d by a small amount does not change the cutoff frequency enough. At $d = .45in$ the higher frequencies begin to approach the cutoff frequency and the amount of energy that propagates through is increased. This makes little changes to d important as it brings the cutoff frequency closer or further away. For $d = .60in$, the lower frequencies remain in evanescence and small changes to d effect the amount of energy decaying in the waveguide insert a larger amount. Once in propagation changes to d effect the uncertainty only slightly. At $d = .75in$, all frequencies are in propagation but as it approaches cutoff frequency at the lower operating frequencies, uncertainty begins to be perceivable. As expected, the $d = .90in$ case is a fully open

waveguide and all frequencies are fully propagating.

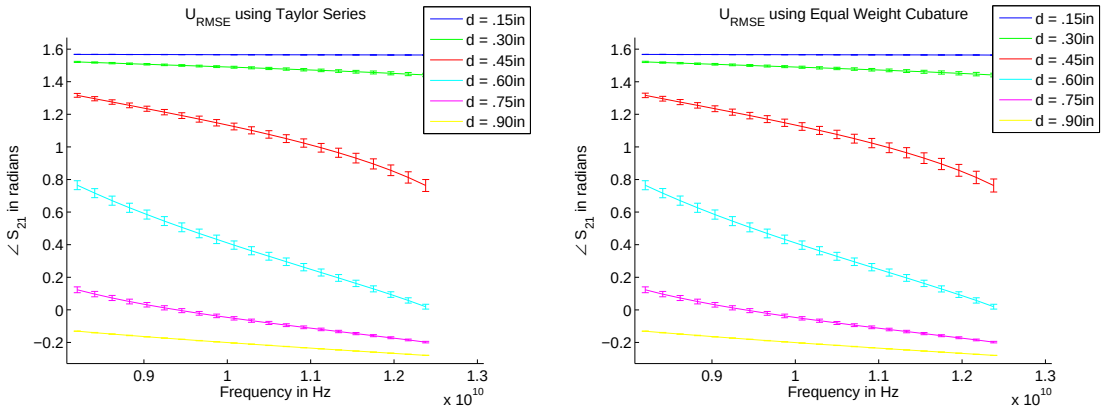

(a) $\angle S_{21}$ Taylor Series RMSE Uncertainty Component d

(b) $\angle S_{21}$ Equal Weight Cubature RMSE Uncertainty Component d

Figure 4.8: $\angle S_{21}$ Component d EWC vs. Taylor Series

For the phase of S_{21} the $d = .15in$ case has a cutoff frequency that is so high that small changes in d do not bring the mode out of evanescence. The magnitude is very close to zero, so the phase is almost meaningless. It is so far from the cutoff frequency that changes to d do not effect the decay of the wave. Waves in evanescence do not have a phase because they are decaying exponentially. However, these waves still have a magnitude that will interact with other modes. For $d = .30in$, the waveguide is now slightly open. The operating frequencies are now a little closer to the cutoff frequency and some energy propagates through. The uncertainty is still very small because changing the d by a small amount does not change the cutoff frequency enough to bring it out of evanescence. At $d = .45in$ the higher frequencies begin to approach the cutoff frequency and the amount of energy that propagates through is increased. This means that reflections within the insert have greater impact on the phase. For $d = .60in$, the lower frequencies remain in evanescence and small changes to d effect the amount of energy decaying in the waveguide insert a larger amount, thus affecting the interactions of phase. In propagation, frequencies closer to cutoff are more sensitive to changes in d as it effects whether reflections in the insert have enough energy to interact. At $d = .75in$, all frequencies are in propagation but as

it approaches cutoff frequency at the lower operating frequencies, uncertainty in d begins again to determine if reflections impact the phase. As expected, the $d = .90in$ case is a fully open waveguide and all frequencies are fully propagating. Small changes to d do not change the cutoff frequency enough to pull the operating frequencies out of propagation which is why there is almost zero uncertainty.

4.3.2 Component ℓ. This section includes the component uncertainty analysis for component ℓ for a Taylor Series and Equal Weight Cubature analysis. Similar to the d component, uncertainties are dependent on both the values of d and frequency. When values of d for particular frequencies are in evanescence, wider values of ℓ allow less energy to travel into Region III. This is because waves in evanescence decay exponentially as a function of distance. The largest uncertainty occurs for a magnitude of approximately ± 0.01 for S_{11} and approximately ± 0.01 for S_{21} at $d = .45in$ and for the phase S_{11} was approximately $\pm 0.03rad$ and approximately $\pm 0.035rad$ for S_{21}. All the largest values of uncertainty occurred as expected when approaching cutoff frequency.

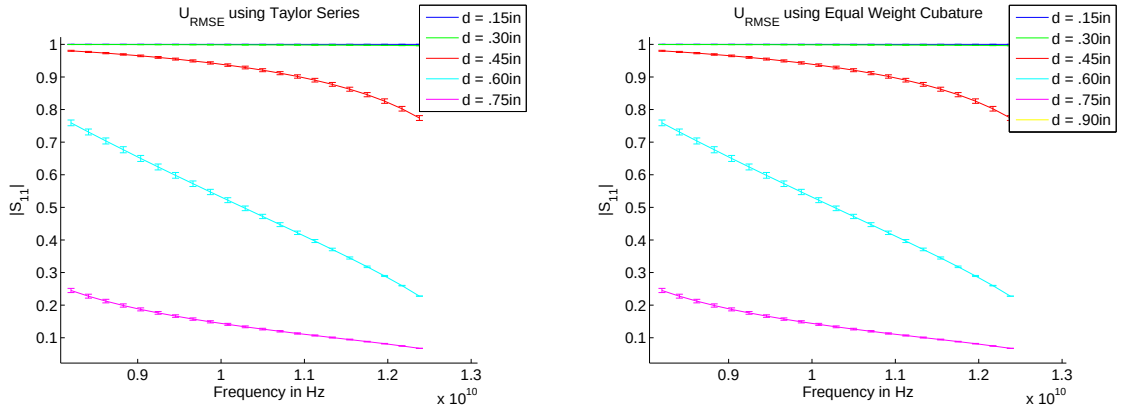

(a) $|S_{11}|$ Taylor Series RMSE Uncertainty Component ℓ

(b) $|S_{11}|$ Equal Weight Cubature RMSE Uncertainty Component ℓ

Figure 4.9: $|S_{11}|$ Component ℓ EWC vs. Taylor Series

Values in this case are much more difficult to evaluate as the uncertainties of the ℓ component are much smaller than those of the d component. However, the trends are very similar to those of the case of d. At $d = .15in$, $.30in$, the cutoff frequency is relatively high. This means that these values will always be in evanescence. The distance from the cutoff frequency means that there will be rapid decay whether ℓ is short or long. The figures show that small changes in ℓ do not have significant effects. At $d = .45in$ it can be seen that the higher frequencies are beginning to approach the cutoff frequency increasing the amount of energy that propagates. Small changes to ℓ begin to effect the energy that propagates but are still relatively small. For $d = .60in$,

the lower frequencies remain in evanescence. In this case small changes to ℓ effect the amount of energy decaying in the waveguide insert. The amount that the wave decays is a function of distance traveled and reflections that occur further decay the wave. Once it passes the cutoff frequencies of 9.84GHz and 7.87GHz for $d = .60in$ and $d = .75in$ respectively, the waves are now propagating. The closer the operating frequency is to the cutoff frequency, the more changes in ℓ effect the value of S_{11}. This occurs because small changes in ℓ effect how rapidly the wave decays.

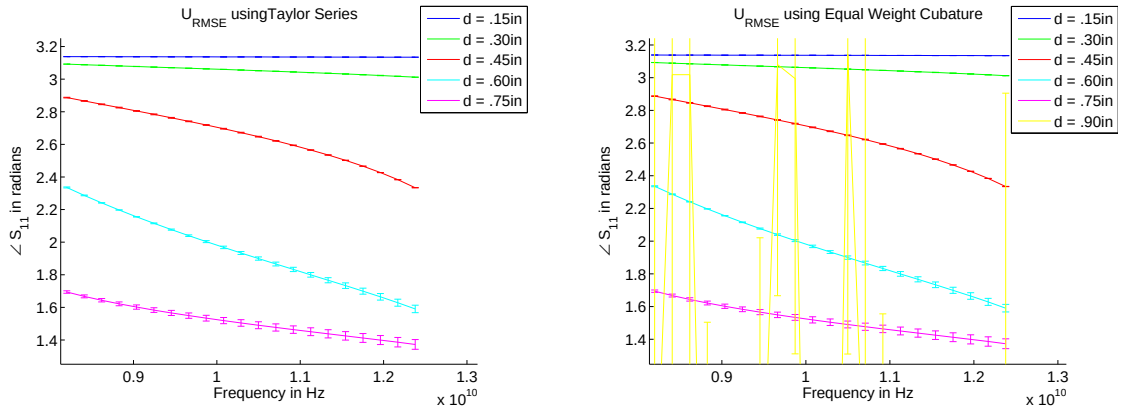

(a) $\angle S_{11}$ Taylor Series RMSE Uncertainty Component ℓ

(b) $\angle S_{11}$ Equal Weight Cubature RMSE Uncertainty Component ℓ

Figure 4.10: $\angle S_{11}$ Component ℓ EWC vs. Taylor Series

The phase is minimal for the first 3 values of d for S_{11}. This is expected because these waves are in evanescence for all operating frequencies. All phase interactions become minimal as the waves travel the distance of ℓ and are reflected back. For the $d = .60in$ and $d = .75in$ case, waves in the propagating region effect the phase because they will interact with waves in Region I and also will be offset by the delay in ℓ.

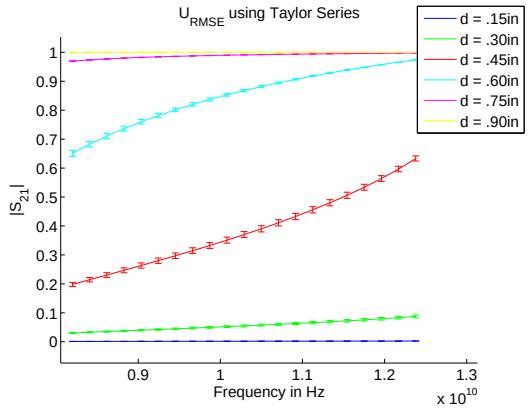

(a) $|S_{21}|$ Taylor Series RMSE Uncertainty Component ℓ

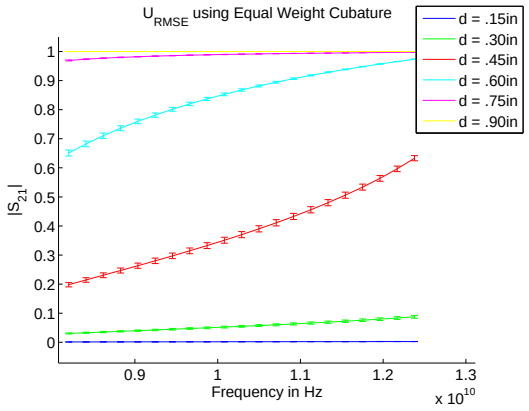

(b) $|S_{21}|$ Equal Weight Cubature RMSE Uncertainty Component ℓ

Figure 4.11: $|S_{21}|$ Component ℓ EWC vs. Taylor Series

When $d = .15in$ the cutoff frequency is much higher than the bandwidth shown here so that all frequencies remain in evanescence. Therefore very little of the energy will propagate through the insert and in this case equates to approximately zero magnitude. For $d = .30in$, the waveguide is now slightly open and at higher frequencies, some energy comes through, but the uncertainty is still very small because the cutoff frequency is so far away. At $d = .45in$ the higher frequencies approach the cutoff frequency but are still in evanescence. Therefore, the amount of energy that propagates is increased. At this point, small changes to ℓ begin to effect the magnitude of S_{21} because waves are propagating through, but decay exponentially depending on the length of ℓ. For $d = .60in$, $.75in$, the lower frequencies remain in evanescence and small changes to ℓ effect the amount of energy decaying in the waveguide insert. But the magnitude for $d = .75in$ is much closer to $+1$ and reflections are somewhat insignificant additions to S_{21}. So even though the uncertainty is greater at the lower frequencies, it is still somewhat imperceptable. Once it passes the cutoff frequencies of 9.84GHz and 7.87GHz for $d = .60in$ and $d = .75in$ respectively, the waves are now propagating and slight changes to ℓ do not effect the magnitude of what travels to S_{21}.

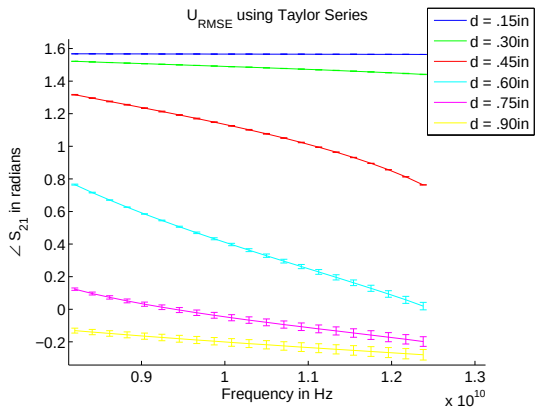

(a) $\angle S_{21}$ Taylor Series RMSE Uncertainty Component ℓ

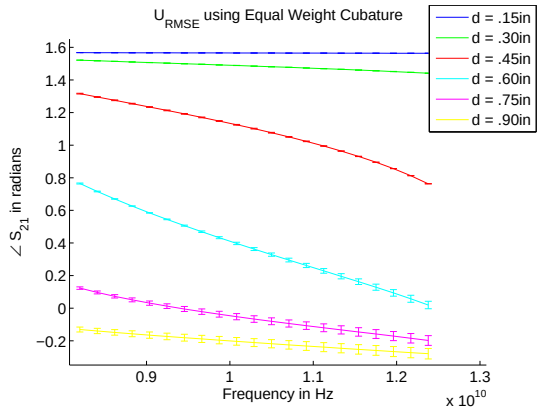

(b) $\angle S_{21}$ Equal Weight Cubature RMSE Uncertainty Component ℓ

Figure 4.12: $\angle S_{21}$ Component ℓ EWC vs. Taylor Series

The phase is minimal for the first 3 values of d for S_{21} similar to S_{11}. This is expected because waves reflected within the waveguide will only have a small amplitude when they meet the Region III boundary as they are in the evanescent modes. The phase of the wave will have the most energy when it reaches the boundary of Region III the first time and it's phase will have the most impact. As reflections happen within the insert the magnitudes decay exponentially. The magnitudes of these three values after reflections will be very small thus contributing very little to the phase. For the $d = .60in$, $d = .75in$, and $d = .90in$ cases, changes to ℓ will have a greater impact in the propagating region because these waves are reflecting within the insert. These reflections effect the phase based on the size of ℓ so error becomes important. As a proof of convergence for TS and Equal Weight Cubature, an example of Real and

Imaginary Uncertainty values is included. The Equal Weight Cubature overlaps very tightly between the 2nd and 3rd orders and even upon magnification, are impossible to distinguish. The Taylor Series method shows values that are converging as the order K is increasing. Figure 13(c) is shown magnified for one frequency in Figure 4.3.2 to display an example of K converging.

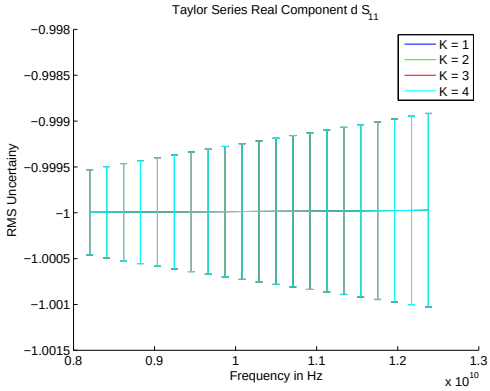

(a) Real S_{11} For d = .15in

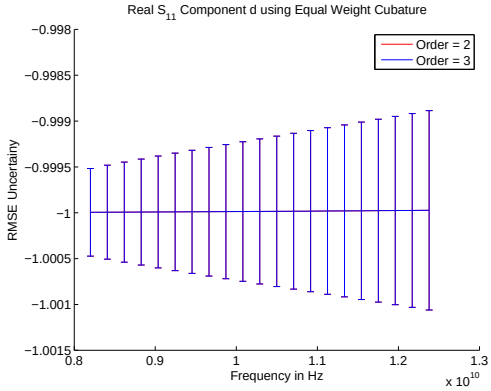

(b) Real S_{11} For d = .15in

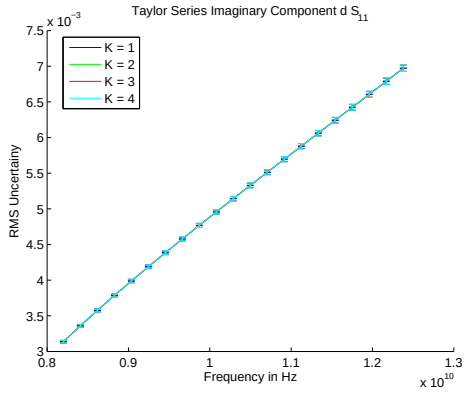

(c) Imag S_{11} For d = .15in

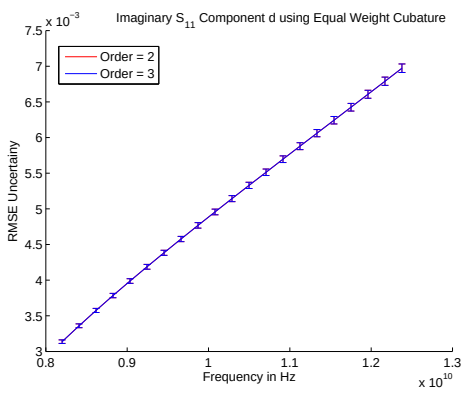

(d) Imag S_{11} For d = .15in

Figure 4.13: True real values and uncertainty increase slightly with frequency. Imaginary uncertainty values are minimal in comparison.

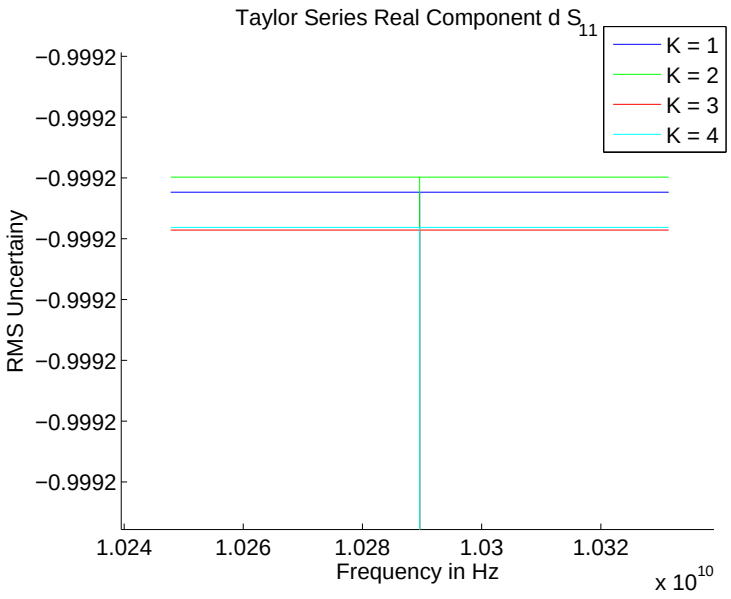

Figure 4.14: Magnification of single real frequency for S_{11} and $d = .15in$

The values of uncertainty were checked using multiple methods. `Matlab`® 's symbolic toolbox took the longest to generate analytic partial derivatives. These values were checked against numerical partials and Mathematica®. The lower orders of K = 1, 2 were much simpler to determine. However, at K = 3, 4 partial derivatives became increasingly complicated and generated some differences between the three methods. There was good correlation between the two methods, EWC and Taylor Series so that confidence was achieved to proceed to composite uncertainty methods.

4.4 Combined Component Analysis

The purpose of the next set of figures is to help determine the component that is most sensitive to uncertainties caused by fabrication errors. Reviewing the previous figures can be beneficial but viewing the results layered on one another may help determine which parameter needs to be fabricated to a tighter tolerance. This section uses Equal Weight Cubature because Taylor Series and EWC are very close in value for the magnitude. The phase values of Taylor Series are also more difficult to trust because there is much more that can go wrong and the values did not match up with EWC. The other major benefit to EWC is computation time.

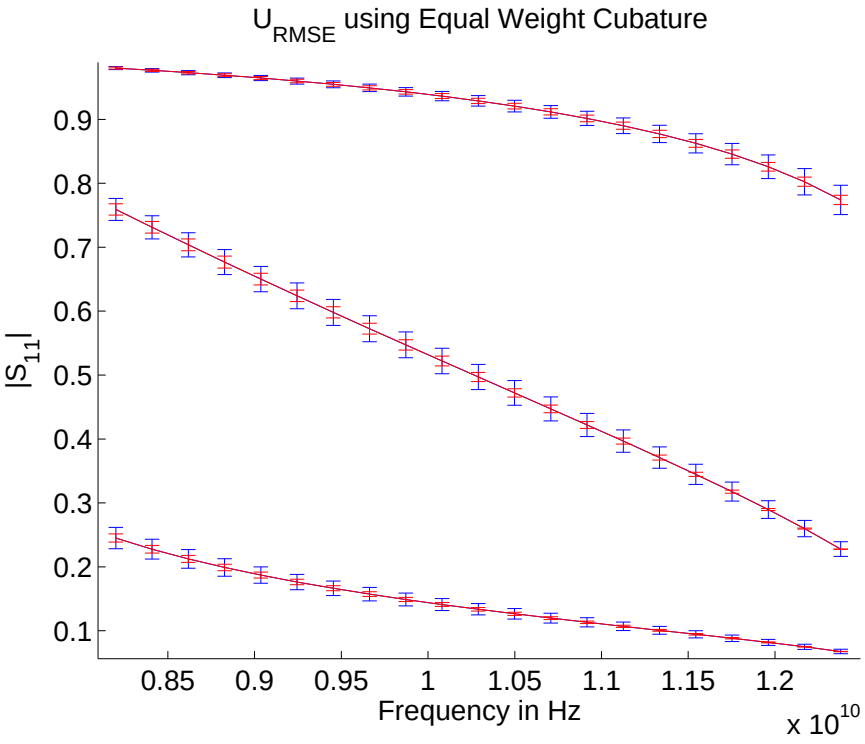

Figure 4.15: Component d vs. ℓ for $|S_{11}|$

The largest uncertainty occurred here for the $d = .45in$ case[1] for the d parameter. Uncertainties tended to be small for the outliers at $d = .15$, $.30in$, and.$90in$ cases so they were removed in order to more clearly see what was happening in the other cases. Small errors in ℓ were still contributors but greater for the cases where

[1] d in blue, ℓ in red; top to bottom: $d = .45in, .60in, .75in$

the operating frequencies were in evanescence and because the magnitude decays as a function of the length ℓ.

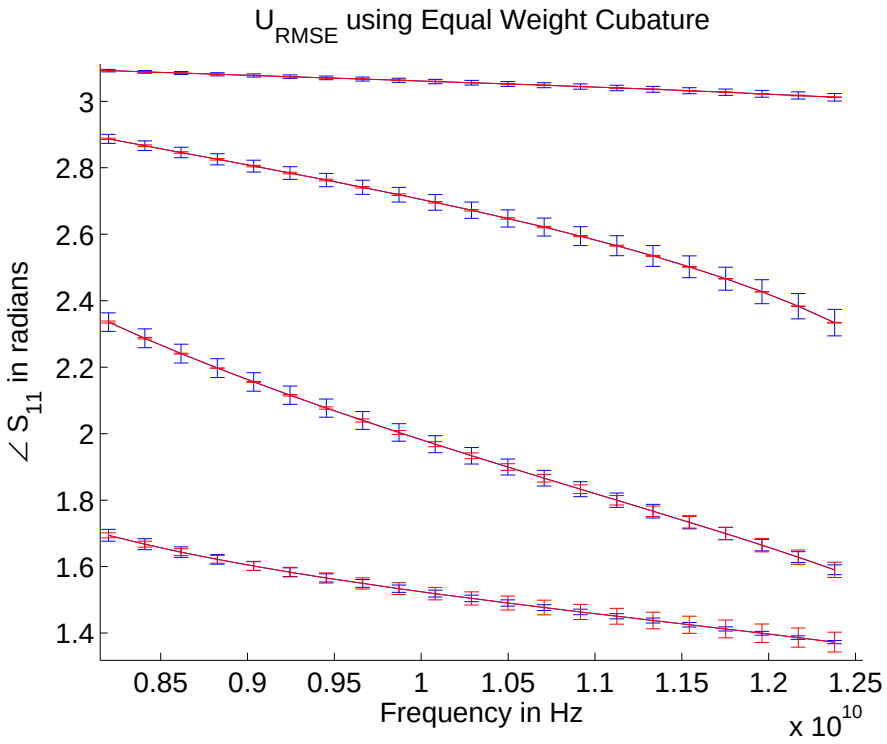

Figure 4.16: Component d vs. ℓ for $\angle S_{11}$

Similar to the discussion earlier, the phase of S_{11} is effected more by changes[2] to d except where the operating frequencies are propagating. This is because in propagation changes to ℓ impact the reflections occurring within the waveguide insert which alter the phase of Region I.

[2] d in blue, ℓ in red; top to bottom: $d = .30in, .45in, .60in, .75in$

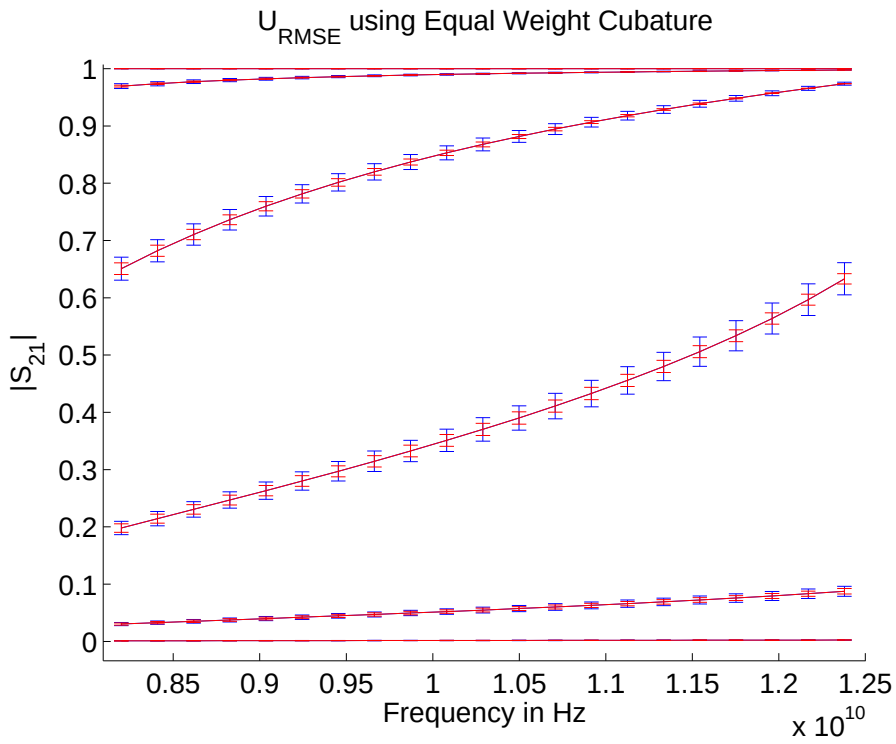

Figure 4.17: Component d vs. ℓ for $|S_{21}|$

Both imperfections in ℓ and d have impacts here at $d = .45in$ because all of the operating frequencies are in evanescence. The impact of d is caused by the fact that the cutoff frequency gets closer to the operating frequencies causing decay in what reaches Region III. Changes[3] to ℓ affect the magnitude greatly because as the cutoff frequency is approached ℓ causes decay less quickly.

[3] d in blue, ℓ in red; bottom to top: $d = .15in, .30in, .45in, .60in, .75in, .90in$

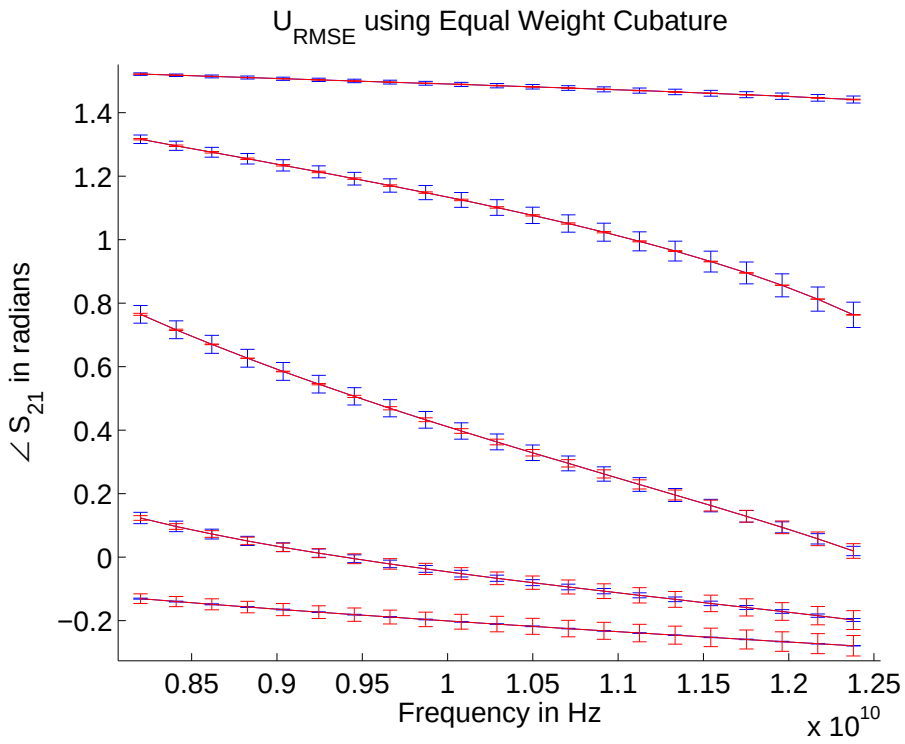

Figure 4.18: Component d vs. ℓ for $\angle S_{21}$

Only for $d = .90in$ does ℓ have a greater impact than d. This is because at $d = .90in$ the waveguide is completely open[4] and the operating frequencies are now in the propagating region. Changes to d never come close to changing the cutoff frequency enough to bring it into the evanescent mode. Changes to ℓ however change the interactions between phase in Region II, the insert region and impact the phase in Region III.

4.5 Composite Uncertainty Analysis Using Equal Weight Cubature and Monte-Carlo

The following figures could be used to define standards of uncertainty using either Equal Weight Cubature or Monte-Carlo methods of uncertainty analysis. Certainly the Equal Weight Cubature method provides a much faster way of determining

[4] d in blue, ℓ in red; bottom to top: $d = .30in, .45in, .60in, .75in, .90in$

these values. Equal Weight Cubature ran for around 40 minutes for 21 X-band frequencies at all six standard widths, 35 frequencies, and composite uncertainty analysis. The Monte-Carlo method on the other hand ran for almost 6 hours for 1001 iterations. To increase confidence in Monte-Carlo results, a more accurate number of iterations would be 10000. This would take around 60 hours to run on a PC. Part of the reason the standards were chosen in the first place for this thesis was speed of computation. The Monte-Carlo method then removes the benefit of speed.

The largest composite uncertainty occurred at $d = .45in$ for $|S_{11}|$ at a value of about

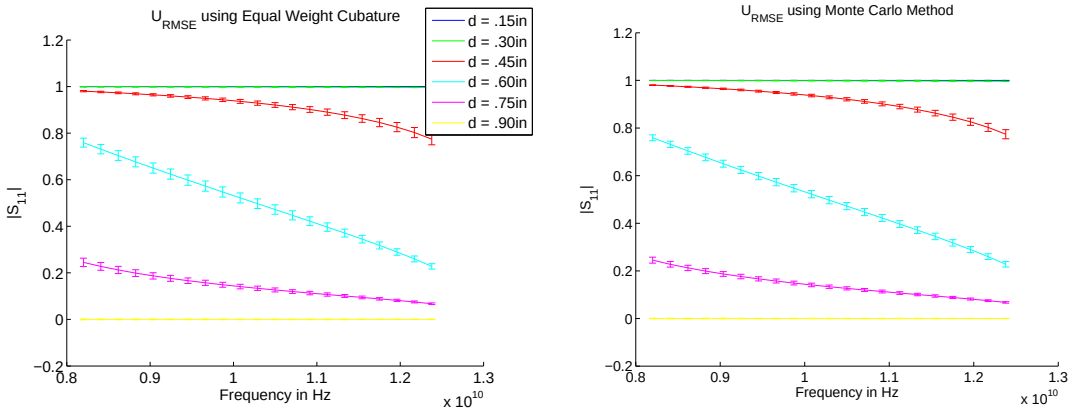

(a) $|S_{11}|$Composite RMSE Uncertainty (b) $|S_{11}|$ Composite RMSE Uncertainty

Figure 4.19: Equal Weight Cubature and Monte-Carlo Techniques produced similar magnitude values

approximately ± 0.025. This occurred when the frequency was near cutoff. As stated previously, when the operating frequency approaches cutoff, changes to d can bring the operating frequency closer to the cutoff frequency and propagation.

The largest value of uncertainty occurs at $d = .45in$ for $\angle S_{11}$ for a value of approximately $\pm 0.04rad$. Again this occurs because the value is approaching cutoff and propagation. Values of d change that cutoff and values of ℓ change how the phase interacts with the reflected values of phase. Values taken using the Monte-Carlo technique were slightly larger most likely because the number of iterations needed to be increased to achieve convergence. When this was attempted for 10000 iterations at

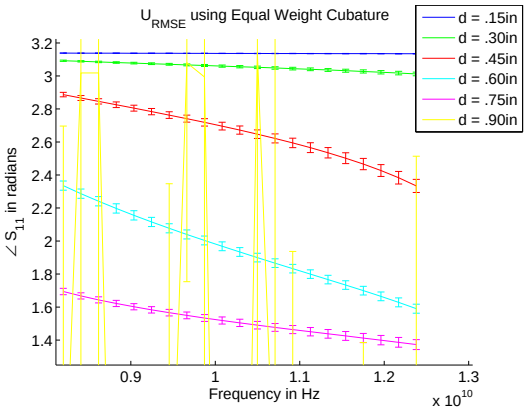

(a) $\angle S_{11}$ Composite RMSE Uncertainty

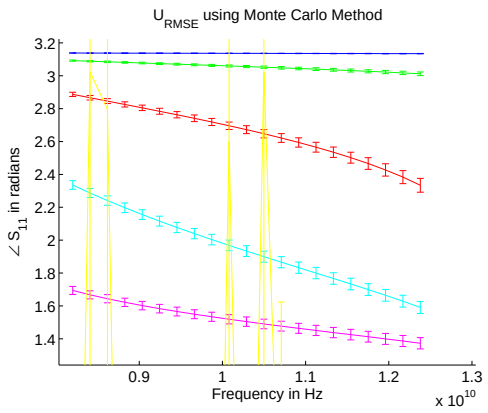

(b) $\angle S_{11}$ Composite RMSE Uncertainty

Figure 4.20: Equal Weight Cubature and Monte-Carlo Techniques produced similar real composite results.

a single frequency, there was a decrease in value of the phase of S_{11}. Most likely as the number of iterations increased again, the value of $\angle S_{11}$ would look more like the EWC value.

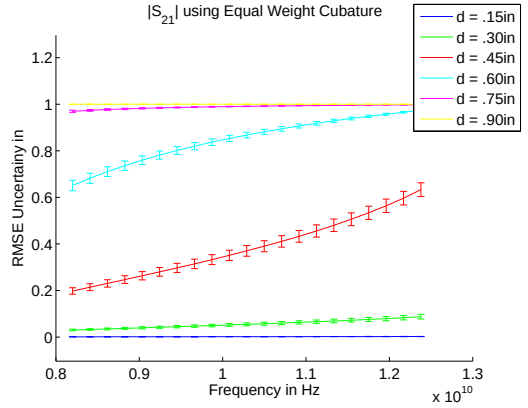

(a) $|S_{21}|$Composite RMSE Uncertainty

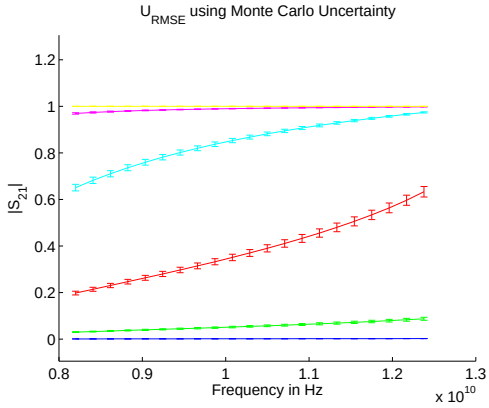

(b) $|S_{21}|$ Composite RMSE Uncertainty

Figure 4.21: Equal Weight Cubature and Monte-Carlo Techniques produced similar real composite results.

The largest value of uncertainty for $|S_{21}|$ occurs at $d = .45in$ for a value of approximately ± 0.03. Composite results tend to follow the trend of the parameter of uncertainty that was the greatest contributor. For this case $d = .45in$ continues to

be the greatest area of uncertainty.

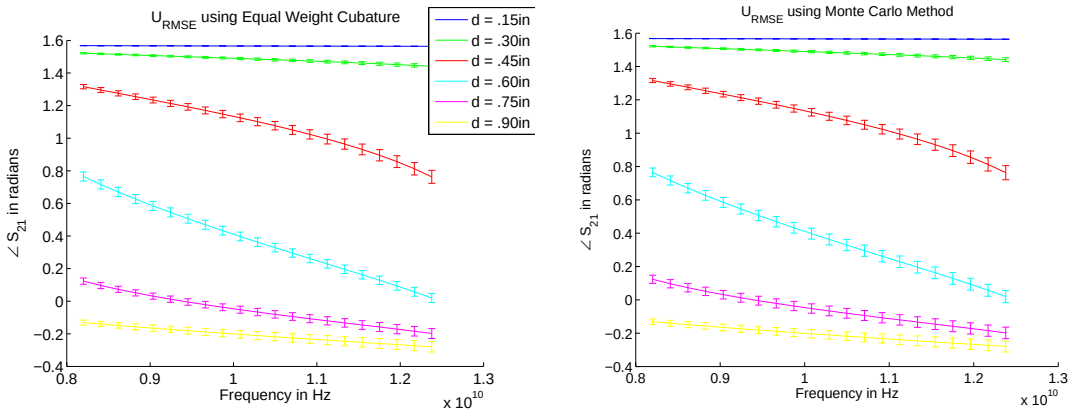

(a) $\angle S_{21}$ Composite RMSE Uncertainty (b) $\angle S_{21}$ Composite RMSE Uncertainty

Figure 4.22: Equal Weight Cubature and Monte-Carlo Techniques produced similar real composite results.

For the $\angle S_{21}$ case, the $d = .45in$ continues to be the greatest contributor at a value of approximately $\pm 0.42rad$. The interesting part about this figure however is that the uncertainty of the $d = .90in$ case is effected most by errors in ℓ. This happens because all of the frequencies of the $d = .90in$ case occur in the propagation region and changes to ℓ affect how reflections within the insert alter the phase in Region III

4.5.1 Tolerance Changes Using EWC. The following graphs show how different tolerances effect the composite EWC uncertainty. The fabrication shop on Wright-Patterson that built the inserts used later in this chapter can fabricate the parameters of uncertainty to $\pm 0.0002in$. Tolerances used for the A600 filter for d were $\pm 0.002in$ for normal, $\pm 0.004in$ for relaxed, and $\pm 0.001in$ for tight measurements. Tolerances for ℓ were ± 0.005 for normal, ± 0.010 for relaxed, and ± 0.002 for loose measurements. The following figures will the same tolerances to identify the usefulness of this standard even though it is possible to get tighter tolerances from the fabrication shop. In previous figures, a loose tolerance of ± 0.010 was used so that values were

visibly discernable. Also, since this was the loosest measurement, this thesis could be matched up well with A600 measurements.

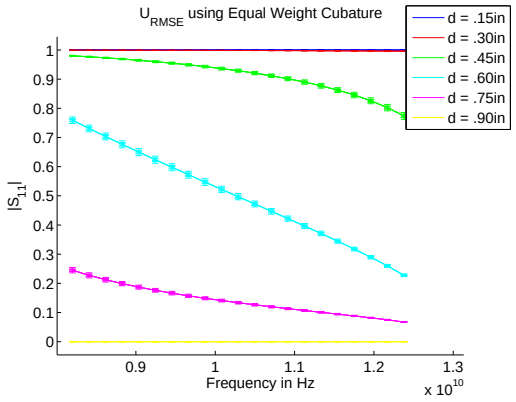

(a) $|S_{11}|$ EWC Uncertainty Changing Tolerances

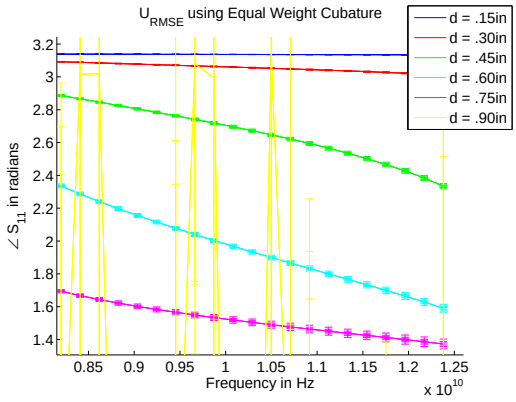

(b) $\angle S_{11}$ EWC Uncertainty Changing Tolerances

Figure 4.23: Tight, Normal, and Loose Tolerances for S_{11}

The largest uncertainty for the magnitude of S_{11} occurs at $d = .45$ for a value of approximately ± 0.0125. The largest uncertainty for the phase of S_{11} occurs at $d = .60$ for a value of approximately $\pm 0.025 rad$.

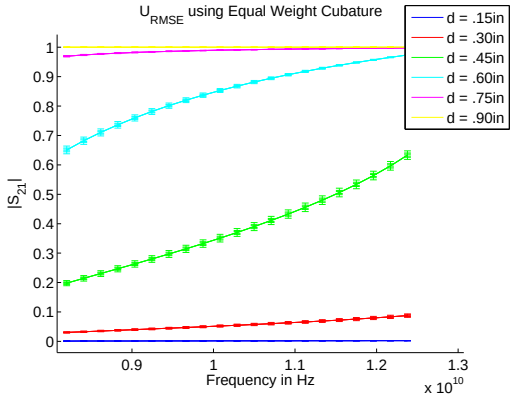

(a) $|S_{21}|$ EWC Uncertainty Changing Tolerances

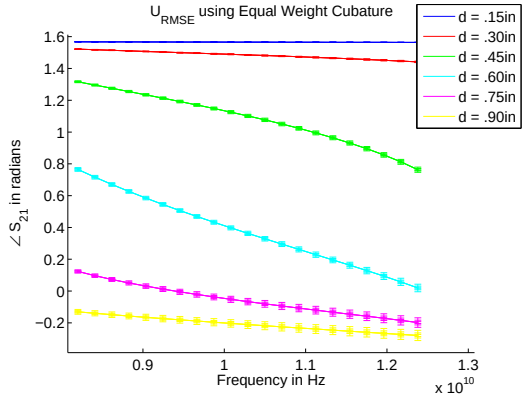

(b) $\angle S_{21}$ EWC Uncertainty Changing Tolerances

Figure 4.24: Tight, Normal, and Loose Tolerances for S_{11}

The largest uncertainty for the magnitude of S_{21} occurs at $d = .45$ for a value of approximately ± 0.015. The largest uncertainty for the phase of S_{21} occurs at $d = .90$ for a value of approximately $\pm 0.03 rad$. For the loose tolerance values chosen here

for uncertainty, the largest absolute RMSE uncertainty for S_{11} and S_{21} for the A600 filter was approximately ± 0.1 for ANALEX's analysis and approximately ± 0.085 for ATK's analysis [1]. These results seem to show these standards performing better than the A600 for the worst case scenario.

4.5.2 Measured Results. The following figures show correlation between true values of uncertainty and the results obtained using an Agilent® PNA Network Analyzer.

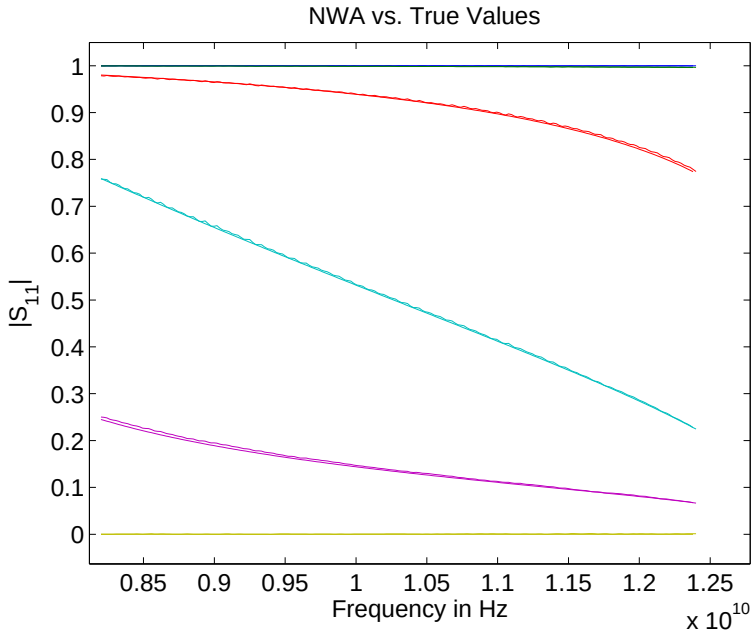

Figure 4.25: $|S_{11}|$ NWA vs. True values

Values for the magnitude of S_{11} were predicted well by the Mode Matching Technique. There is some slight ripple effect to the measured values which might be accounted for by poor handling of cabling attached to the NWA.

Differences occurred for the phase of S_{11} for $d = .45in, .60in,$ & $.75in$. These

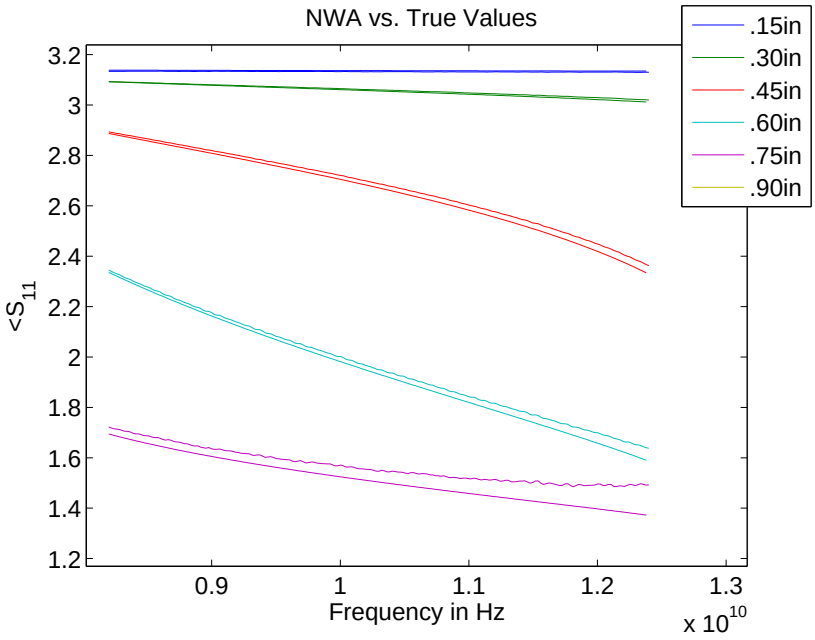

Figure 4.26: $\angle S_{11}$ NWA vs. True values

differences were most likely due to human error caused by roughly handling cabling as this was noticed during measurement. These errors could also have been caused by poor fabrication techniques which introduced new errors of uncertainty into the system. Specifically, precision guidance pinholes were not drilled properly which affect the alignment of the entire system.

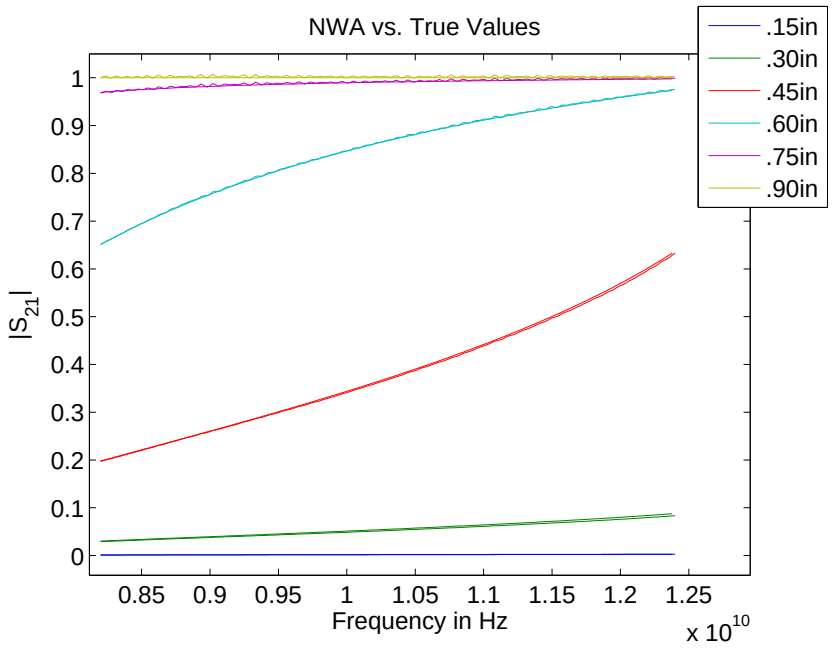

Figure 4.27: $|S_{21}|$ NWA vs. True values

A slight ripple effect is seen in the magnitude of S_{21}. This may be errors caused by the environment of the NWA system described in Chapter I rather than the fabrication of the $d = .15in$ and $d = .30in$ inserts. The ripple occurs at the same point for both values and neither value comes close to changing from evanescent modes to propagating. This means changes to d or ℓ would have almost no impact on the value of S_{21}.

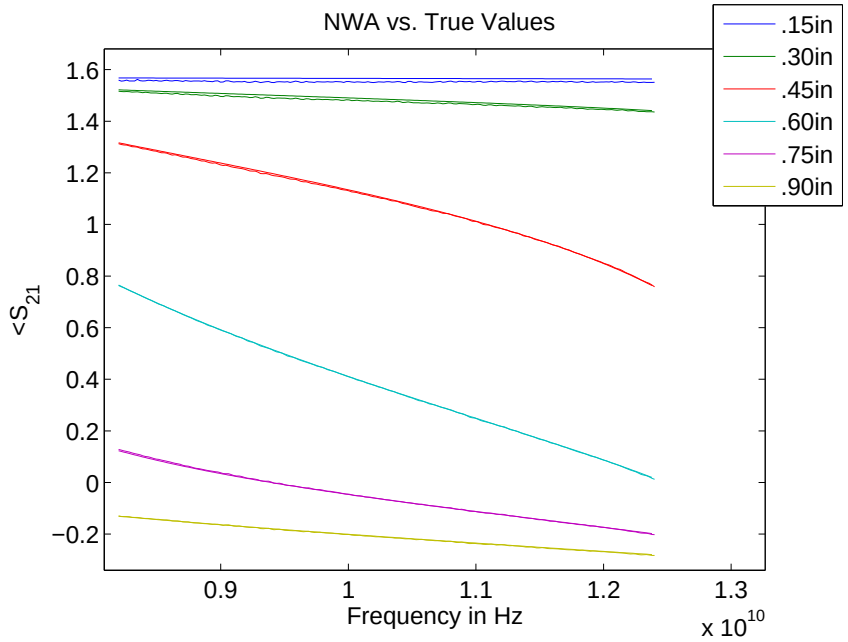

Figure 4.28: $\angle S_{21}$ NWA vs. True values

Values of phase for S_{21} correlated well for all values of d as shown in the figure above. Only the almost fully closed aperture region produced any noticeable difference in results. Again, this may be caused by the poor handling of cables attached to the NWA.

Finally, a set of results taken using the NWA were overlaid on loose tolerance EWC uncertainty values. Remember from Chapter II that these are RMSE uncertainty values and not confidence values. The measured results should line up well with the expected values but will not represent every possible value within the error of Δd and $\Delta \ell$.

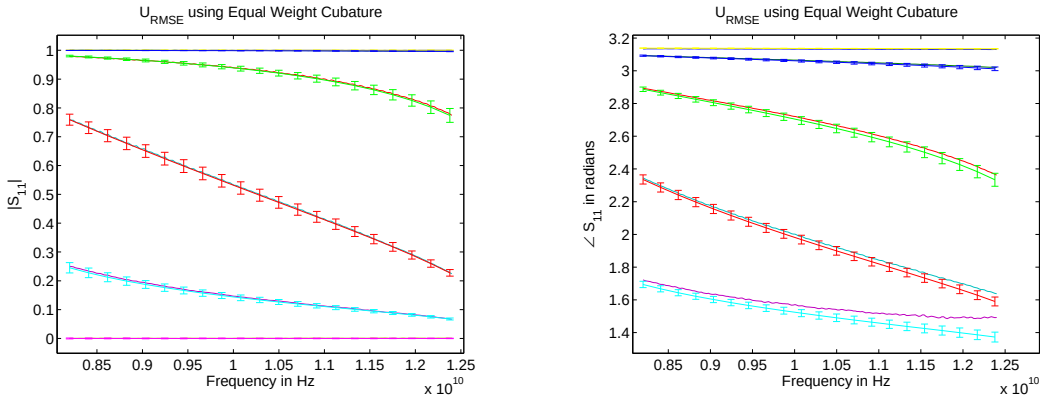

(a) $|S_{11}|$ NWA Results vs EWC

(b) $\angle S_{11}$ NWA Results vs EWC

Figure 4.29: NWA S_{11} results with Equal Weight Cubature uncertainty

As shown above, magnitude values lined up well inside of uncertainty error bars for EWC. Some values of phase fell outside of the error bars. There are two possible reasons this occurred. First, the system itself contains errors and may need to be recallibrated or the user may need to be gentler with the equipment. This first problem is why the standards were developed in the first place. To determine how well a system is measuring S-parameters. A second possibility may be that the standards themselves were not fabricated properly. This second possibility is likely as precision guidance holes were not cut in the standards used for these measurements.

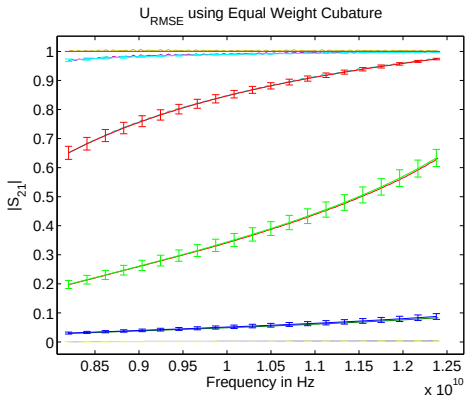

(a) $|S_{21}|$ NWA Results vs EWC

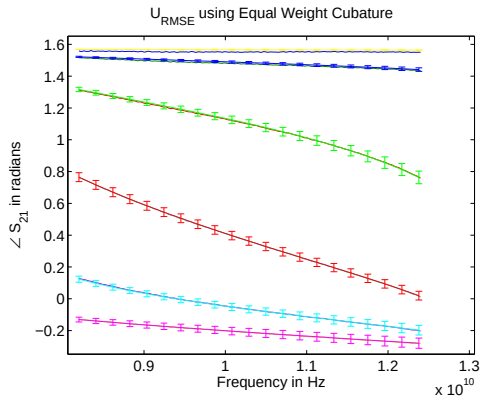

(b) $\angle S_{21}$ NWA Results vs EWC

Figure 4.30: NWA S_{21} results with Equal Weight Cubature uncertainty

Magnitude and phase measurements for S_{21} lined up well in this case and all values fell within the uncertainty values of EWC. It seems that these standards, if fabricated properly and calibrated well should produce a good standard for determining how well a system is taking measurements.

V. Conclusions

5.1 Results and Recommendations

The purpose of this thesis was to determine if a suite of metallic verification standards could be developed that would be simple to fabricate, require short computation time, and have small uncertainty values associated with fabrication errors. The A600 notch filter, while retaining somewhat small uncertainty values, has a great deal of computation time and is more complex in fabrication. In Chapter II, the MMT theory for determining true values of S-parameters was clearly developed for these possible standards. The MMT theory is fundamental to an understanding of the uncertainty of measurements. One of the major benefits to using MMT was that it produced a function which was differentiable and integrable. The A600 filter had to be modeled using HFSS and MWS which does not produce a differentiable function above the first order. This makes using Taylor Series somewhat unreliable. The Monte-Carlo technique was used for both the A600 analysis and the suite of metallic standards. Two methods were used for each of the two methods of analysis: component and composite. This added confidence that values gained through the analysis were correct.

The most difficult of these three methods was the Taylor Series method. The Taylor Series method required computation of partial derivatives for each element of the 4Nx4N A matrix described in Chapter II. These elements were partially differentiated analytically using `Matlab`® 's symbolic toolbox and Mathematica® up to the 4th order. For some of these equations, the partial derivatives for a single element were more than a page in length and could not be integrated back to their original form using the two methods. There were two problems identified when using the Taylor Series. In many cases the partial differentiations left a possible non-zero number divided by zero leading to an undefined number. The other issue relates to the complexity of the functions being used. `Matlab`® and Mathematica® may have had problems differentiating the higher order equations as they grew more and more complex.

Even though there were difficulties in using the Taylor Series method, it correlated well with the Equal Weight Cubature method. This was the stimulus for movement into the composite analysis. The composite analysis in Chapter IV was performed using EWC and Monte-Carlo methods. EWC was a very fast method of defining RMSE uncertainty. The problem with EWC is that it must be verified using another method of analysis. If the function being evaluated by EWC is poorly modeled by either a square or cubic function within the Weighting function, the results obtained are poor. To verify that the function is modeled well a secondary method was used. This is the motivation behind using the slower Monte-Carlo method for composite analysis. Both functions allow for multiple parameters of uncertainty. The Monte-Carlo method's results lined up well with results obtained using EWC. The slight differences were most likely due a lack in the number of iterations taken using the Monte-Carlo method. Higher iterations showed that uncertainty values began to converge on EWC values but would've taken days of computations time.

The results obtained in Chapter IV matched up well with what was physically expected. The dominant mode or TE_{10} allowed for easy calculation of cutoff frequencies. Once the cutoff frequencies were known, it was easy to see when variations in d or ℓ would affect the magnitude and phase of S_{11} and S_{21}. In fact, the closer values of frequency and d got to the cutoff frequency, the greater the uncertainties. For d the uncertainties occurred because the changing of d affected where the cutoff frequency would occur, thus changing the amount of decay in evanescence and determining how much of the signal would propagate. The changing of ℓ produced different magnitudes while in evanescent modes because the longer the ℓ value, the more decay would occur within the insert. The changes in ℓ also produced differences in phase in propagating modes because it caused more interactions with reflecting waves within the insert. Overall it seemed that the d variable was the dominant parameter of uncertainty. There was only one case where the uncertainty of ℓ was the dominant uncertainty and that was for only one value of d rather than the whole set.

On the other hand, most of the analysis of Chapter IV resided in the loose toler-

ance range of $\pm 0.01in$ and for both parameters of uncertainty which was significantly worse than the fabrication shop's possible tolerance of $\pm 0.0002in$. One of the most important parts of this analysis come from Figures 4.24 and 4.25. These figures show that for a loose tolerance, the worst magnitude RMSE uncertainty value is ± 0.0125 for S_{11} and ± 0.015 for S_{21}. The largest phase uncertainties were $\pm 0.025rad$ for S_{11} and $\pm 0.03rad$ for S_{21}. ANALEX and ATK worst case results were similar for S_{11} and S_{21}. The worst case magnitude RMSE uncertainty value of ± 0.97 and ± 0.85 for ANALEX and ATK analysis respectively [1]. Phase values for the A600 resided at around $\pm 0.027rad$ and $\pm 0.025rad$ for S_{11} and for the worst case values. The phase uncertainty for both the A600 and the suite of metallic standards were both small in value in comparison to magnitude values. On the other hand, the maximum magnitude uncertainty for the A600 is an order of magnitude larger than the suite of metallic standards.

Table 5.1: A600 vs. Suite of Metallic Standards (SMS) U_{RMSE}

	A600			SMS		
Parameter	tight	relaxed	normal	tight	relaxed	normal
$\lvert S_{11}\rvert$	0.025	0.097	0.047	0.0027	0.0119	0.0060
$\angle S_{11}$	-	0.027	-	0.0060	0.0300	0.0150
$\lvert S_{21}\rvert$	0.025	0.097	0.047	0.0034	0.0147	0.0074
$\angle S_{21}$	-	0.023	-	0.0064	0.0322	0.016

Advantages of the A600 are that the A600 is a single standard that can be used to determine NWA error. Disadvantages of the A600 are that it is a narrow band standard, is sensitive to slot width, is computationally intensive in terms of run time, and fabrication is somewhat difficult. Advantages of the suite of metallic standards are broadband standard with different levels of response, relatively insensitive to dimension errors, machining is simple, and is not as computationally intensive in

terms of time. Disadvantages of the suite of metallic standards are that multiple standards are necessary.

5.2 Recommendations

In this case results for the A600 were used as the current standard to evaluate the performance of the suite of metallic standards. Specifically, the greatest weakness of the A600 was chosen as the parameter measured against. It makes sense that the slot width should be the greatest area of uncertainty as it directly affects where the cutoff frequency occurs as was shown in the results of this thesis. During testing of the fabricated metallic standards, a possible other area of uncertainty was determined as the precision alignment pins were not fabricated correctly. This could introduce some additional uncertainty. Even with the possibility of this additional error, most values measured using the NWA fell within the uncertainty bars for loose measurement. The phase values differed the most. With more gentle care of equipment, these phase values would most likely improve. In general, the suite of metallic standards provides a broadband standard with different levels of response as shown through repeated plots of S-parameters. The uncertainty analysis would seem to show that these standards are relatively insensitive to dimensional errors and because machining is simple, tolerances can be tight. Finally, run time for Equal Weight Cubature and Taylor Series methods were on the order of minutes compared to hours for the Monte-Carlo method. It seems that the suite of metallic standards may in fact be a good verification standard.

5.3 Improvements and Future Analysis

The biggest improvements to this analysis would be in the area of fabrication and measurement. The precision holes for the metallic verification standards were not cut so the measurements performed by the NWA were not as precise as they could have been. A future analysis might also determine how slight imperfections in the precision alignment holes affect uncertainty. More care could also be taken to ensure

that parts of the system such as cables and waveguides were handled more gently to ensure errors were not caused by these movements. For further gratification that the composite analysis was accurate, the Taylor Series could be used. The problem would lie in the complexity of the equations used. Further analysis can be done as a follow-up to this thesis that could explore the use of a material of some type as a non-metallic standard. It was important in this analysis to use a metallic standard as a verification because it removes some of the possible errors due to production, humidity, and environment of non-metallic standards. It would be interesting to determine if there is some non-metallic material that reduces these possible errors as well.

Appendix A. Derivation of Taylor Series and Monte Carlo RMSE Uncertainty

Derivation of $\beta_{S_{11}}$ and $Var(\Delta S_{11})$ can be found using the following [4]:

$$\hat{y} = f(\hat{x}) = f(x + \Delta x) \approx f(x) + \sum_{k=1}^{K} \frac{f^{(k)}(x)}{k!}(\Delta x)^k,$$

Since$f(x) = y + \beta_0$:

$$\Delta y = \hat{y} - y \approx \beta_0 + \sum_{k=1}^{K} \frac{f^{(k)}(x)}{k!}(\Delta x)^k,$$

Therefore, $\langle \Delta y \rangle \approx \langle \beta_0 + \sum_{k=1}^{K} \frac{f^{(k)}(x)}{k!}(\Delta x)^k \rangle$,

$$\beta_{S_{11}} = \langle \Delta y \rangle \approx \beta_0 + \sum_{k=1}^{K} \frac{f^{(k)}(x)}{k!} \langle (\Delta x)^k \rangle, \tag{A.1}$$

$$Var(\beta_{S_{11}})Var(\Delta y) \approx Var(\beta_0 + \sum_{k=1}^{K} \frac{f^{(k)}(x)}{k!}(\Delta x)^k) = Var(\sum_{k=1}^{K} \frac{f^{(k)}(x)}{k!}(\Delta x)^k)$$

Let$a_k = \frac{f^{(k)}(x)}{k!}andz = \sum_{k=1}^{K} a_k(\Delta x)^k$

$Var(\Delta y) \approx Var(z) = \langle |z|^2 \rangle - |\langle z \rangle|^2 = \langle z z^* \rangle - \langle z \rangle \langle z \rangle^*$

where * denotes complex conjugate

$$\langle \sum_{i=1}^{K} a_i(\Delta x)^i \sum_{j=1}^{K} a_j^*(\Delta^* x)^j \rangle - \langle \sum_{i=1}^{K} a_i(\Delta x)^i \rangle \langle \sum_{j=1}^{K} a_j^*(\Delta^* x)^j \rangle$$

$$\langle \sum_{i=1}^{K} \sum_{j=1}^{K} a_i a_j^*(\Delta x)^i(\Delta^* x)^j \rangle - \sum_{i=1}^{K} a_i \langle (\Delta x)^i \rangle \sum_{j=1}^{K} a_j^* \langle (\Delta^* x)^j \rangle$$

$$\sum_{i=1}^{K} \sum_{j=1}^{K} a_i a_j^* \langle (\Delta x)^i(\Delta^* x)^j \rangle - \sum_{i=1}^{K} \sum_{j=1}^{K} a_i a_j^* \langle (\Delta x)^i \rangle \langle (\Delta^* x)^j \rangle$$

$$\sum_{i=1}^{K} \sum_{j=1}^{K} a_i a_j^* [\langle (\Delta x)^i(\Delta^* x)^j \rangle - \langle (\Delta x)^i \rangle \langle (\Delta^* x)^j \rangle],$$

$$\sum_{i=1}^{K} \sum_{j=1}^{K} a_i a_j^* Cov[(\Delta x)^i, (\Delta x)^j]$$

Appendix B. Additional Figures Using S_{21}

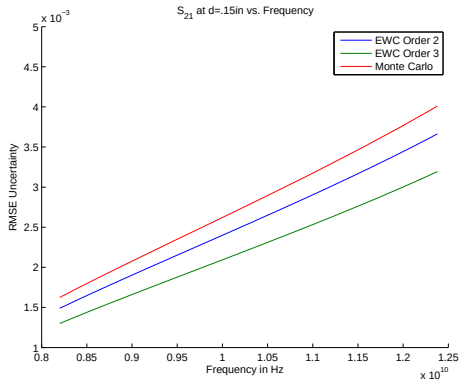

(a) S_{21} For d = .15in

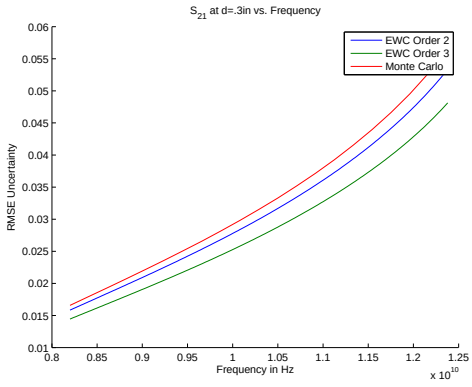

(b) S_{21} For d = .30in

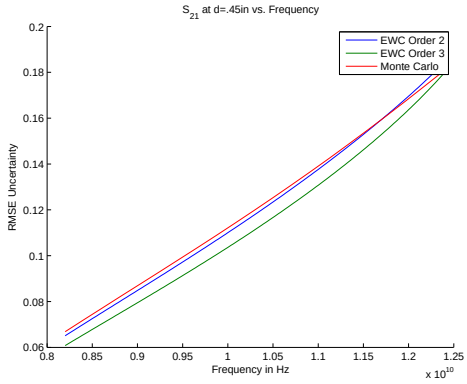

(c) S_{21} For d = .45in

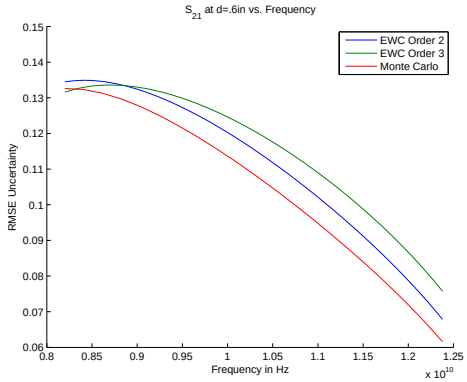

(d) S_{21} For d = .60in

Figure B.1: Composite Uncertainty Analysis Using Equal Weight Cubature and Monte Carlo Techniques

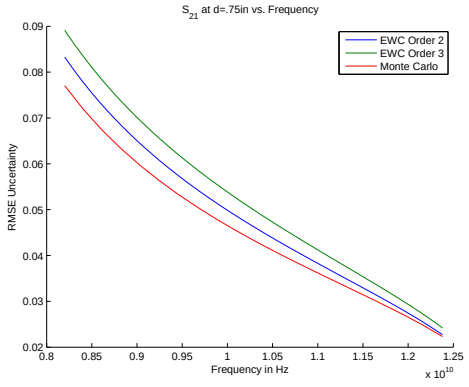

(e) S_{21} For d = .75in

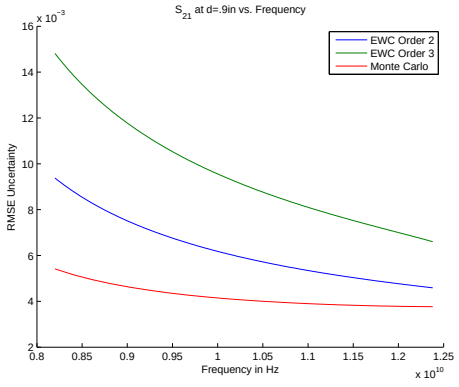

(f) S_{21} For d = .90in

Figure B.1: Composite Uncertainty Analysis Using Equal Weight Cubature and Monte Carlo Techniques (cont'd)

These figures show S_{21} values as the number of modes increases. An excel file is included in Appendix D that marks the place where each value of S_{21} becomes slowly varying. At $d = .15in$ and $d = .90in$ the point of slow variance was almost instantaneous while the slowest values to converge were $d = .45in$ and $d = .6in$.

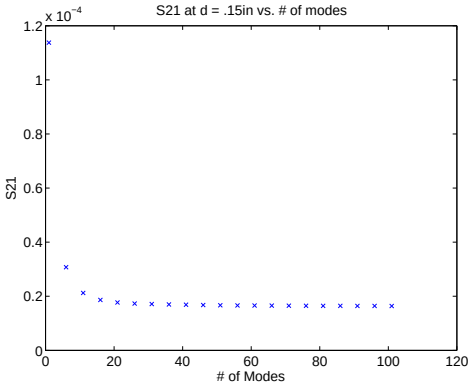

(g) d = 0.15in

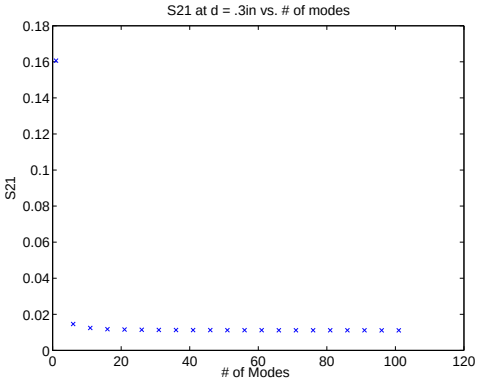

(h) d = 0.30in

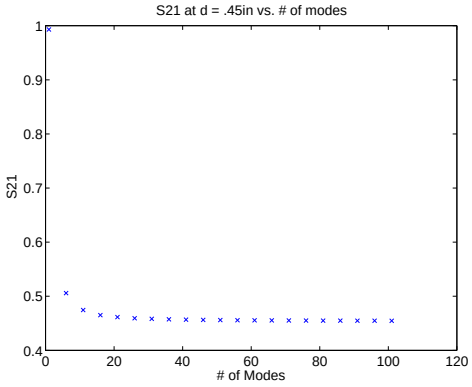

(i) d = 0.45in

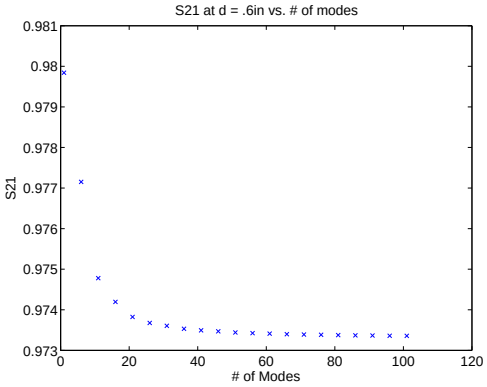

(j) d = 0.60in

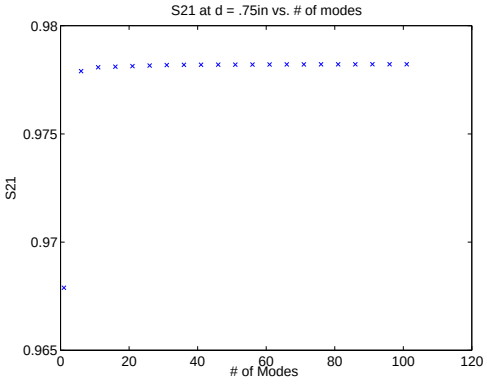

(k) d = 0.75in

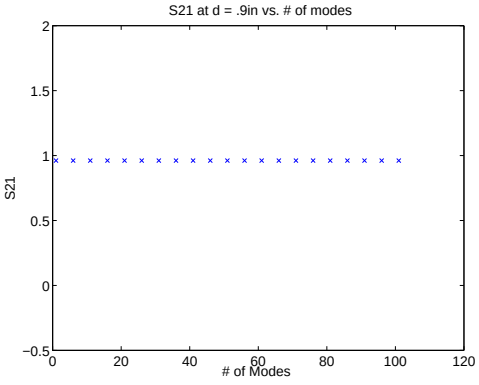

(l) d = 0.90in

Figure B.1: 6 $'d'$ widths with increasing mode inclusion with respect to real S_{21}

```
%Brian Witthoeft
%The following code will be used as a simulation to develop a set of
%waveguide insert standards that will ensure the values provided by the
%Network Analyser are accurate.  This code uses the mode matching technique
%to determine the values of S11 and S21.

clear all
clc

%Global Variables
a = 0.9*2.54*10^(-2);  %inches in height of waveguide in the x direction in the 1st and 3rd sections
%d = 0 to 0.9in;  %height of waveguide in the x direction from the 2nd
%section

l = .05*2.54*10^(-2);  %width of gap produced by insert
mux = 4*pi*10^-7;    %free space permissivity
eps = 1/((3e8)^2*mux);  %free space permittivity
tol = 1e-6;

freq = 8.2e09:0.020896e09:12.4e09;%subdivides the number of
                                  %frequencies into 201 data points
N = 35;  %35 modes was determined in finalmultfreqmultmode.m
M = 35;  %to be the number of modes needed for a slowly varying
         %S11 and S21 to 10^-3 decimal places.

R = 6; % Somewhat arbitrary number of divisions to cut the insert into.

% In order to speed up runtime of the code, the following parameters are
% preallocated.
AmnMat = zeros(M,N);
BmnMat = zeros(M,N);
CmnMat = zeros(M,N);
DmnMat = zeros(M,N);
EmnMat = zeros(M,N);
FmnMat = zeros(M,N);
GmnMat = zeros(M,N);
HmnMat = zeros(M,N);
Xm1Mat = zeros(M,1);
Ym1Mat = zeros(M,1);
ZeroMat = zeros(M,N);
ZeroSol = zeros(M,1);
Sparam11 = zeros(R,1);
Sparam21 = zeros(R,1);
S11complex = zeros(R,length(freq));
```

```
S21complex = zeros(R,length(freq));
magmultfreq11= zeros(R,length(freq));
phasemultfreq11= zeros(R,length(freq));
magmultfreq21= zeros(R,length(freq));
phasemultfreq21= zeros(R,length(freq));
S11realmultfreq= zeros(R,length(freq));
S11imagmultfreq= zeros(R,length(freq));
S21realmultfreq= zeros(R,length(freq));
S21imagmultfreq= zeros(R,length(freq));
S11 = zeros(N,M);
S21 = zeros(N,M);

for q = 1:length(freq)
    %local variables
    w = 2*pi*freq(q);

    for r = 1:R  %this varies the width of the insert from almost ...
       closed
                 %to completely open

        %local variables
        d = r*0.15*2.54*10^(-2);  %width of the insert/2nd section...
            in the x direction
        %b = .4*2.54*10^(-2);  %width of waveguide in the y ...
           direction for all sections

        for m = 1:M  %M is the mode number for the field expansion
            for n = 1:N  %N is the mode number for the testing ...
               operator

            kxm = m*pi/a;  %the wavenumber of section 1&3
            kxn = n*pi/a;  %wavenumber for the testing operator ...
               section 1&3
            kxtilm = m*pi/d; %the wavenumber of section 2
            kxtiln = n*pi/d; %wavenumber for testing operator ...
               section 2
            gammantil = sqrt((kxtiln)^2-w^2*eps*mux);
            gamman = sqrt((kxn)^2-w^2*eps*mux);
            gammamtil = sqrt((kxtilm)^2-w^2*eps*mux);
            gammam = sqrt((kxm)^2-w^2*eps*mux);
            %%Using the mode matching technique to solve the ...
               matrix for
            % the S-parameters
            % In this case consider the matrix equation Ax = b
            % The portions below fill the 'A' and 'b' matrices for...
                each
            % mode.  The S-parameters are determined by the 'x' ...
               matrix
            % There are two cases for each integral equation.
            if m==n
                Amn = 1;
                Dmn = gammantil*gammamtil/((j*w*mux)^2);
```

```
        Gmn = Dmn*exp(-gammantil*l);
        Hmn = Dmn*exp(gammantil*l);
    else
        Amn = 0;
        Dmn = 0;
        Gmn = 0;
        Hmn = 0;
    end

    if abs(kxm-kxtiln) <= tol
        Bmn = sqrt(d/a);
        Emn = Bmn*exp(-gammantil*l);
        Fmn = Bmn*exp(gammantil*l);
    else
        Bmn = 1/sqrt(a*d)*2*kxtiln*(-1)^n*sin(kxm*d)/(kxm...
            ^2-kxtiln^2);
        Emn = Bmn*exp(-gammantil*l);
        Fmn = Bmn*exp(gammantil*l);
    end
    % Because of rounding errors, this code checks to ...
        ensure kxtilm is equal to
    % pi/a within a certain tolerance
    if abs(kxtilm-kxn) <= tol
        Cmn = sqrt(d/a)*gamman*gammamtil/((j*w*mux)^2);
    else
        Cmn = 1/sqrt(a*d)*gamman*gammamtil/((j*w*mux)^2)...
            *2*kxtilm*(-1)^m*sin(kxn*d)/(kxn^2-kxtilm^2);
    end

    AmnMat(m,n) = Amn;
    BmnMat(m,n) = Bmn;
    CmnMat(m,n) = Cmn;
    DmnMat(m,n) = Dmn;
    EmnMat(m,n) = Emn;
    FmnMat(m,n) = Fmn;
    GmnMat(m,n) = Gmn;
    HmnMat(m,n) = Hmn;

    %This part inserts Forcing Function values into the ...
        matrix according to mode matching

    if m == 1
        Xm1 = 1;
    else
        Xm1 = 0;
    end

    if abs(kxtilm-pi/a) <= tol
        Ym1 = sqrt(d/a)*sqrt((pi/a)^2-w^2*eps*mux)*...
            gammamtil/((j*w*mux)^2);
    else
```

```
                Ym1 = 1/sqrt(a*d)*sqrt((pi/a)^2-w^2*eps*mux)*...
                    gammamtil/((j*w*mux)^2)*2*kxtilm*(-1)^m*sin(pi/...
                    a*d)/((pi/a)^2-kxtilm^2);
            end
            Xm1Mat(m,1)= Xm1;
            Ym1Mat(m,1)= Ym1;
            ZeroMat(m,n) = 0;
            ZeroSol(m,1) = 0;

            end
        end
        A_mat = [AmnMat -BmnMat -BmnMat ZeroMat; CmnMat -DmnMat ...
            DmnMat ZeroMat; ZeroMat FmnMat EmnMat -AmnMat; ZeroMat ...
            HmnMat -GmnMat CmnMat];
        b_mat = [-Xm1Mat; Ym1Mat; ZeroSol; ZeroSol];
        x_mat = A_mat\b_mat;
        %Another command that inverts A_mat is invA_mat = inv(...
            A_mat);

        % The following makes sure Matlab does not leave any stray...
             values in the
        % matrices
        clear A_mat; clear b_mat; clear AmnMat; clear BmnMat; ...
            clear ZeroMat;
        clear CmnMat; clear DmnMat; clear FmnMat; clear EmnMat; ...
            clear HmnMat;
        clear GmnMat; clear Xm1Mat; clear Ym1Mat; clear ZeroSol;

        % Now the S-parameters are pulled out of the x_mat
        S11 = x_mat(1,1); % These are the reflection coefficients
        S21 = x_mat(3*N+1,1); % These are the transmission ...
            coefficients
        Sparam11(r,1)= S11; %This takes each Ref coef. and stores ...
            it for
                            %each value of 'd'
        Sparam21(r,1)= S21; %This takes each Trans coef. and ...
            stores it for
                            %each value of 'd'

        % Either the real and imaginary values or the magnitude ...
            and phase
        % can be used in the development of these standards
        mag11 = abs(Sparam11);
        phase11 = atan2(imag(Sparam11),real(Sparam11));
        mag21 = abs(Sparam21);
        phase21 = atan2(imag(Sparam21),real(Sparam21));
        S11real = real(Sparam11);
        S11imag = imag(Sparam11);
        S21real = real(Sparam21);
        S21imag = imag(Sparam21);

    end
```

```
        %This fills in all of the S-parameter values for the 201 ...
           frequency
        %values
176     S11complex(:,q) = Sparam11;
        S21complex(:,q) = Sparam21;

        magmultfreq11(:,q) = mag11(:,1);
        phasemultfreq11(:,q) = phase11(:,1);
181     magmultfreq21(:,q) = mag21(:,1);
        phasemultfreq21(:,q) = phase21(:,1);

        S11realmultfreq(:,q) = S11real;
        S11imagmultfreq(:,q) = S11imag;
186     S21realmultfreq(:,q) = S21real;
        S21imagmultfreq(:,q) = S21imag;

    end

191 %The following will plot multiple frequencies against S-parameters...
        for real
    %and imaginary values
    figure()
    plot(freq,S11realmultfreq(1,1:length(freq)),freq,S11imagmultfreq...
       (1,1:length(freq)));
    title('S_{11} at d = .15in vs. freq')
196 xlabel('Frequency')
    ylabel('S_{11}')
    axis([8.1e09 12.4e09 -1.2 0.5])
    legend('Real','Imag')
    hold on
201 figure()
    plot(freq,S11realmultfreq(2,1:length(freq)),freq,S11imagmultfreq...
       (2,1:length(freq)));
    title('S_{11} at d = .3in vs. freq')
    xlabel('Frequency')
    ylabel('S_{11}')
206 legend('Real','Imag')
    hold on
    figure()
    plot(freq,S11realmultfreq(3,1:length(freq)),freq,S11imagmultfreq...
       (3,1:length(freq)));
    title('S_{11} at d = .45in vs. freq')
211 xlabel('Frequency')
    ylabel('S_{11}')
    legend('Real','Imag')
    figure()
    hold on
216 plot(freq,S11realmultfreq(4,1:length(freq)),freq,S11imagmultfreq...
       (4,1:length(freq)));
    title('S_{11} at d = .6in vs. freq')
    xlabel('Frequency')
    ylabel('S_{11}')
```

```
    legend('Real','Imag')
221 hold on
    figure()
    plot(freq,S11realmultfreq(5,1:length(freq)),freq,S11imagmultfreq...
        (5,1:length(freq)));
    title('S_{11} at d = .75in vs. freq')
    xlabel('Frequency')
226 ylabel('S_{11}')
    legend('Real','Imag')
    hold on
    figure()
    plot(freq,S11realmultfreq(6,1:length(freq)),freq,S11imagmultfreq...
        (6,1:length(freq)));
231 title('S_{11} at d = .9in vs. freq')
    xlabel('Frequency')
    ylabel('S_{11}')
    legend('Real','Imag')
    hold on
236 figure()
    plot(freq,S21realmultfreq(1,1:length(freq)),freq,S21imagmultfreq...
        (1,1:length(freq)));
    title('S_{21} at d = .15in vs. freq')
    xlabel('Frequency')
    ylabel('S_{21}')
241 legend('Real','Imag')
    hold on
    figure()
    plot(freq,S21realmultfreq(2,1:length(freq)),freq,S21imagmultfreq...
        (2,1:length(freq)));
    title('S_{21} at d = .3in vs. freq')
246 xlabel('Frequency')
    ylabel('S_{21}')
    legend('Real','Imag')
    hold on
    figure()
251 plot(freq,S21realmultfreq(3,1:length(freq)),freq,S21imagmultfreq...
        (3,1:length(freq)));
    title('S_{21} at d = .45in vs. freq')
    xlabel('Frequency')
    ylabel('S_{21}')
    legend('Real','Imag')
256 hold on
    figure()
    plot(freq,S21realmultfreq(4,1:length(freq)),freq,S21imagmultfreq...
        (4,1:length(freq)));
    title('S_{21} at d = .6in vs. freq')
    xlabel('Frequency')
261 ylabel('S_{21}')
    legend('Real','Imag')
    hold on
    figure()
```

```
    plot(freq,S21realmultfreq(5,1:length(freq)),freq,S21imagmultfreq...
        (5,1:length(freq)));
266 title('S_{21} at d = .75in vs. freq')
    xlabel('Frequency')
    ylabel('S_{21}')
    legend('Real','Imag')
    hold on
271 figure()
    plot(freq,S21realmultfreq(6,1:length(freq)),freq,S21imagmultfreq...
        (6,1:length(freq)));
    title('S_{21} at d = .9in vs. freq')
    xlabel('Frequency')
    ylabel('S_{21}')
276 legend('Real','Imag')

    %The following will plot S-parameters for magnitude and phase
    figure()
    plot(freq,magmultfreq11(1,1:length(freq)),freq,magmultfreq11(2,1:...
        length(freq)),freq,magmultfreq11(3,1:length(freq)),freq,...
        magmultfreq11(4,1:length(freq)),freq,magmultfreq11(5,1:length(...
        freq)),freq,magmultfreq11(6,1:length(freq)));
281 title('Magnitude S_{11} vs. Frequency For Multiple Insert Widths')
    xlabel('Frequency in Hz')
    ylabel('|S_{11}|')
    axis([8.1e09 12.4e09 -0.2 1.2])
    legend('.15in','.30in','.45in','.60in','.75in','.90in')
286 figure()
    plot(freq,phasemultfreq11(1,1:length(freq)),freq,phasemultfreq11...
        (2,1:length(freq)),freq,phasemultfreq11(3,1:length(freq)),freq,...
        phasemultfreq11(4,1:length(freq)),freq,phasemultfreq11(5,1:...
        length(freq)),freq,phasemultfreq11(6,1:length(freq)));
    title('Phase S_{11} vs. Frequency For Multiple Insert Widths')
    xlabel('Frequency in Hz')
    ylabel('<S_{11}')
291 legend('.15in','.30in','.45in','.60in','.75in','.90in')
    figure()
    plot(freq,magmultfreq21(1,1:length(freq)),freq,magmultfreq21(2,1:...
        length(freq)),freq,magmultfreq21(3,1:length(freq)),freq,...
        magmultfreq21(4,1:length(freq)),freq,magmultfreq21(5,1:length(...
        freq)),freq,magmultfreq21(6,1:length(freq)));
    title('Magnitude S_{21} vs. Frequency For Multiple Insert Widths')
    xlabel('Frequency in Hz')
296 ylabel('|S_{21}|')
    axis([8.1e09 12.4e09 -0.2 1.2])
    legend('.15in','.30in','.45in','.60in','.75in','.90in')
    figure()
    plot(freq,phasemultfreq21(1,1:length(freq)),freq,phasemultfreq21...
        (2,1:length(freq)),freq,phasemultfreq21(3,1:length(freq)),freq,...
        phasemultfreq21(4,1:length(freq)),freq,phasemultfreq21(5,1:...
        length(freq)),freq,phasemultfreq21(6,1:length(freq)));
301 title('Phase S21 vs. Frequency For Multiple Insert Widths')
    xlabel('Frequency in Hz')
```

```
ylabel('<S_{21}')
legend('.15in','.30in','.45in','.60in','.75in','.90in')
```

Appendix D. Mode Determination

Real S_{11} For Determining Number of Modes

		max mode	d in inches										
Frequency	# of modes			1	3	5	7	9	11	13	15	17	19
		3	0.15	-0.999975	-0.99997	-0.999984	-0.999992	-0.999993	-0.999993	-0.9999939	-0.999994	-0.999994	-0.999994
8.20E09		7	0.3	-0.977684	-0.997148	-0.99765	-0.99807	-0.998139	-0.998186	-0.9982427	-0.99825	-0.998271	-0.998290
		15	0.45	-0.37967	-0.915311	-0.936895	-0.942510	-0.944857	-0.946082	-0.9468123	-0.94728	-0.947616	-0.947857
		29	0.6	-0.012796	-0.453948	-0.481832	-0.496416	-0.511698	-0.515458	-0.517076	-0.520478	-0.521610	-0.522088
		29	0.75	0.003242	-0.003751	-0.024178	-0.025160	-0.026021	-0.028514	-0.0285439	-0.028729	-0.029471	-0.029464
		1	0.9	0.00E00	0.00E00	0.00E00	0.00E00	0.00E00	0.00E00	0.00E00	0.00E00	0.00E00	0.00E00
		1	0.15	-0.999971	-0.999974	-0.999981	-0.999991	-0.999992	-0.999992	-0.999993	-0.999993	-0.999993	-0.999993
8.41E09		5	0.3	-0.974028	-0.99668	-0.997280	-0.997761	-0.997841	-0.997896	-0.997962	-0.997979	-0.997995	-0.998017
		19	0.45	-0.333501	-0.901428	-0.926417	-0.932935	-0.935661	-0.937087	-0.9379353	-0.938481	-0.938870	-0.93915
		27	0.6	-0.007926	-0.407997	-0.436010	-0.450529	-0.465875	-0.469681	-0.4713105	-0.474740	-0.475889	-0.476372
		11	0.75	0.003395	-0.000784	-0.017082	-0.017873	-0.018581	-0.020626	-0.0206488	-0.020801	-0.021417	-0.021405
		1	0.9	0.00E00	0.00E00	0.00E00	0.00E00	0.00E00	0.00E00	0.00E00	0.00E00	0.00E00	0.00E00
		1	0.15	-0.999968	-0.99997	-0.999985	-0.999990	-0.999991	-0.999991	-0.9999921	-0.999992	-0.999992	-0.999992
8.62E09		7	0.3	-0.970150	-0.996181	-0.996887	-0.997434	-0.997527	-0.997590	-0.9976658	-0.997685	-0.997704	-0.997729
		15	0.45	-0.292156	-0.886684	-0.915245	-0.922716	-0.925846	-0.927480	-0.9284542	-0.92908	-0.929528	-0.929845
		27	0.6	-0.004281	-0.365781	-0.393564	-0.407816	-0.423008	-0.426807	-0.4284251	-0.431835	-0.432982	-0.433461
		11	0.75	0.003458	0.001532	-0.011444	-0.012081	-0.012665	-0.014346	-0.0143633	-0.014488	-0.014991	-0.014986
		1	0.9	0.00E00	0.00E00	0.00E00	0.00E00	0.00E00	0.00E00	0.00E00	0.00E00	0	0.00E00
		1	0.15	-0.999964	-0.999967	-0.999983	-0.999989	-0.999990	-0.999990	-0.9999911	-0.999991	-0.999991	-0.999991
8.83E09		7	0.3	-0.966035	-0.995654	-0.996454	-0.997089	-0.997195	-0.997267	-0.9973529	-0.997375	-0.997396	-0.997425
		15	0.45	-0.255106	-0.871029	-0.903321	-0.911791	-0.915352	-0.917209	-0.9183161	-0.919034	-0.919536	-0.919901
		29	0.6	-0.001556	-0.32697	-0.354225	-0.368049	-0.382910	-0.386658	-0.3882446	-0.391591	-0.392726	-0.393196
		28	0.75	0.003454	0.003372	-0.006895	-0.007400	-0.007871	-0.009257	-0.0092701	-0.009372	-0.009781	-0.009782
		1	0.9	0.00E00	0.00E00	0.00E00	0.00E00	0.00E00	0.00E00	0.00E00	0.00E00	0.00E00	0.00E00
		1	0.15	-0.999964	-0.999961	-0.999981	-0.999984	-0.999989	-0.999989	-0.9999901	-0.999990	-0.999990	-0.999990
9.04E09		3	0.3	-0.961667	-0.995091	-0.99601	-0.996724	-0.996841	-0.996925	-0.9970221	-0.997041	-0.997071	-0.997104
		19	0.45	-0.221926	-0.854381	-0.890586	-0.900111	-0.904121	-0.906214	-0.9074614	-0.908273	-0.908831	-0.909248
		27	0.6	0.000473	-0.291261	-0.317752	-0.331021	-0.345408	-0.349067	-0.3506066	-0.353866	-0.354967	-0.355427
		5	0.75	0.003400	0.004850	-0.003164	-0.003561	-0.003949	-0.005071	-0.0050858	-0.005168	-0.005509	-0.005505
		1	0.9	0.00E00	0.00E00	0.00E00	0.00E00	0.00E00	0.00E00	0.00E00	0.00E00	0.00E00	0.00E00
		1	0.15	-0.999956	-0.999959	-0.999979	-0.999981	-0.999981	-0.999988	-0.9998891	-0.999988	-0.999988	-0.999989
9.25E09		7	0.3	-0.957023	-0.994489	-0.995534	-0.996334	-0.996471	-0.996563	-0.9966721	-0.996700	-0.996721	-0.996764
		21	0.45	-0.192201	-0.836671	-0.876954	-0.887605	-0.892084	-0.894426	-0.8958231	-0.896732	-0.897364	-0.897824
		21	0.6	0.001962	-0.258389	-0.283926	-0.296542	-0.310342	-0.313881	-0.3153605	-0.318492	-0.319561	-0.320007
		11	0.75	0.003306	0.006049	-7.52E-05	-0.000380	-0.000691	-0.001604	-0.0016118	-0.001678	-0.001954	-0.001952

21	23	25	27	29	31	33	35	37	39	41	43	45	47	49
-0.99999	-0.99999	-0.99999	-0.99999	-0.99999	-0.99999	-0.99999	-0.99999	-0.99999	-0.99999	-0.99999	-0.99999	-0.9999946	-0.99999	-0.99999
-0.99829	-0.99830	-0.99831	-0.99831	-0.99831	-0.99832	-0.99832	-0.99832	-0.99833	-0.99833	-0.99833	-0.99833	-0.9983379	-0.99833	-0.99834
-0.94803	-0.94818	-0.94829	-0.94838	-0.94846	-0.94853	-0.94858	-0.94863	-0.94867	-0.94871	-0.94874	-0.94877	-0.9487997	-0.94882	-0.94884
-0.52341	-0.52389	-0.52411	-0.52479	-0.52504	-0.52516	-0.52557	-0.52572	-0.52580	-0.52607	-0.52616	-0.52622	-0.5264105	-0.52647	-0.52651
-0.02951	-0.02984	-0.02984	-0.02985	-0.03003	-0.03003	-0.03003	-0.03014	-0.03015	-0.03014	-0.03022	-0.03022	-0.0302214	-0.03027	-0.03027
0.00E00	0.00E00	0.00E00	0.00E00	0.00E00	0.00E00	0.00E00	0.00E00	0.00E00	0.00E00	0.00E00	0.00E00	0.00E00	0.00E00	0.00E00
-0.99999	-0.99999	-0.99999	-0.99999	-0.99999	-0.99999	-0.99999	-0.99999	-0.99999	-0.99999	-0.99999	-0.99999	-0.9999938	-0.99999	-0.99999
-0.99802	-0.99803	-0.99804	-0.99804	-0.99805	-0.99805	-0.99805	-0.99806	-0.99806	-0.99806	-0.99806	-0.99807	-0.9980727	-0.99807	-0.99807
-0.93936	-0.93952	-0.93965	-0.93976	-0.93985	-0.93993	-0.93999	-0.94005	-0.94010	-0.94014	-0.94018	-0.94021	-0.9402458	-0.94027	-0.94029
-0.47771	-0.47820	-0.47841	-0.47910	-0.47935	-0.47948	-0.47989	-0.48004	-0.48012	-0.48039	-0.48049	-0.48055	-0.4807419	-0.48080	-0.48084
-0.02144	-0.02171	-0.02171	-0.02172	-0.02187	-0.02187	-0.02187	-0.02196	-0.02197	-0.02196	-0.02203	-0.02203	-0.0220289	-0.02207	-0.02207
0.00E00	0.00E00	0.00E00	0.00E00	0.00E00	0.00E00	0.00E00	0.00E00	0.00E00	0.00E00	0.00E00	0.00E00	0.00E00	0.00E00	0.00E00
-0.99999	-0.99999	-0.99999	-0.99999	-0.99999	-0.99999	-0.99999	-0.99999	-0.99999	-0.99999	-0.99999	-0.99999	-0.999993	-0.99999	-0.99999
-0.99773	-0.99774	-0.99775	-0.99776	-0.99776	-0.99777	-0.99777	-0.99777	-0.99778	-0.99778	-0.99778	-0.99779	-0.9977929	-0.99779	-0.99779
-0.93009	-0.93028	-0.93043	-0.93055	-0.93066	-0.93074	-0.93082	-0.93086	-0.93094	-0.93099	-0.93103	-0.93107	-0.9311068	-0.93113	-0.93116
-0.4348	-0.43528	-0.43550	-0.43618	-0.43643	-0.43656	-0.43697	-0.43712	-0.43720	-0.43747	-0.43756	-0.43762	-0.4378177	-0.43788	-0.43792
-0.01502	-0.01524	-0.01524	-0.01525	-0.01537	-0.01537	-0.01537	-0.01545	-0.01545	-0.01545	-0.01550	-0.01550	-0.0155009	-0.01553	-0.01553
0.00E00	0.00E00	0.00E00	0.00E00	0.00E00	0.00E00	0.00E00	0.00E00	0.00E00	0.00E00	0.00E00	0.00E00	0.00E00	0.00E00	0.00E00
-0.99999	-0.99999	-0.99999	-0.99999	-0.99999	-0.99999	-0.99999	-0.99999	-0.99999	-0.99999	-0.99999	-0.99999	-0.9999921	-0.99999	-0.99999
-0.99743	-0.99744	-0.99745	-0.99746	-0.99746	-0.99747	-0.99747	-0.99748	-0.99748	-0.99749	-0.99749	-0.99749	-0.9974975	-0.99749	-0.99750
-0.92017	-0.92039	-0.92056	-0.92070	-0.92082	-0.92092	-0.92100	-0.92107	-0.92114	-0.92119	-0.92124	-0.92129	-0.921331	-0.92136	-0.92139
-0.39451	-0.39499	-0.39520	-0.39588	-0.39612	-0.39625	-0.39665	-0.39680	-0.39688	-0.39714	-0.39724	-0.39729	-0.3974854	-0.39754	-0.39759
-0.00981	-0.00999	-0.00999	-0.01000	-0.01010	-0.01010	-0.01010	-0.01016	-0.01016	-0.01016	-0.01020	-0.01020	-0.0102067	-0.01023	-0.01023
0.00E00	0.00E00	0.00E00	0.00E00	0.00E00	0.00E00	0.00E00	0.00E00	0.00E00	0.00E00	0.00E00	0.00E00	0.00E00	0.00E00	0.00E00
-0.99999	-0.99999	-0.99999	-0.99999	-0.99999	-0.99999	-0.99999	-0.99999	-0.99999	-0.99999	-0.99999	-0.99999	-0.9999913	-0.99999	-0.99999
-0.99711	-0.99712	-0.99714	-0.99714	-0.99715	-0.99716	-0.99716	-0.99716	-0.99717	-0.99717	-0.99717	-0.99718	-0.9971853	-0.99718	-0.99719
-0.90956	-0.90980	-0.90999	-0.91015	-0.91028	-0.91040	-0.91049	-0.91057	-0.91064	-0.91071	-0.91076	-0.91081	-0.9108601	-0.91089	-0.91093
-0.35670	-0.35717	-0.35738	-0.35803	-0.35828	-0.35840	-0.35879	-0.35893	-0.35901	-0.35927	-0.35936	-0.35941	-0.359602	-0.35966	-0.35970
-0.00552	-0.00568	-0.00567	-0.00568	-0.00576	-0.00576	-0.00576	-0.00582	-0.00582	-0.00581	-0.00585	-0.00585	-0.0058538	-0.00587	-0.00587
0.00E00	0.00E00	0.00E00	0.00E00	0.00E00	0.00E00	0.00E00	0.00E00	0.00E00	0.00E00	0.00E00	0.00E00	0.00E00	0.00E00	0.00E00
-0.99998	-0.99998	-0.99999	-0.99999	-0.99999	-0.99999	-0.99999	-0.99999	-0.99999	-0.99999	-0.99999	-0.99999	-0.9999904	-0.99999	-0.99999
-0.99677	-0.99678	-0.99680	-0.99681	-0.99681	-0.99682	-0.99683	-0.99683	-0.99684	-0.99684	-0.99684	-0.99685	-0.9968551	-0.99685	-0.99686
-0.89817	-0.89844	-0.89866	-0.89884	-0.89898	-0.89911	-0.89921	-0.89931	-0.89939	-0.89946	-0.89952	-0.89957	-0.8996283	-0.89967	-0.89971
-0.32123	-0.32169	-0.32189	-0.32252	-0.32275	-0.32287	-0.32325	-0.32339	-0.32346	-0.32371	-0.32380	-0.32385	-0.3240341	-0.32409	-0.32413
-0.00197	-0.00209	-0.00209	-0.00209	-0.00216	-0.00216	-0.00216	-0.00220	-0.00220	-0.00220	-0.00223	-0.00223	-0.0022366	-0.00225	-0.00225

		1	0.9	0.00E00	0.00E00	0.00E00	0.00E00	0.00E00	0.00E00	0.00E00	0.00E00	0.00E00	0.00E00
	# of modes			1	3	5	7	9	11	13	15	17	19
		1	0.15	-0.99995	-0.999956	-0.99997	-0.999985	-0.999986	-0.999987	-0.999988	-0.999988	-0.999988	-0.999988
9.46E09		9	0.3	-0.95210	-0.993846	-0.995029	-0.995928	-0.99607	-0.996186	-0.996301	-0.996332	-0.996362	-0.996404
		17	0.45	-0.16562	-0.81782	-0.86235	-0.87418	-0.87916	-0.88177	-0.883324	-0.88433	-0.88504	-0.88555
		27	0.6	0.003018	-0.22812	-0.25255	-0.26444	-0.27756	-0.28095	-0.28236	-0.28535	-0.28638	-0.28680
		5	0.75	0.003179	0.007026	0.002502	0.002275	0.002032	0.001297	0.0012954	0.001243	0.001018	0.001022
		1	0.9	0.00E00	0.00E00	0.00E00	0.00E00	0.00E00	0.00E00	0.00E00	0.00E00	0	0.00E00
		1	0.15	-0.99994	-0.99995	-0.99997	-0.999984	-0.999985	-0.999985	-0.999987	-0.999987	-0.999987	-0.999987
9.67E09		7	0.3	-0.94687	-0.993157	-0.99449	-0.99549	-0.995658	-0.995771	-0.9959079	-0.995943	-0.995976	-0.996022
		23	0.45	-0.14186	-0.79774	-0.84668	-0.85976	-0.86527	-0.86815	-0.8698791	-0.87100	-0.87177	-0.87234
		23	0.6	0.003719	-0.20024	-0.22345	-0.23456	-0.24693	-0.25016	-0.2514974	-0.25432	-0.25530	-0.25570
		5	0.75	0.003024	0.007822	0.004663	0.004504	0.004320	0.003740	0.0037418	0.003702	0.003523	0.003526
		1	0.9	0.00E00	0.00E00	0.00E00	0.00E00	0.00E00	0.00E00	0.00E00	0.00E00	0.00E00	0.00E00
		1	0.15	-0.999942	-0.99994	-0.99997	-0.999983	-0.999984	-0.999984	-0.9999858	-0.999986	-0.999986	-0.999986
9.88E09		7	0.3	-0.941309	-0.992418	-0.993918	-0.995030	-0.995213	-0.995341	-0.9954902	-0.995529	-0.995565	-0.995616
		19	0.45	-0.120688	-0.776330	-0.829851	-0.844234	-0.850305	-0.853481	-0.855387	-0.856624	-0.857483	-0.858110
		23	0.6	0.004127	-0.174586	-0.196474	-0.206767	-0.218340	-0.221381	-0.2226334	-0.225285	-0.226208	-0.226585
		5	0.75	0.002847	0.008470	0.006481	0.006380	0.006248	0.005803	0.0058069	0.005779	0.005639	0.005642
		1	0.9	0.00E00	0.00E00	0.00E00	0.00E00	0.00E00	0.00E00	0.00E00	0.00E00	0.00E00	0.00E00
		1	0.15	-0.999936	-0.99994	-0.99997	-0.999981	-0.999983	-0.999983	-0.9999847	-0.999985	-0.999985	-0.999985
1.01E10		7	0.3	-0.935396	-0.991623	-0.993307	-0.994538	-0.994739	-0.994881	-0.9950457	-0.995086	-0.995129	-0.995185
		21	0.45	-0.101843	-0.75347	-0.81174	-0.827488	-0.83415	-0.837646	-0.8397332	-0.84109	-0.84203	-0.84272
		21	0.6	0.004290	-0.150970	-0.17146	-0.180920	-0.19165	-0.194505	-0.1956661	-0.19813	-0.19899	-0.19934
		7	0.75	0.002649	0.008992	0.008009	0.007960	0.007875	0.007545	0.0075515	0.007534	0.007427	0.007431
		1	0.9	0.00E00	0.00E00	0.00E00	0.00E00	0.00E00	0.00E00	0.00E00	0.00E00	0	0.00E00
		1	0.15	-0.999933	-0.999938	-0.999969	-0.999980	-0.999981	-0.999982	-0.9999835	-0.999983	-0.999984	-0.999984
1.03E10		7	0.3	-0.929108	-0.990766	-0.992652	-0.994012	-0.994234	-0.994391	-0.9945721	-0.994619	-0.994664	-0.994725
		23	0.45	-0.085124	-0.729044	-0.792195	-0.809386	-0.816672	-0.820495	-0.8227843	-0.82427	-0.82530	-0.82606
		23	0.6	0.004242	-0.129254	-0.148306	-0.156909	-0.166782	-0.169432	-0.1704964	-0.17277	-0.17357	-0.17389
		3	0.75	0.002434	0.009407	0.009291	0.009286	0.009243	0.009014	0.0090224	0.009013	0.008937	0.008940
		1	0.9	0.00E00	0.00E00	0.00E00	0.00E00	0.00E00	0.00E00	0.00E00	0.00E00	0.00E00	0.00E00
	# of modes			1	3	5	7	9	11	13	15	17	19
		1	0.15	-0.999928	-0.999933	-0.999966	-0.999978	-0.999980	-0.999980	-0.9999823	-0.999982	-0.999982	-0.999983
1.05E10		7	0.3	-0.922418	-0.989840	-0.991957	-0.993450	-0.993694	-0.993867	-0.9940662	-0.994118	-0.994167	-0.994235
		23	0.45	-0.070346	-0.702910	-0.771074	-0.789768	-0.797712	-0.801888	-0.8043839	-0.80601	-0.80714	-0.80796
		23	0.6	0.004014	-0.109310	-0.126876	-0.134627	-0.143625	-0.146064	-0.1470342	-0.14911	-0.14985	-0.15015
		5	0.75	0.002203	0.009729	0.010358	0.010392	0.010387	0.010245	0.0102556	0.010255	0.010204	0.010208

0.00E00	0.00E00	0.00E00	0.00E00	0.00E00	0.00E00	0.00E00	0.00E00	0.00E00	0.00E00	0.00E00	0.00E00	0.00E00	0.00E00	0.00E00
21	23	25	27	29	31	33	35	37	39	41	43	45	47	49
-0.999984	-0.999984	-0.999985	-0.999985	-0.999985	-0.999985	-0.999985	-0.999985	-0.999985	-0.999985	-0.999985	-0.999985	-0.9999895	-0.999985	-0.999985
-0.996417	-0.996429	-0.996450	-0.996457	-0.996464	-0.996475	-0.996480	-0.996484	-0.996492	-0.996495	-0.996497	-0.996503	-0.9965054	-0.996507	-0.996511
-0.885940	-0.886243	-0.886486	-0.886684	-0.886849	-0.886987	-0.887106	-0.887208	-0.887297	-0.887375	-0.887444	-0.887505	-0.8875608	-0.887610	-0.887654
-0.287982	-0.288416	-0.288609	-0.289214	-0.289438	-0.289548	-0.28991	-0.290042	-0.290114	-0.290353	-0.290437	-0.290488	-0.2906568	-0.290714	-0.290752
0.001008	0.000906	0.000908	0.000905	0.000849	0.000849	0.000849	0.000814	0.000814	0.000815	0.000792	0.000791	0.0007932	0.000776	0.000775
0.00E00	0.00E00	0.00E00	0.00E00	0.00E00	0.00E00	0.00E00	0.00E00	0.00E00	0.00E00	0.00E00	0.00E00	0.00E00	0.00E00	0.00E00
-0.999987	-0.999987	-0.999988	-0.999988	-0.999988	-0.999988	-0.999988	-0.999988	-0.999988	-0.999988	-0.999988	-0.999988	-0.9999885	-0.999988	-0.999988
-0.996036	-0.996050	-0.996073	-0.996081	-0.996088	-0.996101	-0.996106	-0.996111	-0.996119	-0.996123	-0.996126	-0.996132	-0.9961347	-0.996136	-0.996141
-0.872771	-0.873113	-0.873382	-0.873601	-0.873783	-0.873933	-0.874068	-0.874181	-0.874280	-0.874366	-0.874443	-0.874511	-0.874572	-0.874626	-0.874676
-0.256816	-0.257229	-0.257413	-0.257985	-0.258198	-0.258303	-0.258646	-0.258772	-0.258840	-0.259066	-0.259146	-0.259195	-0.2593544	-0.259405	-0.259445
0.003516	0.003435	0.003437	0.003434	0.003389	0.003390	0.003390	0.003362	0.003362	0.003363	0.003344	0.003344	0.0033453	0.003331	0.003331
0.00E00	0.00E00	0.00E00	0.00E00	0.00E00	0.00E00	0.00E00	0.00E00	0.00E00	0.00E00	0.00E00	0.00E00	0.00E00	0.00E00	0.00E00
-0.999986	-0.999986	-0.999987	-0.999987	-0.999987	-0.999987	-0.999987	-0.999987	-0.999987	-0.999987	-0.999987	-0.999987	-0.9999875	-0.999987	-0.999987
-0.995632	-0.995648	-0.995671	-0.995681	-0.995690	-0.995704	-0.995710	-0.995715	-0.995724	-0.995728	-0.995731	-0.995738	-0.9957411	-0.995743	-0.995748
-0.858584	-0.858955	-0.859251	-0.859493	-0.859694	-0.859864	-0.860009	-0.860133	-0.860242	-0.860337	-0.860422	-0.860496	-0.860564	-0.860624	-0.860676
-0.227631	-0.228027	-0.228193	-0.228731	-0.228932	-0.229031	-0.229353	-0.229471	-0.229536	-0.229748	-0.229824	-0.229869	-0.2300193	-0.230071	-0.230104
0.005635	0.005571	0.005573	0.005572	0.005536	0.005537	0.005537	0.005515	0.005515	0.005516	0.005501	0.005501	0.0055022	0.005491	0.005491
0.00E00	0.00E00	0.00E00	0.00E00	0.00E00	0.00E00	-1.00E-15	-1.00E-15	-1.00E-15	-1.00E-15	-1.00E-15	-1.00E-15	-1.00E-15	-1.00E-15	-1.00E-15
-0.999985	-0.999985	-0.999986	-0.999986	-0.999986	-0.999986	-0.999986	-0.999986	-0.999986	-0.999986	-0.999986	-0.999986	-0.9999865	-0.999986	-0.999986
-0.995203	-0.995220	-0.995247	-0.995257	-0.995266	-0.995282	-0.995288	-0.995294	-0.995304	-0.995308	-0.995312	-0.995319	-0.9953226	-0.995325	-0.995330
-0.843248	-0.843659	-0.843981	-0.844247	-0.844468	-0.844654	-0.844813	-0.844950	-0.84507	-0.845174	-0.845267	-0.845345	-0.8454232	-0.845489	-0.845545
-0.200321	-0.200684	-0.200849	-0.201350	-0.201538	-0.201630	-0.201931	-0.202041	-0.202101	-0.202299	-0.202370	-0.202412	-0.2025522	-0.202600	-0.202632
0.007427	0.007378	0.007380	0.007379	0.007352	0.007352	0.007353	0.007336	0.007336	0.007337	0.007325	0.007325	0.0073267	0.007318	0.007318
0.00E00	0.00E00	0.00E00	0.00E00	0.00E00	0.00E00	0.00E00	0.00E00	0.00E00	0.00E00	0.00E00	0.00E00	0.00E00	0.00E00	0.00E00
-0.999984	-0.999984	-0.999984	-0.999985	-0.999985	-0.999985	-0.999985	-0.999985	-0.999985	-0.999985	-0.999985	-0.999985	-0.9999855	-0.999985	-0.999985
-0.994745	-0.994764	-0.994794	-0.994805	-0.994815	-0.994832	-0.994839	-0.994845	-0.994857	-0.994861	-0.994865	-0.994873	-0.9948768	-0.994879	-0.994885
-0.826635	-0.827081	-0.827438	-0.827729	-0.827972	-0.828176	-0.828350	-0.828500	-0.82863	-0.828745	-0.828847	-0.828937	-0.8290179	-0.829090	-0.829156
-0.174799	-0.175138	-0.175286	-0.175749	-0.175924	-0.176009	-0.176281	-0.176389	-0.176445	-0.176628	-0.176694	-0.176731	-0.1768615	-0.176906	-0.176936
0.008939	0.008903	0.008905	0.008905	0.008885	0.008886	0.008887	0.008874	0.008874	0.008875	0.008866	0.008866	0.0088674	0.008861	0.008861
0.00E00	0.00E00	0.00E00	0.00E00	0.00E00	0.00E00	0.00E00	0.00E00	0.00E00	0.00E00	0.00E00	0.00E00	0.00E00	0.00E00	0.00E00
21	23	25	27	29	31	33	35	37	39	41	43	45	47	49
-0.999983	-0.999983	-0.999983	-0.999983	-0.999983	-0.999984	-0.999984	-0.999984	-0.999984	-0.999984	-0.999984	-0.999984	-0.9999844	-0.999984	-0.999984
-0.994256	-0.994277	-0.994310	-0.994322	-0.994333	-0.994352	-0.994359	-0.994366	-0.994379	-0.994384	-0.994388	-0.994397	-0.994401	-0.994404	-0.994410
-0.808590	-0.809078	-0.809468	-0.809786	-0.81005	-0.810274	-0.810464	-0.810628	-0.810770	-0.810896	-0.811006	-0.811105	-0.8111933	-0.811272	-0.811344
-0.150973	-0.151285	-0.151421	-0.151845	-0.152006	-0.152084	-0.152338	-0.152432	-0.152483	-0.152651	-0.152711	-0.152747	-0.1528655	-0.152906	-0.152933
0.010209	0.010184	0.010186	0.010187	0.010173	0.010173	0.010175	0.010166	0.010166	0.010167	0.010161	0.010161	0.0101619	0.010157	0.010157

		1	0.9	0.00E00	0.00E00	0.00E00	0.00E00	0.00E00	0.00E00	0.00E00	0.00E00	0	0.00E00
		1	0.15	-0.999923	-0.999929	-0.999964	-0.999977	-0.999978	-0.999979	-0.999981	-0.99998	-0.99998	-0.999982
1.07E10		9	0.3	-0.915297	-0.988835	-0.991197	-0.992848	-0.993115	-0.993306	-0.9935247	-0.99358	-0.993635	-0.993710
		27	0.45	-0.05734	-0.674910	-0.74818	-0.768449	-0.777084	-0.781629	-0.7843474	-0.786120	-0.787352	-0.788250
		23	0.6	0.003629	-0.091025	-0.107076	-0.113983	-0.122101	-0.124323	-0.1251988	-0.127082	-0.127755	-0.128023
		5	0.75	0.001958	0.009968	0.011236	0.011304	0.011332	0.011267	0.0112792	0.011286	0.011257	0.011261
		1	0.9	0.00E00	0.00E00	0.00E00	0.00E00	0.00E00	0.00E00	0.00E00	0.00E00	0.00E00	0.00E00
		1	0.15	-0.999917	-0.999921	-0.999961	-0.999975	-0.999977	-0.999978	-0.9999797	-0.999980	-0.999980	-0.999980
1.09E10		7	0.3	-0.907716	-0.987741	-0.990383	-0.992201	-0.992493	-0.992704	-0.9929434	-0.993009	-0.993065	-0.993146
		23	0.45	-0.04596	-0.644863	-0.723300	-0.745206	-0.754568	-0.759501	-0.7624542	-0.764380	-0.76572	-0.766696
		21	0.6	0.003105	-0.074302	-0.088818	-0.094895	-0.102135	-0.104138	-0.1049185	-0.106605	-0.107211	-0.107451
		7	0.75	0.001700	0.010132	0.011943	0.012041	0.012100	0.012100	0.0121140	0.012128	0.012118	0.012122
		1	0.9	0.00E00	0.00E00	0.00E00	0.00E00	0.00E00	0.00E00	0.00E00	0.00E00	0	0.00E00
		1	0.15	-0.999912	-0.999918	-0.999959	-0.999974	-0.999976	-0.999976	-0.9999784	-0.999978	-0.999979	-0.999979
1.11E10		11	0.3	-0.899642	-0.986545	-0.989502	-0.991502	-0.991823	-0.992059	-0.9923173	-0.992385	-0.992450	-0.992540
		31	0.45	-0.036070	-0.612569	-0.696170	-0.719774	-0.729896	-0.735238	-0.7384375	-0.740526	-0.741978	-0.743037
		17	0.6	0.002459	-0.059058	-0.072025	-0.077292	-0.083664	-0.085447	-0.0861336	-0.087623	-0.088162	-0.088375
		5	0.75	0.001431	0.010226	0.012492	0.012616	0.012704	0.012759	0.0127754	0.012795	0.012802	0.012806
		1	0.9	0.00E00	0.00E00	0.00E00	0.00E00	0.00E00	0.00E00	0.00E00	0.00E00	0.00E00	0.00E00
		1	0.15	-0.999906	-0.999911	-0.999956	-0.999972	-0.999974	-0.999975	-0.999977	-0.999977	-0.999977	-0.999978
1.14E10		9	0.3	-0.891040	-0.985230	-0.988545	-0.990746	-0.991097	-0.991352	-0.9916404	-0.991714	-0.991787	-0.991884
		25	0.45	-0.027546	-0.577781	-0.666476	-0.691826	-0.702740	-0.708510	-0.711969	-0.714228	-0.715799	-0.716945
		15	0.6	0.001704	-0.045225	-0.056636	-0.061118	-0.066637	-0.068199	-0.0687934	-0.070089	-0.070561	-0.070746
		9	0.75	0.001150	0.010252	0.012893	0.01304	0.013152	0.013255	0.0132730	0.013298	0.013319	0.013323
		11	0.9	0.00E00	0.00E00	0.00E00	0.00E00	0.00E00	0.00E00	0.00E00	0.00E00	0.00E00	0.00E00
	# of modes			1	3	5	7	9	11	13	15	17	19
		1	0.15	-0.999900	-0.999907	-0.999953	-0.999970	-0.999972	-0.999973	-0.9999756	-0.999976	-0.999976	-0.999977
1.16E10		9	0.3	-0.881873	-0.983776	-0.987499	-0.989924	-0.990308	-0.990589	-0.9909052	-0.990986	-0.991066	-0.991173
		29	0.45	-0.020279	-0.540212	-0.633825	-0.660961	-0.672692	-0.678907	-0.6826374	-0.685074	-0.686770	-0.688007
		17	0.6	0.000850	-0.032756	-0.042605	-0.046331	-0.051017	-0.052359	-0.0528627	-0.053968	-0.054374	-0.054532
		5	0.75	0.000860	0.010211	0.013149	0.013313	0.013449	0.013592	0.0136108	0.013641	0.013673	0.013677
		1	0.9	0.00E00	0.00E00	0.00E00	0.00E00	0.00E00	0.00E00	0.00E00	0.00E00	0.00E00	0.00E00
		1	0.15	-0.999894	-0.999901	-0.999950	-0.999969	-0.999971	-0.999972	-0.9999741	-0.999974	-0.999974	-0.999975
1.18E10		7	0.3	-0.872100	-0.982156	-0.986349	-0.989023	-0.989444	-0.989759	-0.9901021	-0.990191	-0.990278	-0.990396
		29	0.45	-0.014169	-0.499516	-0.597725	-0.626656	-0.639227	-0.645902	-0.6499131	-0.652536	-0.654361	-0.655693
		15	0.6	-9.26E-05	-0.021621	-0.029903	-0.032907	-0.036784	-0.037909	-0.0383237	-0.039245	-0.039585	-0.039716
		5	0.75	0.000560	0.010099	0.013255	0.013435	0.013590	0.013765	0.0137858	0.013821	0.013862	0.013867

0.00E00	0.00E00	0.00E00	0.00E00	0.00E00	0.00E00	0.00E00	0.00E00	0.00E00	0.00E00	0.00E00	0.00E00	0.00E00	0.00E00	0.00E00
-0.999982	-0.999982	-0.999982	-0.999982	-0.999982	-0.999982	-0.999983	-0.999983	-0.999983	-0.999983	-0.999983	-0.999983	-0.9999833	-0.999983	-0.999983
-0.993731	-0.993756	-0.993791	-0.993805	-0.993817	-0.993831	-0.993846	-0.993854	-0.993864	-0.993871	-0.993878	-0.993884	-0.993892	-0.993895	-0.993902
-0.788931	-0.789462	-0.789881	-0.790234	-0.790521	-0.790765	-0.790977	-0.791154	-0.791306	-0.791442	-0.791563	-0.791670	-0.7917662	-0.791852	-0.791930
-0.128761	-0.129051	-0.129171	-0.129561	-0.129701	-0.129771	-0.130001	-0.130091	-0.130141	-0.130291	-0.130348	-0.130381	-0.1304882	-0.130525	-0.130550
0.011264	0.011249	0.011251	0.011253	0.011244	0.011245	0.011246	0.011240	0.011241	0.011242	0.011238	0.011238	0.0112390	0.011236	0.011236
0.00E00	0.00E00	0.00E00	0.00E00	0.00E00	0.00E00	0.00E00	0.00E00	0.00E00	0.00E00	0.00E00	0.00E00	0.00E00	0.00E00	0.00E00
-0.999981	-0.999981	-0.999981	-0.999981	-0.999981	-0.999981	-0.999981	-0.999981	-0.999982	-0.999982	-0.999982	-0.999982	-0.9999821	-0.999982	-0.999982
-0.993171	-0.993191	-0.993231	-0.993251	-0.993264	-0.993281	-0.993296	-0.993304	-0.993319	-0.993325	-0.993331	-0.993341	-0.9933459	-0.993349	-0.993357
-0.767436	-0.768011	-0.768471	-0.768852	-0.769161	-0.769421	-0.769654	-0.769844	-0.770011	-0.770161	-0.770296	-0.770411	-0.7705172	-0.770616	-0.770695
-0.108126	-0.108376	-0.108481	-0.108831	-0.108961	-0.109021	-0.109234	-0.109311	-0.109352	-0.109489	-0.109533	-0.109568	-0.109664	-0.109697	-0.109719
0.012127	0.012121	0.012122	0.012125	0.012121	0.012121	0.012123	0.012120	0.012120	0.012122	0.012119	0.012119	0.0121207	0.012119	0.012119
0.00E00	0.00E00	0.00E00	0.00E00	0.00E00	0.00E00	0.00E00	0.00E00	0.00E00	0.00E00	0.00E00	0.00E00	0.00E00	0.00E00	0.00E00
-0.999975	-0.999975	-0.999986	-0.999986	-0.999986	-0.999986	-0.999986	-0.999986	-0.999986	-0.999986	-0.999986	-0.999986	-0.999981	-0.999981	-0.999981
-0.992568	-0.992596	-0.992635	-0.992654	-0.992668	-0.992694	-0.992704	-0.992711	-0.992729	-0.992734	-0.992742	-0.992753	-0.9927582	-0.992762	-0.992770
-0.743835	-0.744465	-0.744966	-0.745375	-0.745715	-0.746001	-0.746245	-0.746455	-0.746634	-0.746795	-0.746941	-0.747067	-0.7471802	-0.747281	-0.747373
-0.088966	-0.089194	-0.089292	-0.089597	-0.089715	-0.089771	-0.089954	-0.090021	-0.090066	-0.090181	-0.090225	-0.090251	-0.0903362	-0.090364	-0.090385
0.012813	0.012814	0.012815	0.012819	0.012818	0.012819	0.012821	0.012820	0.012821	0.012822	0.012821	0.012822	0.0128229	0.012822	0.012822
0.00E00	0.00E00	0.00E00	0.00E00	0.00E00	0.00E00	0.00E00	0.00E00	0.00E00	0.00E00	0.00E00	0.00E00	0.00E00	0.00E00	0.00E00
-0.999979	-0.999979	-0.999979	-0.999979	-0.999979	-0.999979	-0.999979	-0.999979	-0.999979	-0.999979	-0.999979	-0.999979	-0.9999798	-0.999979	-0.999979
-0.991915	-0.991946	-0.991991	-0.992005	-0.992026	-0.992054	-0.992064	-0.992074	-0.992091	-0.992096	-0.992104	-0.992114	-0.9921234	-0.992126	-0.992137
-0.717811	-0.718491	-0.719031	-0.719475	-0.719841	-0.720151	-0.720416	-0.720641	-0.720841	-0.721015	-0.721166	-0.721305	-0.7214272	-0.721536	-0.721636
-0.071262	-0.071462	-0.071541	-0.071814	-0.071916	-0.071966	-0.072126	-0.072186	-0.072216	-0.072321	-0.072362	-0.072385	-0.0724593	-0.072485	-0.072502
0.013332	0.013339	0.013340	0.013345	0.013347	0.013348	0.013350	0.013352	0.013352	0.013353	0.013354	0.013354	0.0133558	0.013356	0.013356
0.00E00	0.00E00	0.00E00	0.00E00	0.00E00	0.00E00	0.00E00	0.00E00	0.00E00	0.00E00	0.00E00	0.00E00	0.00E00	0.00E00	0.00E00
21	23	25	27	29	31	33	35	37	39	41	43	45	47	49
-0.999971	-0.999971	-0.999971	-0.999971	-0.999971	-0.999975	-0.999975	-0.999975	-0.999975	-0.999975	-0.999975	-0.999975	-0.9999785	-0.999978	-0.999978
-0.991206	-0.991246	-0.991292	-0.991316	-0.991326	-0.991354	-0.991366	-0.991386	-0.991406	-0.991408	-0.991415	-0.991428	-0.9914345	-0.991439	-0.991449
-0.688944	-0.689675	-0.690261	-0.690736	-0.691135	-0.691466	-0.691754	-0.691999	-0.692211	-0.692401	-0.692566	-0.692711	-0.6928454	-0.692963	-0.693070
-0.054971	-0.055145	-0.055215	-0.055447	-0.055535	-0.055571	-0.055714	-0.055766	-0.055794	-0.055884	-0.055918	-0.055931	-0.0560010	-0.056023	-0.056038
0.013689	0.013700	0.013702	0.013707	0.013712	0.013713	0.013715	0.013718	0.013719	0.013720	0.013722	0.013722	0.0137235	0.013724	0.013724
0.00E00	0.00E00	0.00E00	0.00E00	0.00E00	0.00E00	0.00E00	0.00E00	0.00E00	0.00E00	0.00E00	0.00E00	0.00E00	0.00E00	0.00E00
-0.999975	-0.999976	-0.999976	-0.999976	-0.999976	-0.999976	-0.999976	-0.999976	-0.999977	-0.999977	-0.999977	-0.999977	-0.9999772	-0.999977	-0.999977
-0.990431	-0.990465	-0.990521	-0.990544	-0.990566	-0.990595	-0.990611	-0.990621	-0.990645	-0.990651	-0.990661	-0.990676	-0.9906827	-0.990684	-0.990699
-0.656702	-0.657485	-0.658115	-0.658634	-0.659061	-0.659420	-0.659721	-0.659992	-0.660222	-0.660421	-0.660601	-0.660760	-0.660902	-0.661029	-0.661144
-0.040085	-0.040225	-0.040296	-0.040481	-0.040556	-0.040597	-0.040706	-0.040745	-0.040771	-0.040844	-0.040876	-0.040893	-0.0409463	-0.040965	-0.040977
0.013879	0.013895	0.013896	0.013902	0.013909	0.013910	0.013913	0.013917	0.013917	0.013919	0.013922	0.013922	0.0139236	0.013925	0.013925

		1	0.9	0.00E00	0.00E00	0.00E00	0.00E00	0.00E00	0.00E00	0.00E00	0.00E00	0	0.00E00
		1	0.15	-0.99988	-0.99989	-0.99994	-0.99996	-0.99996	-0.99997	-0.99997	-0.99997	-0.99997	-0.99997
1.20E10		7	0.3	-0.86168	-0.98033	-0.98507	-0.98803	-0.98849	-0.98883	-0.98921	-0.98931	-0.98941	-0.98954
		31	0.45	-0.00912	-0.45525	-0.55753	-0.58822	-0.60164	-0.60879	-0.61309	-0.61590	-0.61786	-0.61929
		17	0.6	-0.00111	-0.01182	-0.01852	-0.02084	-0.02394	-0.02485	-0.02518	-0.02592	-0.02620	-0.02630
		5	0.75	0.000251	0.009907	0.013200	0.013392	0.013565	0.013764	0.013785	0.013825	0.013873	0.013878
		1	0.9	0.00E00	0.00E00	0.00E00	0.00E00	0.00E00	0.00E00	0.00E00	0.00E00	0.00E00	0.00E00
		1	0.15	-0.99988	-0.99988	-0.99994	-0.99996	-0.99996	-0.99996	-0.99997	-0.99997	-0.99997	-0.99997
1.22E10		13	0.3	-0.85056	-0.97825	-0.98364	-0.98692	-0.98743	-0.98781	-0.98823	-0.98834	-0.98845	-0.98859
		31	0.45	-0.00506	-0.40683	-0.51235	-0.54473	-0.55898	-0.56660	-0.57119	-0.57419	-0.57629	-0.57782
		15	0.6	-0.00221	-0.00340	-0.00852	-0.01019	-0.01254	-0.01324	-0.01348	-0.01405	-0.01427	-0.01435
		7	0.75	-6.64E-05	0.009620	0.012959	0.013158	0.013346	0.013561	0.013584	0.013626	0.013679	0.013684
		1	0.9	0.00E00	0.00E00	0.00E00	0.00E00	0.00E00	0.00E00	0.00E00	0.00E00	0	0.00E00
		1	0.15	-0.99987	-0.99988	-0.99994	-0.99996	-0.99996	-0.99996	-0.99996	-0.99997	-0.99997	-0.99997
1.24E10		13	0.3	-0.83871	-0.97584	-0.98201	-0.98567	-0.98623	-0.98666	-0.98712	-0.98724	-0.98736	-0.98752
		35	0.45	-0.00190	-0.35342	-0.46089	-0.49476	-0.50980	-0.51787	-0.52274	-0.52593	-0.52816	-0.52979
		11	0.6	-0.00338	0.003515	1.13E-05	-0.00106	-0.00269	-0.00318	-0.00335	-0.00375	-0.00390	-0.00396
		5	0.75	-0.00039	0.009204	0.012477	0.012680	0.012880	0.013101	0.013125	0.013170	0.013225	0.013230
		1	0.9	0.00E00	0.00E00	0.00E00	0.00E00	0.00E00	0.00E00	0.00E00	0.00E00	0.00E00	0.00E00
		1339	1285										
		10.62698412	15.29761904										

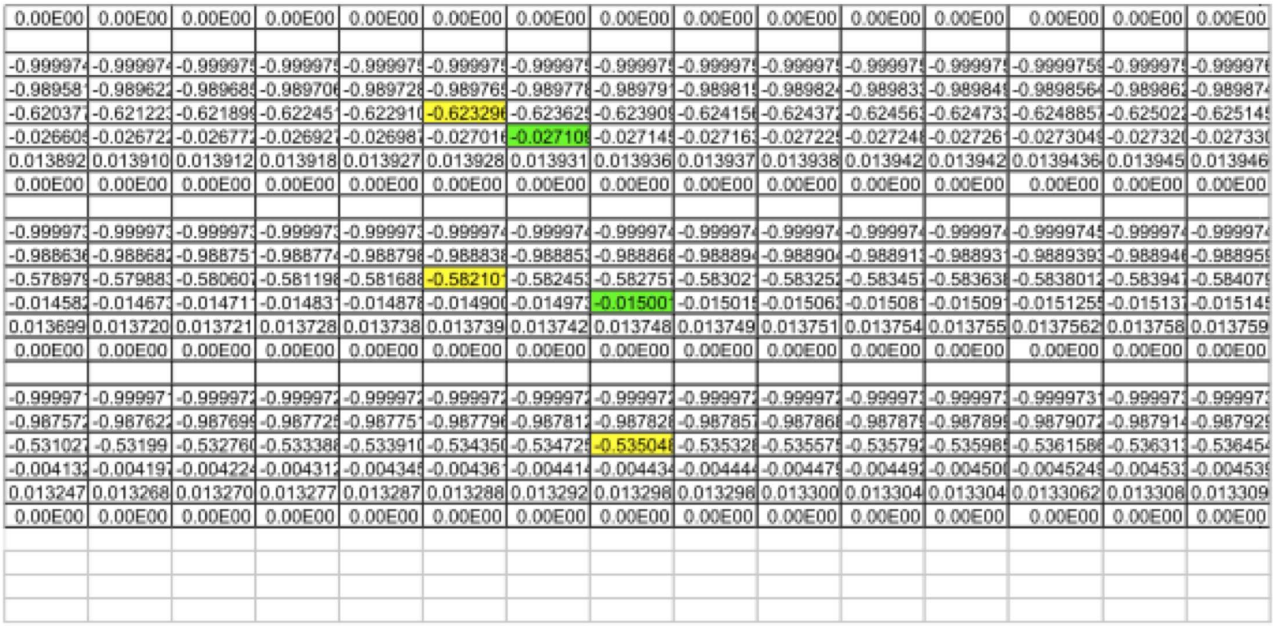

Figure D.1: Varying Number of Modes for S_{11}

Real S_{21} For Determining Number of Modes

			max mode	d in inches										
Frequency	# of modes				1	3	5	7	9	11	13	15	17	19
		49	1	0.15	2.22E-05	1.88E-05	8.37E-06	4.65E-06	4.20E-06	4.10E-06	3.73E-06	3.61E-06	3.59E-06	3.48E-06
8.20E09		25	7	0.3	0.022180	0.002672	0.002151	0.001742	0.001674	0.001627	0.001573	0.001560	0.001546	0.001528
		33	17	0.45	0.619232	0.083235	0.061579	0.055945	0.053594	0.052370	0.051643	0.051171	0.050844	0.050606
		21	21	0.6	0.983534	0.541652	0.513553	0.498897	0.483605	0.479824	0.478199	0.474803	0.473665	0.473186
		11	11	0.75	0.996266	0.988699	0.968212	0.967172	0.966278	0.963787	0.963749	0.963554	0.962817	0.962820
		1	1	0.9	0.991457	0.991457	0.991457	0.991457	0.991457	0.991457	0.991457	0.991457	0.991457	0.991457
		55	1	0.15	2.56E-05	2.16E-05	9.62E-06	5.34E-06	4.83E-06	4.71E-06	4.28E-06	4.15E-06	4.13E-06	4.00E-06
8.41E09		27	9	0.3	0.025816	0.003114	0.002500	0.002023	0.001944	0.001890	0.001827	0.001811	0.001796	0.001775
		41	15	0.45	0.665239	0.096906	0.071834	0.065295	0.062562	0.061140	0.060294	0.059746	0.059366	0.059089
		21	21	0.6	0.987878	0.586969	0.558709	0.544108	0.528751	0.52492	0.523282	0.519858	0.518704	0.518220
		11	11	0.75	0.995417	0.990586	0.974216	0.973360	0.972614	0.970572	0.970539	0.970376	0.969770	0.969773
		1	1	0.9	0.990233	0.990233	0.990233	0.990233	0.990233	0.990233	0.990233	0.990233	0.990233	0.990233
		49	1	0.15	2.90E-05	2.46E-05	1.09E-05	6.06E-06	5.48E-06	5.34E-06	4.86E-06	4.70E-06	4.68E-06	4.54E-06
8.62E09		31	5	0.3	0.029674	0.003584	0.002671	0.002321	0.002231	0.002168	0.002096	0.002077	0.002060	0.002036
		41	15	0.45	0.706428	0.111428	0.082778	0.075282	0.072147	0.070514	0.069544	0.068914	0.068477	0.068160
		27	27	0.6	0.990976	0.628529	0.600471	0.586126	0.570922	0.567094	0.565467	0.562064	0.560910	0.560429
		11	11	0.75	0.994455	0.991793	0.978731	0.978023	0.977398	0.975721	0.975692	0.975554	0.975056	0.975058
		1	1	0.9	0.988978	0.988978	0.988978	0.988978	0.988978	0.988978	0.988978	0.988978	0.988978	0.988978
		67	1	0.15	3.25E-05	2.76E-05	1.23E-05	6.80E-06	6.15E-06	5.99E-06	5.45E-06	5.28E-06	5.25E-06	5.09E-06
8.83E09		31	7	0.3	0.033769	0.004085	0.003264	0.002637	0.002534	0.002462	0.002380	0.002359	0.002339	0.002312
		39	19	0.45	0.743309	0.126863	0.094466	0.085962	0.082402	0.080546	0.079443	0.078727	0.078231	0.077870
		25	25	0.6	0.993150	0.666671	0.639107	0.625180	0.610305	0.606525	0.604929	0.601588	0.600448	0.599974
		11	11	0.75	0.993401	0.992496	0.982139	0.981551	0.981026	0.979650	0.979624	0.979508	0.979099	0.979100
		1	1	0.9	0.987694	0.987694	0.987694	0.987694	0.987694	0.987694	0.987694	0.987694	0.987694	0.987694
		55	1	0.15	3.62E-05	3.08E-05	1.37E-05	7.57E-06	6.84E-06	6.67E-06	6.07E-06	5.87E-06	5.85E-06	5.67E-06
9.04E09		33	7	0.3	0.038116	0.004620	0.003681	0.002972	0.002856	0.002774	0.002682	0.002658	0.002635	0.002604
		45	21	0.45	0.776328	0.143278	0.106965	0.097397	0.093387	0.091296	0.090052	0.089245	0.088685	0.088278
		21	21	0.6	0.994616	0.701693	0.674860	0.661477	0.647074	0.643379	0.64183	0.638584	0.63747	0.637009
		11	11	0.75	0.992272	0.992811	0.984696	0.984208	0.983767	0.982643	0.982620	0.982522	0.982188	0.982188
		1	1	0.9	0.986379	0.986379	0.986379	0.986379	0.986379	0.986379	0.986379	0.986379	0.986379	0.986379
		61	1	0.15	4.00E-05	3.41E-05	1.51E-05	8.37E-06	7.56E-06	7.36E-06	6.70E-06	6.48E-06	6.46E-06	6.26E-06
9.25E09		35	7	0.3	0.042732	0.005193	0.004125	0.003328	0.003197	0.003105	0.003001	0.002975	0.002949	0.002915
		49	17	0.45	0.805870	0.160747	0.120346	0.109657	0.105171	0.102830	0.101438	0.100534	0.099907	0.099452
			23	0.6	0.995525	0.73386	0.707947	0.695205	0.681389	0.677811	0.676320	0.673197	0.672117	0.671673
			11	0.75	0.991077	0.992818	0.986584	0.986179	0.985810	0.984899	0.984878	0.984795	0.984524	0.984523

21	23	25	27	29	31	33	35	37	39	41	43	45	47	49	51
3.43E-06	3.43E-06	3.38E-06	3.35E-06	3.35E-06	3.32E-06	3.31E-06	3.30E-06	3.29E-06	3.28E-06	3.27E-06	3.26E-06	3.25E-06	3.25E-06	3.24E-06	3.24E-06
0.001523	0.001517	0.001509	0.001506	0.001503	0.001498	0.001496	0.001494	0.001491	0.001490	0.001488	0.001486	0.001485	0.001484	0.001483	0.001482
0.050426	0.050286	0.050174	0.050083	0.050007	0.049943	0.049888	0.049841	0.049800	0.049764	0.049732	0.049704	0.049679	0.049656	0.049636	0.049617
0.471861	0.471381	0.471165	0.470486	0.470238	0.470115	0.469709	0.469564	0.469483	0.469215	0.469122	0.469065	0.468877	0.468813	0.468771	0.468632
0.962764	0.962438	0.962441	0.962425	0.962247	0.962247	0.962244	0.962134	0.962133	0.962134	0.962060	0.962058	0.962061	0.962008	0.962006	0.962010
0.991457	0.991457	0.991457	0.991457	0.991457	0.991457	0.991457	0.991457	0.991457	0.991457	0.991457	0.991457	0.991457	0.991457	0.991457	0.991457
3.95E-06	3.94E-06	3.88E-06	3.85E-06	3.85E-06	3.81E-06	3.80E-06	3.80E-06	3.77E-06	3.76E-06	3.76E-06	3.75E-06	3.74E-06	3.74E-06	3.73E-06	3.72E-06
0.001769	0.001762	0.001752	0.001749	0.001745	0.001739	0.001737	0.001735	0.001731	0.001730	0.001728	0.001726	0.001725	0.001724	0.001722	0.001721
0.058880	0.058717	0.058587	0.058481	0.058392	0.058318	0.058254	0.058200	0.058152	0.058110	0.058073	0.058040	0.058011	0.057985	0.057961	0.057939
0.516883	0.516396	0.516177	0.515492	0.515241	0.515116	0.514706	0.514559	0.514477	0.514207	0.514113	0.514055	0.513865	0.513801	0.513758	0.513618
0.969725	0.969458	0.969460	0.969446	0.969300	0.969300	0.969297	0.969207	0.969206	0.969206	0.969146	0.969145	0.969147	0.969103	0.969102	0.969104
0.990233	0.990233	0.990233	0.990233	0.990233	0.990233	0.990233	0.990233	0.990233	0.990233	0.990233	0.990233	0.990233	0.990233	0.990233	0.990233
4.47E-06	4.47E-06	4.40E-06	4.37E-06	4.36E-06	4.33E-06	4.31E-06	4.30E-06	4.28E-06	4.27E-06	4.26E-06	4.25E-06	4.24E-06	4.24E-06	4.22E-06	4.22E-06
0.002028	0.002021	0.002009	0.002005	0.002001	0.001995	0.001992	0.001990	0.001985	0.001984	0.001982	0.001979	0.001978	0.001977	0.001975	0.001974
0.067920	0.067733	0.067583	0.067461	0.067359	0.067274	0.067201	0.067138	0.067084	0.067036	0.066993	0.066955	0.066922	0.066891	0.066864	0.066839
0.559098	0.558612	0.558394	0.557712	0.557461	0.557337	0.556929	0.556782	0.556700	0.556432	0.556337	0.556280	0.556091	0.556027	0.555984	0.555845
0.975017	0.974798	0.974799	0.974787	0.974667	0.974667	0.974664	0.974590	0.974589	0.974589	0.974540	0.974539	0.974540	0.974505	0.974503	0.974505
0.988978	0.988978	0.988978	0.988978	0.988978	0.988978	0.988978	0.988978	0.988978	0.988978	0.988978	0.988978	0.988978	0.988978	0.988978	0.988978
5.02E-06	5.01E-06	4.94E-06	4.90E-06	4.90E-06	4.85E-06	4.83E-06	4.83E-06	4.80E-06	4.79E-06	4.79E-06	4.77E-06	4.76E-06	4.75E-06	4.74E-06	4.73E-06
0.002303	0.002295	0.002282	0.002277	0.002273	0.002265	0.002262	0.002259	0.002255	0.002253	0.002251	0.002247	0.002246	0.002245	0.002242	0.002241
0.077597	0.077384	0.077214	0.077075	0.076960	0.076863	0.076780	0.076709	0.076646	0.076592	0.076544	0.076501	0.076462	0.076428	0.076397	0.076368
0.598667	0.598187	0.597972	0.597302	0.597054	0.596932	0.596531	0.596386	0.596306	0.596042	0.595949	0.595892	0.595707	0.595643	0.595601	0.595464
0.979065	0.978885	0.978886	0.978875	0.978777	0.978777	0.978774	0.978713	0.978713	0.978713	0.978672	0.978671	0.978672	0.978643	0.978642	0.978644
0.987694	0.987694	0.987694	0.987694	0.987694	0.987694	0.987694	0.987694	0.987694	0.987694	0.987694	0.987694	0.987694	0.987694	0.987694	0.987694
5.59E-06	5.58E-06	5.49E-06	5.45E-06	5.45E-06	5.40E-06	5.38E-06	5.37E-06	5.34E-06	5.33E-06	5.32E-06	5.30E-06	5.29E-06	5.29E-06	5.27E-06	5.27E-06
0.002595	0.002585	0.002570	0.002565	0.002560	0.002551	0.002548	0.002545	0.002540	0.002538	0.002535	0.002532	0.002530	0.002529	0.002526	0.002525
0.087971	0.087731	0.087539	0.087382	0.087252	0.087143	0.08705	0.086969	0.086899	0.086837	0.086783	0.086735	0.086692	0.086653	0.086618	0.086586
0.635738	0.635268	0.635059	0.634408	0.634166	0.634047	0.633657	0.633515	0.633437	0.633181	0.633090	0.633035	0.632855	0.632792	0.632752	0.632619
0.982158	0.982011	0.982012	0.982002	0.981922	0.981922	0.981919	0.981869	0.981869	0.981869	0.981835	0.981835	0.981835	0.981812	0.981811	0.981812
0.986379	0.986379	0.986379	0.986379	0.986379	0.986379	0.986379	0.986379	0.986379	0.986379	0.986379	0.986379	0.986379	0.986379	0.986379	0.986379
6.17E-06	6.16E-06	6.07E-06	6.02E-06	6.02E-06	5.97E-06	5.94E-06	5.94E-06	5.90E-06	5.88E-06	5.88E-06	5.86E-06	5.85E-06	5.84E-06	5.83E-06	5.82E-06
0.002904	0.002893	0.002876	0.002871	0.002865	0.002855	0.002852	0.002848	0.002842	0.002840	0.002837	0.002833	0.002831	0.002830	0.002827	0.002825
0.099107	0.098838	0.098623	0.098448	0.098303	0.098180	0.098075	0.097985	0.097907	0.097838	0.097777	0.097723	0.097675	0.097631	0.097592	0.097556
0.670450	0.669995	0.669794	0.669166	0.668932	0.668817	0.668442	0.668305	0.668230	0.667983	0.667895	0.667842	0.667668	0.667608	0.667569	0.667441
0.984498	0.984379	0.984379	0.984371	0.984306	0.984306	0.984303	0.984263	0.984263	0.984262	0.984235	0.984235	0.984235	0.984216	0.984215	0.984216

			1	0.9	0.985034	0.985034	0.985034	0.985034	0.985034	0.985034	0.985034	0.985034	0.985034	0.985034
		67	1	0.15	4.39E-05	3.75E-05	1.66E-05	9.19E-06	8.30E-06	8.09E-06	7.36E-06	7.12E-06	7.09E-06	6.87E-06
9.46E09		31	7	0.3	0.047635	0.005806	0.004598	0.003705	0.003560	0.003457	0.003341	0.003312	0.003283	0.003244
		17	17	0.45	0.832276	0.179352	0.134689	0.12282	0.117831	0.115227	0.113677	0.112670	0.111973	0.111465
		21	21	0.6	0.995986	0.763404	0.738562	0.726536	0.713397	0.709960	0.708538	0.705560	0.704524	0.704099
		5	5	0.75	0.989825	0.992577	0.987933	0.987598	0.987291	0.986561	0.986542	0.986472	0.986255	0.986254
		1	1	0.9	0.983659	0.983659	0.983659	0.983659	0.983659	0.983659	0.983659	0.983659	0.983659	0.983659
Frequency	# of modes				1	3	5	7	9	11	13	15	17	19
		61	1	0.15	4.79E-05	4.10E-05	1.82E-05	1.00E-05	9.07E-06	8.83E-06	8.04E-06	7.78E-06	7.74E-06	7.51E-06
9.67E09		41	9	0.3	0.052846	0.006463	0.005103	0.004108	0.003946	0.003831	0.003703	0.003670	0.003638	0.003595
		21	21	0.45	0.855844	0.199183	0.150089	0.136975	0.131456	0.128572	0.126855	0.125740	0.124967	0.124404
		23	23	0.6	0.996079	0.790536	0.766884	0.755626	0.743233	0.739958	0.738614	0.735798	0.734811	0.734409
		11	11	0.75	0.988520	0.992128	0.988839	0.988562	0.988309	0.987735	0.987717	0.987658	0.987488	0.987486
		1	1	0.9	0.982254	0.982254	0.982254	0.982254	0.982254	0.982254	0.982254	0.982254	0.982254	0.982254
		73	1	0.15	5.21E-05	4.47E-05	1.98E-05	1.09E-05	9.86E-06	9.61E-06	8.74E-06	8.46E-06	8.42E-06	8.16E-06
9.88E09		37	7	0.3	0.058384	0.007170	0.005641	0.004537	0.004358	0.004230	0.004087	0.004051	0.004015	0.003968
		21	21	0.45	0.876838	0.220340	0.166648	0.152227	0.146146	0.142966	0.141073	0.139842	0.138989	0.138369
		21	21	0.6	0.995867	0.815439	0.793070	0.782618	0.771023	0.767926	0.766665	0.764025	0.763091	0.762713
		9	9	0.75	0.987168	0.991503	0.989373	0.989146	0.988940	0.988501	0.988484	0.988435	0.988304	0.988302
		1	1	0.9	0.980819	0.980819	0.980819	0.980819	0.980819	0.980819	0.980819	0.980819	0.980819	0.980819
		67	1	0.15	5.64E-05	4.85E-05	2.15E-05	1.18E-05	1.07E-05	1.04E-05	9.47E-06	9.16E-06	9.12E-06	8.84E-06
1.01E10		41	7	0.3	0.064273	0.007932	0.006218	0.004994	0.004797	0.004656	0.004498	0.004458	0.004418	0.004366
		21	21	0.45	0.895493	0.242933	0.184486	0.168691	0.162018	0.158525	0.156445	0.155092	0.154154	0.153472
		23	23	0.6	0.995394	0.838277	0.817264	0.807638	0.796880	0.793973	0.792800	0.790345	0.789469	0.789117
		5	5	0.75	0.985770	0.990726	0.989591	0.989406	0.989241	0.988918	0.988902	0.988862	0.988765	0.988763
		1	1	0.9	0.979354	0.979354	0.979354	0.979354	0.979354	0.979354	0.979354	0.979354	0.979354	0.979354
		79	1	0.15	6.08E-05	5.24E-05	2.32E-05	1.28E-05	1.15E-05	1.12E-05	1.02E-05	9.88E-06	9.84E-06	9.54E-06
1.03E10		47	7	0.3	0.070537	0.008755	0.006836	0.005484	0.005267	0.005111	0.004937	0.004893	0.004849	0.004791
		23	23	0.45	0.912018	0.267088	0.203741	0.186503	0.179206	0.175383	0.173104	0.171622	0.170594	0.169846
		21	21	0.6	0.994698	0.859196	0.839592	0.830805	0.820906	0.818200	0.817118	0.814855	0.814040	0.813715
		3	3	0.75	0.984330	0.989814	0.989535	0.989385	0.989256	0.989034	0.989019	0.988986	0.988920	0.988917
		1	1	0.9	0.977859	0.977859	0.977859	0.977859	0.977859	0.977859	0.977859	0.977859	0.977859	0.977859
	# of modes													
		85	1	0.15	6.54E-05	5.66E-05	2.51E-05	1.38E-05	1.24E-05	1.21E-05	1.10E-05	1.06E-05	1.06E-05	1.03E-05
1.05E10		43	9	0.3	0.077203	0.009646	0.007500	0.006010	0.005771	0.005598	0.005407	0.005359	0.005310	0.005246
		27	27	0.45	0.926597	0.292942	0.224571	0.205823	0.197868	0.193695	0.191206	0.189587	0.188464	0.187647
		21	21	0.6	0.993808	0.878324	0.860169	0.852221	0.843197	0.840698	0.839708	0.837642	0.836890	0.836593
		5	5	0.75	0.982849	0.988782	0.989237	0.989116	0.989020	0.988885	0.988871	0.988844	0.988805	0.988801

0.985034	0.985034	0.985034	0.985034	0.985034	0.985034	0.985034	0.985034	0.985034	0.985034	0.985034	0.985034	0.985034	0.985034	0.985034	0.985034
6.78E-06	6.76E-06	6.66E-06	6.61E-06	6.61E-06	6.55E-06	6.52E-06	6.52E-06	6.48E-06	6.46E-06	6.46E-06	6.43E-06	6.42E-06	6.42E-06	6.40E-06	6.39E-06
0.003232	0.003220	0.003202	0.003195	0.003189	0.003178	0.003174	0.003170	0.003163	0.003161	0.003158	0.003153	0.003151	0.003149	0.003146	0.003144
0.111081	0.110782	0.110543	0.110348	0.110185	0.110049	0.109933	0.109832	0.109745	0.109668	0.109601	0.109540	0.109486	0.109438	0.109394	0.109355
0.702932	0.702496	0.702303	0.701705	0.701480	0.701370	0.701012	0.700880	0.700809	0.700573	0.700489	0.700439	0.700273	0.700215	0.700178	0.700056
0.986232	0.986136	0.986137	0.986129	0.986077	0.986077	0.986074	0.986043	0.986042	0.986042	0.986020	0.98602	0.986020	0.986005	0.986004	0.986004
0.983659	0.983659	0.983659	0.983659	0.983659	0.983659	0.983659	0.983659	0.983659	0.983659	0.983659	0.983659	0.983659	0.983659	0.983659	0.983659
21	23	25	27	29	31	33	35	37	39	41	43	45	47	49	51
7.40E-06	7.39E-06	7.28E-06	7.22E-06	7.22E-06	7.15E-06	7.12E-06	7.12E-06	7.08E-06	7.06E-06	7.05E-06	7.02E-06	7.01E-06	7.01E-06	6.99E-06	6.98E-06
0.003582	0.003568	0.003547	0.003540	0.003533	0.003521	0.003517	0.003512	0.003505	0.003502	0.003499	0.003493	0.003491	0.003489	0.003485	0.003484
0.123979	0.123647	0.123382	0.123166	0.122987	0.122835	0.122706	0.122595	0.122498	0.122414	0.122339	0.122272	0.122212	0.122159	0.122110	0.122066
0.733305	0.732889	0.732706	0.732140	0.731926	0.731822	0.731484	0.731359	0.731291	0.731068	0.730988	0.730940	0.730784	0.730729	0.730693	0.730578
0.987467	0.987392	0.987392	0.987386	0.987345	0.987345	0.987342	0.987317	0.987317	0.987316	0.9873	0.987299	0.987299	0.987287	0.987287	0.987287
0.982254	0.982254	0.982254	0.982254	0.982254	0.982254	0.982254	0.982254	0.982254	0.982254	0.982254	0.982254	0.982254	0.982254	0.982254	0.982254
8.05E-06	8.03E-06	7.91E-06	7.85E-06	7.85E-06	7.78E-06	7.74E-06	7.74E-06	7.69E-06	7.67E-06	7.67E-06	7.64E-06	7.62E-06	7.62E-06	7.59E-06	7.58E-06
0.003953	0.003938	0.003915	0.003908	0.003899	0.003886	0.003881	0.003877	0.003868	0.003865	0.003861	0.003856	0.003853	0.003851	0.003847	0.003845
0.137899	0.137533	0.137241	0.137002	0.136804	0.136637	0.136495	0.136372	0.136266	0.136172	0.136089	0.136016	0.135950	0.135891	0.135837	0.135789
0.761678	0.761285	0.761114	0.760583	0.760381	0.760283	0.759966	0.759848	0.759784	0.759575	0.7595	0.759455	0.759308	0.759256	0.759223	0.759115
0.988286	0.988229	0.988228	0.988222	0.988192	0.988191	0.988189	0.988170	0.988170	0.988169	0.988156	0.988156	0.988156	0.988147	0.988146	0.988146
0.980819	0.980819	0.980819	0.980819	0.980819	0.980819	0.980819	0.980819	0.980819	0.980819	0.980819	0.980819	0.980819	0.980819	0.980819	0.980819
8.71E-06	8.70E-06	8.57E-06	8.50E-06	8.50E-06	8.42E-06	8.38E-06	8.38E-06	8.33E-06	8.31E-06	8.30E-06	8.27E-06	8.25E-06	8.25E-06	8.22E-06	8.21E-06
0.004350	0.004333	0.004308	0.004299	0.004290	0.004276	0.004270	0.004265	0.004256	0.004252	0.004248	0.004242	0.004239	0.004237	0.004232	0.004230
0.152956	0.152554	0.152232	0.151970	0.151752	0.151568	0.151412	0.151277	0.151160	0.151057	0.150966	0.150885	0.150813	0.150748	0.150689	0.150636
0.788155	0.787786	0.787627	0.787133	0.786944	0.786853	0.786558	0.786447	0.786388	0.786194	0.786123	0.786081	0.785945	0.785897	0.785866	0.785765
0.988749	0.988708	0.988707	0.988702	0.988679	0.988679	0.988677	0.988663	0.988663	0.988662	0.988653	0.988652	0.988652	0.988646	0.988645	0.988645
0.979354	0.979354	0.979354	0.979354	0.979354	0.979354	0.979354	0.979354	0.979354	0.979354	0.979354	0.979354	0.979354	0.979354	0.979354	0.979354
9.40E-06	9.39E-06	9.25E-06	9.18E-06	9.17E-06	9.09E-06	9.05E-06	9.04E-06	8.99E-06	8.96E-06	8.96E-06	8.92E-06	8.90E-06	8.90E-06	8.87E-06	8.86E-06
0.004774	0.004755	0.004727	0.004718	0.004708	0.004692	0.004686	0.004680	0.004670	0.004666	0.004662	0.004654	0.004652	0.004649	0.004643	0.004641
0.169281	0.168840	0.168487	0.168200	0.167961	0.167760	0.167589	0.167441	0.167313	0.167200	0.167100	0.167012	0.166933	0.166861	0.166797	0.166739
0.812828	0.812485	0.812338	0.811883	0.811707	0.811623	0.811351	0.811249	0.811194	0.811015	0.81095	0.810911	0.810786	0.810741	0.810712	0.810620
0.988906	0.988877	0.988877	0.988872	0.988857	0.988857	0.988854	0.988845	0.988845	0.988844	0.988838	0.988838	0.988837	0.988833	0.988833	0.988832
0.977859	0.977859	0.977859	0.977859	0.977859	0.977859	0.977859	0.977859	0.977859	0.977859	0.977859	0.977859	0.977859	0.977859	0.977859	0.977859
1.01E-05	1.01E-05	9.95E-06	9.87E-06	9.86E-06	9.78E-06	9.73E-06	9.73E-06	9.67E-06	9.64E-06	9.64E-06	9.60E-06	9.58E-06	9.57E-06	9.54E-06	9.53E-06
0.005227	0.005207	0.005176	0.005166	0.005155	0.005137	0.005131	0.005124	0.005113	0.005108	0.005104	0.005096	0.005093	0.005090	0.005084	0.005082
0.187029	0.186547	0.186162	0.185848	0.185587	0.185368	0.185181	0.185019	0.184879	0.184756	0.184647	0.184550	0.184464	0.184386	0.184316	0.184252
0.835782	0.835467	0.835332	0.834917	0.834755	0.834678	0.834430	0.834335	0.834286	0.834123	0.834062	0.834027	0.833913	0.833871	0.833845	0.833761
0.988792	0.988775	0.988774	0.988770	0.988762	0.988761	0.988759	0.988754	0.988754	0.988752	0.988749	0.988749	0.988748	0.988746	0.988746	0.988745

		1	1	0.9	0.976334	0.976334	0.976334	0.976334	0.976334	0.976334	0.976334	0.976334	0.976334	0.976334
		33	1	0.15	7.01E-05	6.08E-05	2.69E-05	1.48E-05	1.33E-05	1.30E-05	1.18E-05	1.14E-05	1.14E-05	1.10E-05
1.07E10		49	7	0.3	0.084298	0.010615	0.008216	0.006574	0.006313	0.006122	0.005912	0.005859	0.005805	0.005735
		23	23	0.45	0.939398	0.320654	0.247162	0.226836	0.218188	0.213646	0.210936	0.209172	0.207949	0.207058
		23	23	0.6	0.992748	0.895774	0.879097	0.871980	0.863835	0.861547	0.860652	0.858784	0.858097	0.857827
		5	5	0.75	0.981330	0.987640	0.988722	0.988625	0.988558	0.988499	0.988485	0.988465	0.988448	0.988444
		1	1	0.9	0.97478	0.97478	0.97478	0.97478	0.97478	0.97478	0.97478	0.97478	0.97478	0.97478
		31	1	0.15	7.50E-05	6.52E-05	2.89E-05	1.58E-05	1.42E-05	1.39E-05	1.26E-05	1.22E-05	1.22E-05	1.18E-05
1.09E10		49	9	0.3	0.091854	0.011672	0.008990	0.007183	0.006896	0.006686	0.006455	0.006397	0.006338	0.006261
		23	23	0.45	0.950571	0.350402	0.271732	0.249763	0.240389	0.235459	0.232514	0.230597	0.229267	0.228299
		21	21	0.6	0.991535	0.911643	0.896463	0.890163	0.882893	0.880821	0.880020	0.878350	0.877729	0.877487
		7	7	0.75	0.979773	0.986396	0.988009	0.987932	0.98789	0.987897	0.987883	0.987868	0.987871	0.987867
		1	1	0.9	0.973195	0.973195	0.973195	0.973195	0.973195	0.973195	0.973195	0.973195	0.973195	0.973195
		37	1	0.15	8.01E-05	6.98E-05	3.09E-05	1.69E-05	1.52E-05	1.48E-05	1.35E-05	1.30E-05	1.30E-05	1.26E-05
1.11E10		53	7	0.3	0.099901	0.012831	0.009830	0.007841	0.007527	0.007296	0.007042	0.006979	0.006914	0.006829
		29	29	0.45	0.960251	0.382393	0.298541	0.274871	0.264736	0.259398	0.256207	0.254128	0.252686	0.251636
		17	17	0.6	0.990187	0.926013	0.912342	0.906839	0.900436	0.898581	0.897872	0.896400	0.895845	0.895631
		5	5	0.75	0.978180	0.985054	0.987112	0.987050	0.987030	0.987094	0.987080	0.987069	0.987089	0.987085
		1	1	0.9	0.971581	0.971581	0.971581	0.971581	0.971581	0.971581	0.971581	0.971581	0.971581	0.971581
Frequency	# of modes				1	3	5	7	9	11	13	15	17	19
		37	1	0.15	8.52E-05	7.46E-05	3.30E-05	1.80E-05	1.62E-05	1.58E-05	1.44E-05	1.39E-05	1.38E-05	1.34E-05
1.14E10		55	11	0.3	0.108477	0.014106	0.010745	0.008556	0.008212	0.007957	0.007679	0.007609	0.007538	0.007445
		27	27	0.45	0.96856	0.416868	0.327907	0.302484	0.291557	0.285791	0.282342	0.280093	0.278533	0.277396
		15	15	0.6	0.988715	0.938950	0.926797	0.922066	0.916514	0.914875	0.914258	0.912981	0.912492	0.912305
		11	11	0.75	0.976550	0.983618	0.986038	0.985988	0.985987	0.986100	0.986086	0.986079	0.986113	0.986109
		1	1	0.9	0.969937	0.969937	0.969937	0.969937	0.969937	0.969937	0.969937	0.969937	0.969937	0.969937
	# of modes													
		37	1	0.15	9.06E-05	7.96E-05	3.52E-05	1.92E-05	1.72E-05	1.68E-05	1.53E-05	1.48E-05	1.47E-05	1.43E-05
1.16E10		49	9	0.3	0.117617	0.015520	0.011748	0.009336	0.008959	0.008678	0.008372	0.008296	0.008218	0.008116
		29	29	0.45	0.975607	0.454113	0.360218	0.333007	0.321260	0.315049	0.311330	0.308904	0.307219	0.305992
		17	17	0.6	0.987132	0.950504	0.939873	0.935883	0.931163	0.929740	0.929212	0.928126	0.927703	0.927543
		5	5	0.75	0.974886	0.982087	0.984791	0.98475	0.984765	0.984918	0.984904	0.984900	0.984947	0.984943
		1	1	0.9	0.968263	0.968263	0.968263	0.968263	0.968263	0.968263	0.968263	0.968263	0.968263	0.968263
		33	1	0.15	9.61E-05	8.48E-05	3.74E-05	2.04E-05	1.83E-05	1.78E-05	1.62E-05	1.57E-05	1.56E-05	1.51E-05
1.18E10		49	9	0.3	0.127362	0.017099	0.012854	0.010193	0.009780	0.009469	0.009133	0.009049	0.008963	0.008851
		33	33	0.45	0.981493	0.494476	0.395968	0.366958	0.354371	0.347700	0.343700	0.341089	0.339275	0.337953
		15	15	0.6	0.985445	0.960700	0.951597	0.948316	0.944403	0.943194	0.942753	0.941852	0.941494	0.941361
		5	5	0.75	0.973188	0.980457	0.983367	0.983331	0.983361	0.983546	0.983531	0.983530	0.983587	0.983583

0.976334	0.976334	0.976334	0.976334	0.976334	0.976334	0.976334	0.976334	0.976334	0.976334	0.976334	0.976334	0.976334	0.976334	0.976334	0.976334
1.08E-05	1.08E-05	1.07E-05	1.06E-05	1.06E-05	1.05E-05	1.04E-05	1.04E-05	1.04E-05	1.03E-05	1.03E-05	1.03E-05	1.03E-05	1.03E-05	1.02E-05	1.02E-05
0.005714	0.005692	0.005658	0.005647	0.005635	0.005615	0.005608	0.005601	0.005588	0.005584	0.005579	0.005570	0.005567	0.005563	0.005557	0.005554
0.206385	0.20586	0.205440	0.205097	0.204813	0.204574	0.204370	0.204194	0.204041	0.203907	0.203789	0.203683	0.203589	0.203504	0.203428	0.203358
0.857095	0.856807	0.856685	0.856310	0.856162	0.856093	0.855869	0.855783	0.855738	0.855591	0.855535	0.855504	0.855401	0.855363	0.855339	0.855263
0.988436	0.988430	0.988429	0.988425	0.988422	0.988422	0.988419	0.988418	0.988418	0.988416	0.988415	0.988415	0.988414	0.988414	0.988414	0.988413
0.97478	0.97478	0.97478	0.97478	0.97478	0.97478	0.97478	0.97478	0.97478	0.97478	0.97478	0.97478	0.97478	0.97478	0.97478	0.97478
1.16E-05	1.16E-05	1.14E-05	1.13E-05	1.13E-05	1.12E-05	1.12E-05	1.12E-05	1.11E-05	1.11E-05	1.11E-05	1.10E-05	1.10E-05	1.10E-05	1.10E-05	1.09E-05
0.006238	0.006213	0.006176	0.006164	0.006151	0.006130	0.006122	0.006114	0.006100	0.006095	0.006090	0.006080	0.006076	0.006073	0.006066	0.006063
0.227567	0.226996	0.226539	0.226167	0.225858	0.225598	0.225376	0.225185	0.225019	0.224873	0.224745	0.224630	0.224528	0.224436	0.224353	0.224277
0.876834	0.876573	0.876464	0.876129	0.875996	0.875934	0.875734	0.875656	0.875616	0.875485	0.875435	0.875407	0.875315	0.875281	0.875260	0.875193
0.987860	0.987863	0.987862	0.987858	0.987860	0.987860	0.987858	0.987859	0.987859	0.987858	0.987859	0.987858	0.987858	0.987858	0.987858	0.987858
0.973195	0.973195	0.973195	0.973195	0.973195	0.973195	0.973195	0.973195	0.973195	0.973195	0.973195	0.973195	0.973195	0.973195	0.973195	0.973195
1.24E-05	1.24E-05	1.22E-05	1.21E-05	1.21E-05	1.20E-05	1.19E-05	1.19E-05	1.18E-05	1.18E-05	1.18E-05	1.18E-05	1.17E-05	1.17E-05	1.17E-05	1.17E-05
0.006804	0.006777	0.006736	0.006723	0.006708	0.006685	0.006677	0.006668	0.006653	0.006647	0.006641	0.006631	0.006627	0.006623	0.006615	0.006612
0.250841	0.250222	0.249727	0.249323	0.248988	0.248706	0.248466	0.248258	0.248078	0.247920	0.247780	0.247656	0.247545	0.247446	0.247355	0.247274
0.895055	0.894823	0.894726	0.894431	0.894312	0.894258	0.894082	0.894013	0.893977	0.893862	0.893818	0.893793	0.893712	0.893682	0.893664	0.893604
0.987080	0.987090	0.987089	0.987086	0.987092	0.987091	0.987089	0.987093	0.987093	0.987092	0.987095	0.987095	0.987094	0.987096	0.987096	0.987095
0.971581	0.971581	0.971581	0.971581	0.971581	0.971581	0.971581	0.971581	0.971581	0.971581	0.971581	0.971581	0.971581	0.971581	0.971581	0.971581
21	23	25	27	29	31	33	35	37	39	41	43	45	47	49	51
1.32E-05	1.32E-05	1.30E-05	1.29E-05	1.29E-05	1.28E-05	1.27E-05	1.27E-05	1.26E-05	1.26E-05	1.26E-05	1.25E-05	1.25E-05	1.25E-05	1.25E-05	1.24E-05
0.007418	0.007388	0.007343	0.007328	0.007313	0.007287	0.007278	0.007268	0.007252	0.007245	0.007239	0.007227	0.007223	0.007218	0.007210	0.007206
0.276536	0.275866	0.275330	0.274893	0.274531	0.274226	0.273965	0.273741	0.273546	0.273375	0.273224	0.273090	0.272970	0.272862	0.272764	0.272676
0.911806	0.911601	0.911517	0.911262	0.911158	0.911110	0.910958	0.910898	0.910867	0.910767	0.910729	0.910707	0.910637	0.910611	0.910595	0.910544
0.986105	0.986122	0.986120	0.986117	0.986127	0.986126	0.986125	0.986131	0.986131	0.986129	0.986134	0.986134	0.986133	0.986136	0.986136	0.986135
0.969937	0.969937	0.969937	0.969937	0.969937	0.969937	0.969937	0.969937	0.969937	0.969937	0.969937	0.969937	0.969937	0.969937	0.969937	0.969937
1.40E-05	1.40E-05	1.38E-05	1.37E-05	1.37E-05	1.36E-05	1.35E-05	1.35E-05	1.34E-05	1.34E-05	1.34E-05	1.33E-05	1.33E-05	1.33E-05	1.33E-05	1.32E-05
0.008086	0.008053	0.008004	0.007988	0.007970	0.007942	0.007932	0.007922	0.007903	0.007896	0.007890	0.007877	0.007872	0.007867	0.007858	0.007854
0.305064	0.304340	0.303761	0.303290	0.302898	0.302569	0.302288	0.302046	0.301835	0.301650	0.301487	0.301343	0.301213	0.301097	0.300991	0.300896
0.927119	0.926943	0.926871	0.926655	0.926564	0.926524	0.926395	0.926343	0.926317	0.926233	0.926199	0.926181	0.926122	0.926099	0.926086	0.926042
0.984939	0.984961	0.984960	0.984957	0.984970	0.98497	0.984968	0.984976	0.984976	0.984974	0.984980	0.984980	0.984979	0.984983	0.984983	0.984982
0.968263	0.968263	0.968263	0.968263	0.968263	0.968263	0.968263	0.968263	0.968263	0.968263	0.968263	0.968263	0.968263	0.968263	0.968263	0.968263
1.49E-05	1.49E-05	1.47E-05	1.46E-05	1.45E-05	1.44E-05	1.43E-05	1.43E-05	1.43E-05	1.42E-05	1.42E-05	1.41E-05	1.41E-05	1.41E-05	1.41E-05	1.40E-05
0.008818	0.008781	0.008728	0.008710	0.008691	0.008660	0.008649	0.008637	0.008617	0.008610	0.008602	0.008588	0.008583	0.008577	0.008567	0.008563
0.336954	0.336174	0.335551	0.335043	0.334622	0.334267	0.333964	0.333703	0.333477	0.333278	0.333103	0.332947	0.332807	0.332682	0.332569	0.332466
0.941010	0.940861	0.940801	0.940623	0.940547	0.940513	0.940407	0.940363	0.940342	0.940272	0.940244	0.940229	0.940181	0.940162	0.940150	0.940115
0.983580	0.983607	0.983605	0.983603	0.983618	0.983618	0.983616	0.983626	0.983625	0.983624	0.983631	0.983631	0.98363	0.983634	0.983634	0.983634

		1	1	0.9	0.966560	0.966560	0.966560	0.966560	0.966560	0.966560	0.966560	0.966560	0.966560	0.966560
		37	1	0.15	0.000101	9.02E-05	3.98E-05	2.16E-05	1.94E-05	1.89E-05	1.72E-05	1.66E-05	1.66E-05	1.60E-05
1.20E10		61	13	0.3	0.137754	0.018880	0.014083	0.011141	0.010686	0.010342	0.009973	0.009880	0.009785	0.009662
		27	27	0.45	0.986309	0.538398	0.435801	0.405019	0.391583	0.384443	0.380155	0.377354	0.375407	0.373988
		17	17	0.6	0.983664	0.969537	0.961969	0.959359	0.956225	0.955228	0.954871	0.954150	0.953856	0.953748
		5	5	0.75	0.971456	0.978722	0.981755	0.981719	0.981761	0.981971	0.981956	0.981957	0.982022	0.982017
		1	1	0.9	0.964827	0.964827	0.964827	0.964827	0.964827	0.964827	0.964827	0.964827	0.964827	0.964827
		45	1	0.15	0.000107	9.59E-05	4.22E-05	2.29E-05	2.06E-05	2.01E-05	1.82E-05	1.76E-05	1.75E-05	1.70E-05
1.22E10		27	13	0.3	0.148838	0.020914	0.015465	0.012202	0.011700	0.011318	0.010909	0.010807	0.010702	0.010566
		31	31	0.45	0.990139	0.586461	0.480603	0.448135	0.433863	0.426254	0.421677	0.418684	0.416603	0.415085
		15	15	0.6	0.981794	0.976970	0.970950	0.968969	0.966584	0.965795	0.965518	0.964971	0.964739	0.964657
		5	5	0.75	0.969691	0.976862	0.979928	0.979889	0.979941	0.980167	0.980151	0.980154	0.980224	0.980219
		1	1	0.9	0.963065	0.963065	0.963065	0.963065	0.963065	0.963065	0.963065	0.963065	0.963065	0.963065
		33	1	0.15	0.000113	0.000101	4.48E-05	2.43E-05	2.18E-05	2.12E-05	1.93E-05	1.86E-05	1.86E-05	1.80E-05
1.24E10		27	13	0.3	0.160663	0.023281	0.017044	0.013404	0.012848	0.012422	0.011969	0.011856	0.011739	0.011588
		33	33	0.45	0.993057	0.639499	0.531670	0.497706	0.482648	0.474588	0.469729	0.466548	0.464334	0.462719
		11	11	0.6	0.979842	0.982876	0.978431	0.977034	0.975363	0.974779	0.97458	0.974198	0.974027	0.973968
		5	5	0.75	0.967893	0.974846	0.977833	0.977788	0.977845	0.978078	0.978061	0.978065	0.978138	0.978133
		1	1	0.9	0.961273	0.961273	0.961273	0.961273	0.961273	0.961273	0.961273	0.961273	0.961273	0.961273
		3127	1286	1244										
		24.81746	10.206349	14.8095238										

0.966560	0.966560	0.966560	0.966560	0.966560	0.966560	0.966560	0.966560	0.966560	0.966560	0.966560	0.966560	0.966560	0.966560	0.966560	0.966560
1.58E-05	1.58E-05	1.56E-05	1.54E-05	1.54E-05	1.53E-05	1.52E-05	1.52E-05	1.51E-05	1.51E-05	1.51E-05	1.50E-05	1.50E-05	1.50E-05	1.49E-05	1.49E-05
0.009625	0.009585	0.009526	0.009507	0.009486	0.009452	0.009439	0.009427	0.009405	0.009396	0.009388	0.009373	0.009367	0.009361	0.009350	0.009345
0.372915	0.372078	0.371409	0.370863	0.370411	0.370029	0.369705	0.369425	0.369181	0.368968	0.368780	0.368612	0.368463	0.368328	0.368207	0.368097
0.953468	0.953346	0.953298	0.953156	0.953094	0.953068	0.952984	0.952948	0.952930	0.952876	0.952853	0.952841	0.952802	0.952787	0.952778	0.952750
0.982015	0.982046	0.982044	0.982042	0.982059	0.982059	0.982057	0.982068	0.982068	0.982066	0.982074	0.982074	0.982073	0.982078	0.982078	0.982077
0.964827	0.964827	0.964827	0.964827	0.964827	0.964827	0.964827	0.964827	0.964827	0.964827	0.964827	0.964827	0.964827	0.964827	0.964827	0.964827
1.67E-05	1.67E-05	1.65E-05	1.63E-05	1.63E-05	1.62E-05	1.61E-05	1.61E-05	1.60E-05	1.60E-05	1.59E-05	1.59E-05	1.58E-05	1.58E-05	1.58E-05	1.58E-05
0.010526	0.010481	0.010416	0.010395	0.010371	0.010334	0.010320	0.010306	0.010282	0.010273	0.010263	0.010247	0.010240	0.010233	0.010221	0.010216
0.413936	0.413041	0.412325	0.411741	0.411257	0.410849	0.410502	0.410202	0.409942	0.409714	0.409513	0.409334	0.409174	0.409030	0.408900	0.408783
0.964445	0.964350	0.964313	0.964206	0.964158	0.964138	0.964075	0.964047	0.964034	0.963993	0.963975	0.963966	0.963938	0.963926	0.963919	0.963898
0.980218	0.980251	0.980249	0.980247	0.980265	0.980265	0.980263	0.980275	0.980275	0.980273	0.980281	0.980281	0.980280	0.980286	0.980286	0.980285
0.963065	0.963065	0.963065	0.963065	0.963065	0.963065	0.963065	0.963065	0.963065	0.963065	0.963065	0.963065	0.963065	0.963065	0.963065	0.963065
1.77E-05	1.77E-05	1.74E-05	1.73E-05	1.73E-05	1.71E-05	1.70E-05	1.70E-05	1.69E-05	1.69E-05	1.69E-05	1.68E-05	1.68E-05	1.68E-05	1.67E-05	1.67E-05
0.011543	0.011494	0.011422	0.011398	0.011372	0.011330	0.011315	0.011300	0.011273	0.011263	0.011252	0.011234	0.011226	0.011219	0.011206	0.011200
0.461497	0.460544	0.459782	0.459160	0.458645	0.458211	0.457841	0.457523	0.457246	0.457003	0.456789	0.456598	0.456428	0.456275	0.456137	0.456012
0.973823	0.973753	0.973727	0.973654	0.973619	0.973605	0.973562	0.973542	0.973533	0.973505	0.973492	0.973486	0.973467	0.973458	0.973454	0.973440
0.978132	0.978166	0.978164	0.978162	0.978182	0.978181	0.978179	0.978192	0.978191	0.978190	0.978198	0.978198	0.978197	0.978203	0.978203	0.978203
0.961273	0.961273	0.961273	0.961273	0.961273	0.961273	0.961273	0.961273	0.961273	0.961273	0.961273	0.961273	0.961273	0.961273	0.961273	0.961273

Figure D.2: Varying Number of Modes for S_{21}

Bibliography

1. Lambert, Kevin M., Carol L. Kory, Gregory L. Wilson, and Thao H. Dinh. "Assessment of a Candidate Metallic Waveguide Standard, Based on S-Parameter Uncertainty Due to Dimensional Manufacturing Errors". 6 p. ;, 2008.

2. Ridler, Nick, Brian Lee, Jon Martens, and Ken Wong. "Measurement Uncertainty, Traceability, and the GUM". *IEEE Microwave Magazine*, (1527-3342):44–53, August 2007.

3. Taylor, B. N., Chris E. Kuyatt, National Institute of Standards, and Technology (U.S.). *Guidelines for evaluating and expressing the uncertainty of NIST measurement results*. U.S. Dept. of Commerce, Technology Administration, National Institute of Standards and Technology ; For sale by the Supt. of Docs., U.S. G.P.O., Gaithersburg, MD : Washington, DC :, 1993.

4. Wilson, Gregory L. "Estimation of Material Parameter Uncertainty". 4–8, 28–36, 42–45 p. ;, 2008.

5. Wittwer, J. W. ""Monte Carlo Simulation Basics" From Vertex42.com", June 1 2004. URL `http://vertex42.com/ExcelArticles/mc/MonteCarloSimulation.html`.

Index

The index is conceptual and does not designate every occurrence of a keyword. Page numbers in bold represent concept definition or introduction.

REPORT DOCUMENTATION PAGE

Form Approved
OMB No. 0704–0188

The public reporting burden for this collection of information is estimated to average 1 hour per response, including the time for reviewing instructions, searching existing data sources, gathering and maintaining the data needed, and completing and reviewing the collection of information. Send comments regarding this burden estimate or any other aspect of this collection of information, including suggestions for reducing this burden to Department of Defense, Washington Headquarters Services, Directorate for Information Operations and Reports (0704–0188), 1215 Jefferson Davis Highway, Suite 1204, Arlington, VA 22202–4302. Respondents should be aware that notwithstanding any other provision of law, no person shall be subject to any penalty for failing to comply with a collection of information if it does not display a currently valid OMB control number. **PLEASE DO NOT RETURN YOUR FORM TO THE ABOVE ADDRESS.**

1. REPORT DATE *(DD–MM–YYYY)*	2. REPORT TYPE	3. DATES COVERED *(From — To)*
26–03–2009	Master's Thesis	Aug 2008 — Mar 2009

4. TITLE AND SUBTITLE

Suite of Standards
for
Electromagnetic Material Characterization
Using Mode Matching
Theory

5a. CONTRACT NUMBER

DACA99–99–C–9999

5b. GRANT NUMBER

5c. PROGRAM ELEMENT NUMBER

6. AUTHOR(S)

Brian J. Witthoeft, 1Lt, USAF

5d. PROJECT NUMBER

09-164

5e. TASK NUMBER

5f. WORK UNIT NUMBER

7. PERFORMING ORGANIZATION NAME(S) AND ADDRESS(ES)

Air Force Institute of Technology
Graduate School of Engineering and Management (AFIT/EN)
2950 Hobson Way
WPAFB OH 45433-7765

8. PERFORMING ORGANIZATION REPORT NUMBER

AFIT/GE/ENG/09-49

9. SPONSORING / MONITORING AGENCY NAME(S) AND ADDRESS(ES)

AFRL/RYS (Mr. Garrett Stenholm)
2230 Tenth St., Suite 1
Wright Patterson AFB, OH 45433-7718
937-255-9179, garrett.stenholm@us.af.mil

10. SPONSOR/MONITOR'S ACRONYM(S)

AFRL/RYS

11. SPONSOR/MONITOR'S REPORT NUMBER(S)

12. DISTRIBUTION / AVAILABILITY STATEMENT

Approval for public release; distribution is unlimited.

13. SUPPLEMENTARY NOTES

14. ABSTRACT

The objective of this research is to determine if an acceptable standard can be developed to access the accuracy and precision of measurements taken using waveguide systems. Tiny changes in material fabrication, processing, and environment can cause problems with accuracy and precision in measurement. There is a great deal of research on uncertainty analysis in the literature. A large portion of the effort will be to determine the levels of uncertainty caused by each of the dimensions of the waveguide insert and to develop a suitable standard capable of verifying system performance. The Mode-Matching Technique will be used to extract input and output S-parameters of a suite of metallic verification waveguide standards. This suite will be used to set a new standard for acceptable tolerances of waveguide systems. After running the theoretical values of Scattering parameters against measured values, it can be determined whether small changes to the parameters of uncertainty greatly effect the measurements. If these changes only cause small changes in measurement, this will be considered an effective standard.

15. SUBJECT TERMS

material measurement, mode matching technique, uncertainty

16. SECURITY CLASSIFICATION OF:			17. LIMITATION OF ABSTRACT	18. NUMBER OF PAGES	19a. NAME OF RESPONSIBLE PERSON
a. REPORT	b. ABSTRACT	c. THIS PAGE			Dr. Michael J. Havrilla
U	U	U	UU	114	19b. TELEPHONE NUMBER *(include area code)* (937)255-3636 ext 4582; michael.havrilla@afit.edu